

2016

# Therapeutic Potential Of Catechins And Derivatives For The Prevention Of Alzheimer's Disease

Shelby Elaine Chastain  
*University of South Carolina*

Follow this and additional works at: <http://scholarcommons.sc.edu/etd>

 Part of the [Biomedical Engineering and Bioengineering Commons](#)

---

## Recommended Citation

Chastain, S. E. (2016). *Therapeutic Potential Of Catechins And Derivatives For The Prevention Of Alzheimer's Disease*. (Doctoral dissertation). Retrieved from <http://scholarcommons.sc.edu/etd/3998>

This Open Access Dissertation is brought to you for free and open access by Scholar Commons. It has been accepted for inclusion in Theses and Dissertations by an authorized administrator of Scholar Commons. For more information, please contact [SCHOLARC@mailbox.sc.edu](mailto:SCHOLARC@mailbox.sc.edu).

THERAPEUTIC POTENTIAL OF CATECHINS AND DERIVATIVES FOR THE  
PREVENTION OF ALZHEIMER'S DISEASE

By

Shelby Elaine Chastain

Bachelor of Science  
Newberry College, 2012

---

Submitted in Partial Fulfillment of the Requirements

For the Degree of Doctor of Philosophy in

Biomedical Engineering

College of Engineering and Computing

University of South Carolina

2016

Accepted by:

Melissa A. Moss, Major Professor

Mark Uline, Committee Member

Susan Lessner, Committee Member

James Chapman, Committee Member

Cheryl L. Addy, Vice Provost and Dean of the Graduate School

© Copyright by Shelby Elaine Chastain, 2016

All Rights Reserved

## ACKNOWLEDGEMENTS

I would like to thank my parents, Ricky and Kelley, for their unconditional love and support. Their faith in me, my abilities, and goals has been a steadfast pillar in my life. I would also like to thank my cherished family and friends, for the multitude of ways you show me your love and support, from being my practice audience to bringing me coffee or sending me messages of encouragement. I am truly thankful for my past and present work cohorts who became my comrades in arms and friends, you have made my graduate experience a period of my life that I will always cherish and look back on fondly. I would like to thank my undergraduate mentor Dr. Christina McCartha and lab mentor Dr. Evelyn Swain, whose mentorship and encouragement lead me to the Biomedical Engineering program at the University of South Carolina. I would like to thank all the past and present lab members, especially my undergraduate research assistant Ryan Geiser, for their mentorship, guidance, and help. I would like to recognize and thank Dr. Mark Uline, Dr. Susan Lessner, and Dr. James Chapman for being members of my committee. Finally, but certainly not least, I would like to thank my professor Dr. Melissa Moss for her excellent guidance, patience, and understanding.

## ABSTRACT

Alzheimer's disease (AD) is a neurodegenerative condition that affects 1 in 9 people over the age of 65, an estimated 5.4 million Americans. It is the only disease among the top 10 that cannot be prevented, cured, or treated. Based on the lack of a viable therapeutic for the prevention or cure of AD, it is vital that therapeutic research for AD continues. AD is characterized by the deposition of extracellular neuritic plaques comprised of insoluble amyloid- $\beta$  ( $A\beta$ ) fibrils. These plaques are formed from the amyloidogenic aggregation of  $A\beta$  monomer, generated from the cleavage of the amyloid precursor protein (APP) by  $\beta$ -secretase (BACE1) and  $\gamma$ -secretase.  $A\beta$  monomer aggregates via a nucleation-dependent pathway to form insoluble  $A\beta$  fibrils ( $fA\beta$ ). Many  $A\beta$  aggregates formed along the nucleation-dependent pathway are neurotoxins, associated with cognitive decline and neuronal loss observed in AD patients. Thus, one therapeutic strategy is to target the production of  $A\beta$  and/or its subsequent aggregation.

Epidemiological studies have associated green tea, rich in catechin polyphenols, and black tea, rich in theaflavin polyphenols, with reduced incidence of AD. The present study sought to explain this correlation, by identifying their potential to act as multi-target therapeutic drugs for AD by 1) altering the mechanistic aggregation of  $A\beta$  and 2) altering  $A\beta_{1-42}$  oligomer-induced expression of key AD-associated mRNAs.

Catechins and theaflavins showed mechanistic inhibition towards  $A\beta$  aggregation.

Catechins inhibit only the late stages of  $A\beta$  soluble aggregate growth, suggesting the

ability to bind only large A $\beta$  aggregate conformations. Theaflavins displayed a more sweeping capability, showing slight to prominent inhibition across the mechanistic steps of A $\beta$  aggregation. Both catechins and theaflavins were able to alter the morphology of fA $\beta$  made in their presence. fA $\beta$  structural conformation, or morphology, has been correlated with cytotoxic effects.

While theaflavins showed promising capabilities to inhibit the overall mechanistic aggregation of A $\beta$ , catechins displayed higher capabilities to alter A $\beta$ -oligomer induced expression of key AD-associated mRNAs. Epigallocatechin (EGC) and epigallocatechin gallate (EGCG) through antioxidant and antiaggregation capabilities, respectively, were able to attenuate the oligomer induced upregulation of APP, thus potentially reducing the APP protein that can be cleaved to release A $\beta$ . Additionally, through antiaggregation capabilities EGC and EGCG were able to significantly increase RNA expression of ADAM10, which cleaves APP in a manner that prevents A $\beta$  release. All catechins were able to attenuate A $\beta$ -induced expression of BACE1 mRNA through antiaggregation capabilities. In combination, these studies identify the capabilities of catechins to alter the pre-processing and post-processing of A $\beta$ , supporting their potential to act as multi-target therapeutics.

## TABLE OF CONTENTS

ACKNOWLEDGEMENTS.....	iii
ABSTRACT.....	iv
LIST OF TABLES.....	viii
LIST OF FIGURES.....	ix
LIST OF SYMBOLS.....	xi
LIST OF ABBREVIATIONS.....	xii
CHAPTER 1: BACKGROUND AND SIGNIFICANCE.....	1
1.1 Alzheimer's Disease Pathogenesis.....	1
1.2 Amyloid- $\beta$ Peptide.....	2
1.3 Therapeutic treatment of Alzheimer's disease by polyphenols.....	3
1.4 Flavanols: Catechins and Theaflavins.....	5
1.5 Study Overview.....	6
CHAPTER 2: MATERIALS AND METHODS.....	13
2.1 Materials.....	13
2.2 A $\beta$ <sub>1-40</sub> Monomer Purification.....	13
2.3 Soluble A $\beta$ <sub>1-40</sub> Aggregate Preparation and Purification.....	14
2.4 Preparation of fA $\beta$ .....	15
2.5 Preparation of Catechins and Theaflavins.....	16

CHAPTER 3: GREEN TEA CATECHINS AND BLACK TEA THEAFLAVINS MECHANISTICALLY INHIBIT AB AGGREGATION IN ALZHEIMER'S DISEASE .....	18
3. 1 Introduction .....	18
3. 2 Materials and Methods.....	20
3. 3 Results.....	28
3. 4 Discussion.....	32
CHAPTER 4: GREEN TEA CATECHINS AND BLACK TEA THEAFLAVINS ALTER KEY RNA EXPRESSION IN ALZHEIMER'S DISEASE .....	47
4. 1 Introduction .....	47
4. 2 Materials and Methods.....	50
4. 3 Results.....	56
4. 4 Discussion.....	59
CHAPTER 5: CONCLUSIONS.....	75
CHAPTER 6: FUTURE PERSPECTIVES .....	79
REFERENCES .....	80



## LIST OF TABLES

TABLE 4.1. PRIMER SEQUENCES USED. ....	64
--	----

## LIST OF FIGURES

FIGURE 1.1. AMYLOIDOGENIC CLEAVAGE OF APP.....	9
FIGURE 1.2. NUCLEATION-DEPENDENT PATHWAY OF AB.....	12
FIGURE 1.3. PROPERTIES BASED CATEGORIZATION OF POLYPHENOLS.....	11
FIGURE 1.4. CATECHINS AND THEAFLAVINS .....	12
FIGURE 3.1. PETKOVA ET AL. MODEL OF AB SECONDARY STRUCTURE AND POTENTIAL FIBRILLAR INTERACTION .....	39
FIGURE 3.1. AB1-40 MONOMER AGGREGATION .....	40
FIGURE 3.3. ABILITY OF CATECHINS AND THEAFLAVINS TO INHIBIT AB1-42 OLIGOMER FORMATION. ....	41
FIGURE 3.4. ALTERED CONFORMATION OF AB1-42 OLIGOMERS CONFIRMED BY ANS. ....	42
FIGURE 3.5. EFFECT OF CATECHINS AND THEAFLAVINS ON SOLUBLE AB1-40 AGGREGATE GROWTH. ....	43
FIGURE 3.6. COMPARISON OF DIFFERENT AB1-40 MONOMER AGGREGATION MONITORING TECHNIQUES. ....	44
FIGURE 3.7. EFFECT OF CATECHINS AND THEAFLAVINS ON AB1-40 MONOMER AGGREGATION. ....	45
FIGURE 3.8. MORPHOLOGY OF AB1-40 AGGREGATES FORMED IN PRESENCE OF CATECHINS AND THEAFLAVINS .....	46
FIGURE 4.1. AMYLOIDOGENIC AND NON-AMYLOIDOGENIC CLEAVAGE OF APP .....	65
FIGURE 4.2. CELL VIABILITY AFTER TREATMENT WITH CATECHINS AND THEAFLAVINS....	66

FIGURE 4.3. ANTIOXIDANT CAPACITY OF CATECHINS. ....	67
FIGURE 4.4. CATECHINS AND THEAFLAVINS ALONE HAVE NEGLIGIBLE EFFECT ON AD-ASSOCIATED MRNAS .....	68
FIGURE 4.5. CELL TREATMENTS DISPLAY NEGLIGIBLE EFFECT ON KI67 MRNA.....	69
FIGURE 4.6. EFFECT OF CATECHINS AND THEAFLAVINS ON AB <sub>1-42</sub> OLIGOMERS-INDUCED UPREGULATION OF APP MRNA.....	70
FIGURE 4.7. EFFECT OF CATECHINS AND THEAFLAVINS ON PS1 MRNA EXPRESSION. ....	71
FIGURE 4.8. EFFECT OF CATECHINS AND THEAFLAVINS ON ADAM9 MRNA EXPRESSION. 72	
FIGURE 4.9. EFFECT OF CATECHINS AND THEAFLAVINS ON ADAM10 MRNA EXPRESSION.....	73
FIGURE 4.10. EFFECT OF CATECHINS AND THEAFLAVINS ON AB <sub>1-42</sub> OLIGOMERS-INDUCED UPREGULATION OF BACE1 MRNA. ....	74

## LIST OF SYMBOLS

M Molar, abbreviation for SI unit mole/L

p p-value test statistic

$R_H$  hydrodynamic radius

$C_t$  threshold cycle

$\Delta C_t = C_{t_{\text{Sequence of Interest}}} - C_{t_{\text{Sequence of Reference}}}$

$\Delta\Delta C_t = \Delta C_{t_{\text{Sample}}} - \Delta C_{t_{\text{Vehicle}}}$

## LIST OF ABBREVIATIONS

A $\beta$	Amyloid- $\beta$ protein
A $\beta$ <sub>1-40</sub>	40 amino acid isoform of A $\beta$
A $\beta$ <sub>1-42</sub>	42 amino acid isoform of A $\beta$
AD	Alzheimer's disease
ADAM	A disintegrin and metalloproteinase
ANOVA	Analysis of Variance
ANS	8-anilino-1-naphthalenesulfonic acid
APP	Amyloid Precursor Protein
BACE1	$\beta$ -secretase1
BACE1-AS	BACE1 antisense transcript
BSA	Bovine Serum Albumin
DLS	Dynamic Light Scattering
DMSO	Dimethyl Sulfoxide
EC	Epicatechin
EGC	Epigallocatechin
EGCG	Epigallocatechin gallate
fA $\beta$	Fibril Amyloid- $\beta$
FBS	Fetal Bovine Serum

FPLC	Fast Protein Liquid Chromatography
HRP	Horseradish Peroxidase
iNOS	interleukin-1
MW	Molecular Weight
NFκB	Nuclear Factor Kappa-light-chain-enhancer of Activated B cells
ORAC	Oxygen Radical Antioxidant Capacity
PCR	Polymerase Chain Reaction
PBS	Phosphate Buffered Saline
PS1	Presenilin-1
qRT-PCR	Quantitative Real Time Polymerase Chain Reaction
ROS	Reactive Oxygen Species
SDS	Sodium Dodecyl Sulfate
SDS-PAGE	SDS-Polyacrylamide Gel Electrophoresis
SEC	Size Exclusion Chromatography
SEM	Standard Error of the Mean
SH-SY5Y	human neuroblastoma cell line
TF	Theaflavin
TFG	Theaflavin Monogallate
TEM	Transmission Electron Microscopy
TNF-α	Tumor Necrosis Factor-α

## CHAPTER 1: BACKGROUND AND SIGNIFICANCE

### 1.1 Alzheimer's Disease Pathogenesis

Alzheimer's disease (AD) is a neurodegenerative condition that affects 1 in 9 people over the age of 65, an estimated 5.4 million Americans.<sup>1</sup> Individuals with AD exhibit a decline in cognitive functions: memory, speech, judgment, planning, etc., which in turn affects their everyday activities ultimately resulting in their need for a caregiver. AD is the most common form of dementia and the 6<sup>th</sup> leading cause of death in the United States. It is the only disease among the top 10 that cannot be prevented, cured, or treated.<sup>1</sup> While other top leading causes of death, such as heart disease, cancer, and stroke, have decreased between the years 2000 and 2013, the number of AD fatalities has increased by 71%. It is estimated that in 2050 13.8 million Americans will be affected with AD.<sup>1</sup> The current FDA approved drugs for AD, such as Aricept, Razadyne, Namenda, and Exelon, cannot stop the disease but can only aid the treatment of the symptoms.<sup>2</sup> Based on the lack of viable therapeutics for the prevention or cure of AD and the drastically increasing number of AD cases, it is vital that therapeutic research for AD continues.

Postmortem examinations of AD-ridden brains have shown several reoccurring abnormal cellular pathologies: loss of synapses, microglial activation, and inflammatory processes.<sup>3</sup> Two additional hallmarks of AD are the deposition of intraneuronal neurofibrillary tangles composed of hyperphosphorylated tau protein and extracellular

neuritic plaques comprised of aggregated amyloid- $\beta$  ( $A\beta$ ).<sup>4,5</sup> *In vivo* studies have shown that when amyloid plaques are targeted and sequentially removed, hyperphosphorylated tau also disperses.<sup>6,7</sup> Additionally, mouse models of AD have demonstrated that  $A\beta$  plaques appear before the neurofibrillary tangles, implicating the accumulation of aggregated  $A\beta$  as the primary pathogenesis of AD.<sup>6,7</sup> Since derivation of this amyloid cascade hypothesis in 1991,<sup>8</sup> it has been the leading focus of research into therapeutic treatments of AD.<sup>9</sup> This hypothesis states that the naturally occurring soluble  $A\beta$  monomer aggregates via a nucleation-dependent pathway to form insoluble  $A\beta$  fibrils ( $fA\beta$ ). All  $A\beta$  aggregates formed along the nucleation-dependent pathway are inflammatory components and neurotoxins, which in turn causes cognitive decline and neuronal loss observed in AD patients.<sup>10</sup>

## 1.2 Amyloid- $\beta$ Peptide

$A\beta$  is an amphipathic peptide that originates from the proteolytic processing of the amyloid precursor protein (APP). APP is a transmembrane glycoprotein that is concentrated in synapses and neurons; the actual function of the protein is still unknown. In AD, APP undergoes sequential cleavage by  $\beta$ -secretase (BACE1) at the N-terminus and  $\gamma$ -secretase at the C-terminus to produce  $A\beta$  (Figure 1.1).<sup>11</sup> Cleavage by  $\gamma$ -secretase occurs within the transmembrane domain of APP and can produce an  $A\beta$  peptide that ranges from 38-43 amino acids. The two most common forms of  $A\beta$  are  $A\beta_{1-40}$  and  $A\beta_{1-42}$ . While  $A\beta_{1-42}$  only encompasses approximately 10% of  $A\beta$  present, it has a higher predisposition to aggregation due to its greater hydrophobicity.<sup>12</sup>



Once released from APP, A $\beta$  can aggregate via a nucleation-dependent pathway (Figure 1.2) in which the A $\beta$  monomer nucleates to form oligomers that then coalesce to form soluble aggregates. These soluble aggregates are then simultaneously thickened through association and lengthened through elongation to form insoluble fibrils that deposit as extracellular neuritic plaques.<sup>4,5</sup> Studies have shown A $\beta$  oligomers to be the most toxic A $\beta$  aggregate,<sup>13-15</sup> placing emphasis on inhibiting the mechanistic aggregation of A $\beta$  at the earlier stages.<sup>16</sup> The rate and method in which A $\beta$  aggregates is dependent upon A $\beta$ 's physiochemical features, such as hydrophobicity, secondary structure, charge, and aromatic interactions.<sup>17</sup> Alterations to these physiochemical features are possible avenues to modulate A $\beta$  aggregation and toxicity of aggregates formed.<sup>18</sup> Each stage of A $\beta$  aggregation presents a possibility for pharmacological manipulation to interrupt the aggregation, thus interrupting the pathogenesis of AD.<sup>19</sup>

### **1.3 Therapeutic treatment of Alzheimer's disease by polyphenols**

The conundrum of the "French paradox" has led to the premise that nature itself may have already created useful therapeutic agents. The "French paradox" identified that a population who consumed moderate amounts of red wine (two to four glasses a day) even in the presence of a high fat diet had a reduced incidence of coronary artery disease and AD. Upon further research into the composition of red wine, the beneficial attributes correlate with the high abundance of natural polyphenols within the beverage. The "French paradox" has led to many epidemiological studies that have researched the beneficial attributes associated with the consumption of large quantities of natural polyphenols in relation to a reduced risk of a multitude of diseases, including AD.<sup>4,20,21</sup>

Polyphenols encompass a large group of natural and synthetic small molecules that are known for containing one or more aromatic rings and possessing antioxidant properties.<sup>17,22</sup> Figure 1.3 shows the different classifications of over 800 known natural polyphenols. Polyphenols can be categorized into subgroups based on their structures, intramolecular interactions, functional groups, and basis of natural or synthetic production. Naturally produced polyphenols are commonly found in high concentrations in wine, tea, cocoa, nuts, berries, and a wide variety of other plants. Synthetically produced polyphenols are commonly used as pH indicators in cell culture media and food additives.<sup>17</sup>

In relation to AD, studies have shown that polyphenols bind to A $\beta$  through different mechanisms. Some polyphenols are sequence specific in their binding, while others are conformation-dependent, thus possessing different inhibitory capabilities at the different mechanistic steps of A $\beta$  aggregation.<sup>17</sup> In addition to inhibiting A $\beta$  aggregation, polyphenols have been shown to scavenge free radicals thereby reducing oxidative stress induced by reactive oxygen species (ROS), stimuli for inflammation.<sup>17,22</sup> A $\beta$  aggregates are associated with the production of ROS,<sup>17,23–26</sup> producing oxidative stress linked with the age-associated cognitive decline and neuronal loss seen in AD.<sup>22</sup> ROS acts as a messenger that activates downstream signaling pathways, such as the activation of iNOS, interleukin-1, nuclear factor kappa B (NF $\kappa$ B), and tumor necrosis factor-  $\alpha$  (TNF- $\alpha$ ). Stimulation of these genes results in the activation of microglia and astrocytes; and oxidative stress-mediated neuroinflammation, characteristics associated with AD.<sup>22</sup>

#### 1.4 Flavanols: Catechins and Theaflavins

Green tea, rich in catechin polyphenols, and black tea, rich in theaflavin polyphenols, have been associated specifically with prevention of obesity, breast cancer, coronary heart and cardiovascular disease, and reduced risk of AD.<sup>21,27,28,29, 30</sup> Catechins and their derivatives are part of the polyphenol subgroup flavanols, which are distinguishable from other anthoxanthin sub-groups by the additional hydroxyl at position 3 (Figure 1.3). Catechins and derivatives are constituents of the *Camellia Sinensis* tealeaf and, along with other flavanols and flavonols, comprise 30% of the dry tealeaf's weight. These polyphenols can be found in green, black, white, and oolong teas. The primary flavanols present in tealeaves are catechins. The parent compound of the catechin family is found in two isomer forms: catechin, the *trans* isomer, and epicatechin (EC), the *cis* isomer. This research focuses on the *cis* parent isomer, EC, structure and its derivatives based on their higher abundance in green tea. Epigallocatechin gallate (EGCG) is the main polyphenolic constituent of green tea leaves. HPLC analysis of green tea leaves revealed it comprises 60% of the total catechins isolated; that is, 10% of the total extracted dry tealeaf weight. EGCG represents the most abundant catechin followed by epigallocatechin (EGC) and then EC.<sup>24</sup> The parent compound EC undergoes hydroxylation to produce EGC; EGC can then be acetylated with gallic acid to form EGCG.

Once tea leaves are harvested, they are either immediately steamed and dried to preserve the "green," un-oxidized characteristics of the leaves or allowed to ferment for a period of time before being heated to stop the enzymatic reaction used to create black tea leaves. During this enzymatic process, the catechins undergo oxidative coupling to

produce oligomeric polyphenolic compounds, theaflavins.<sup>31-33</sup> Coupling of EC and EGC produces theaflavin (TF), while the oxidative coupling of EGC and EGCG produces theaflavin monogallate (TFG) (Figure 1.4).<sup>31</sup>

Catechins and derivatives are of great interest because of their natural role in plants, their association with decreased cognitive impairment, and their known bioavailability. Research has shown that EC, EGC and EGCG are bioavailable after oral consumption, and can be found in the plasma.<sup>34-40</sup> Additionally, EGCG<sup>40</sup> and EC<sup>36</sup> have been found to cross the blood brain barrier.<sup>22</sup> EC metabolites in glucuronides, methylated and sulfated forms have been identified to reach and accumulate in the brain at ~400nM concentrations.<sup>37</sup> Research has shown that through continual daily intake the bioavailability of EC increases.<sup>39</sup> The bioavailability of theaflavins is still not understood and continued research is needed to determine their ability to cross the blood brain barrier and their produced metabolites. Catechins and their derivatives will be analyzed for their strongest point of action in the modulation of pre-processing and post-processing of A $\beta$ , investigating their capabilities to become a multi-target drug.

### **1.5 Study Overview**

This study investigated the hypothesis that green tea catechins and their derivatives can act as multi-target therapeutics by altering pre-processing and post-processing pathways in AD. Catechins and their derivatives' individual capabilities to alter the pre-processing and post-processing of A $\beta$  were examined separately. These studies comprise the two aims of this work and are described below.

#### *1. 4. 1 Green tea catechins and black tea theaflavins mechanistically inhibit A $\beta$ aggregation in Alzheimer's disease*

The first aim tested the hypothesis that green tea catechins and black tea theaflavins can inhibit the overall and individual mechanistic steps of A $\beta$  monomer aggregation. Four assays were used to target unique steps along the aggregation pathway: a monomer aggregation assay to monitor the overall aggregation process; an oligomerization assay to monitor the initial nucleation step; an association assay to monitor the late stage lateral binding of soluble aggregates; and an elongation assay to monitor the late stage lengthening of soluble aggregates. The objective is to identify catechins and theaflavins that can prevent or reduce the amount of different A $\beta$  aggregate species formed. By comparing the inhibitory capabilities of this family of dietary relevant catechins and their polyphenolic oligomers, theaflavins, the proposed studies will elucidate key structural elements within these naturally occurring inhibitors of A $\beta$  aggregation. These structural observations can aid in the development of a better inhibitor compound.

#### *1. 4. 2 Green tea catechins and black tea theaflavins alter key RNA expression in Alzheimer's disease*

This chapter tested the hypothesis that green tea catechins and black tea theaflavins can alter the expression of key RNAs in AD. Research has shown that stressors such as A $\beta$  can result in increased levels of long non coding RNA (lncRNA) BACE1-antisense transcript (BACE1-AS) in human SH-SY5Y neuroblastoma cells, a regulator of  $\beta$ -secretase-1 (BACE1).<sup>41,42</sup> BACE1-AS regulates BACE1 expression by increasing BACE1 mRNA stability

and generating additional BACE1 through a 'post-transcriptional feed-forward mechanism' that results in increased levels of BACE1 and subsequently increased A $\beta$ .<sup>42</sup> This aim examined the capabilities of catechins and theaflavins to attenuate this 'post-transcriptional feed-forward mechanism' by altering BACE1 mRNA and other key AD-associated mRNAs expression. Real time quantitative polymerase chain reaction (qRT-PCR) will be used to analyze alterations in the relative RNA expression of BACE1, ADAM9, ADAM10, APP, and presenilin 1 (PS1). Alterations in each of these RNA expressions can have an effect on prognosis of AD.

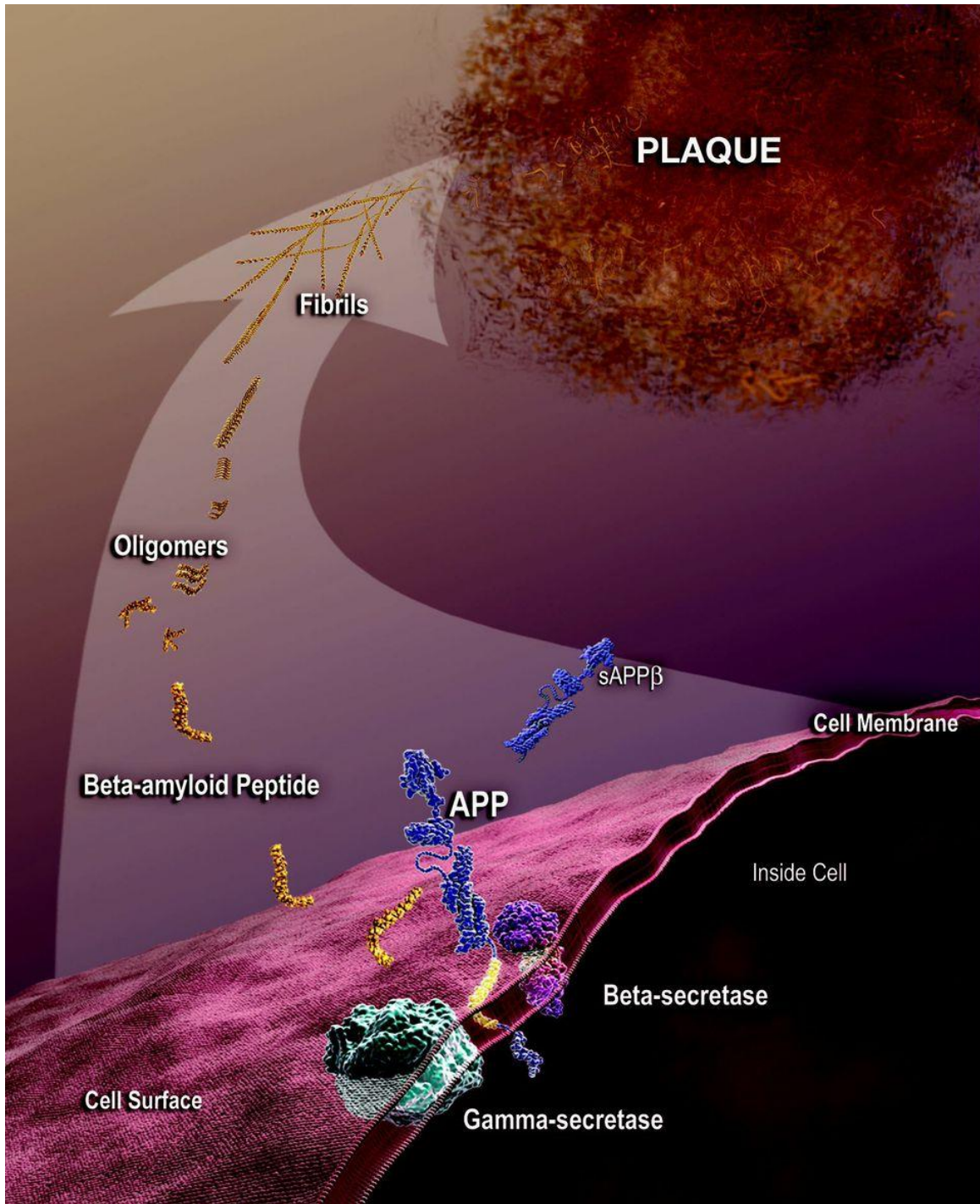


**Figure 1.1. Amyloidogenic cleavage of APP.**<sup>43</sup> APP is sequentially cleaved by  $\beta$ -secretase (BACE1) and  $\gamma$ -secretase to produce the  $A\beta$  peptide. This peptide can follow an amyloidogenic pathway resulting in  $A\beta$  aggregation. These aggregates accumulate extracellularly with in the brain as neuritic plaques.

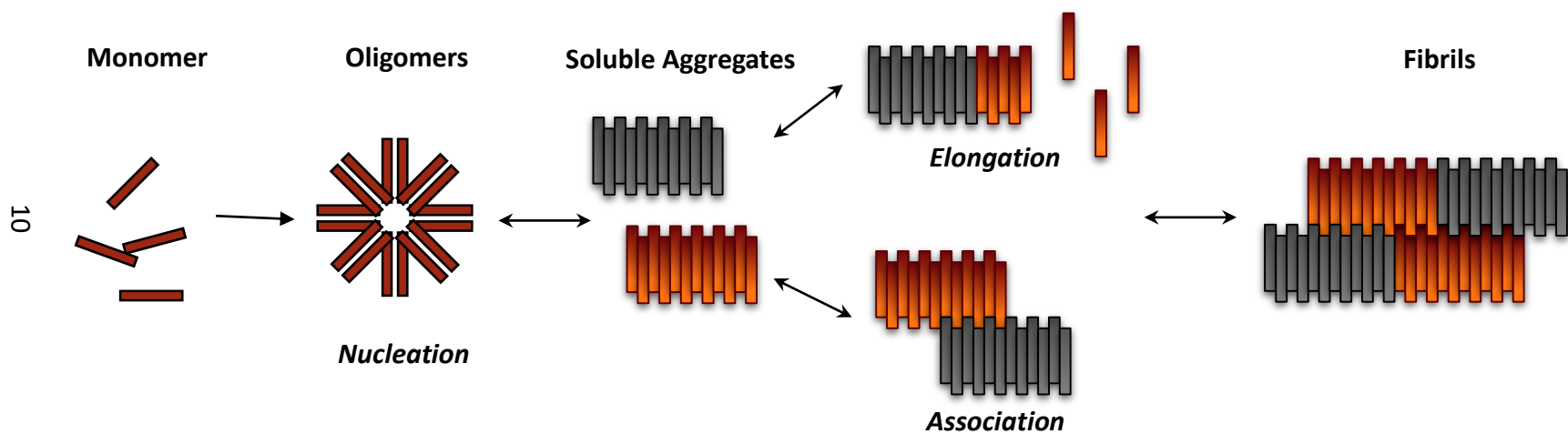


**Figure 1.2. Nucleation-dependent pathway of A $\beta$ .** A $\beta$  aggregation occurs by the nucleation of A $\beta$  monomer to oligomers, oligomers then coalesce to form soluble aggregates that grow through simultaneous elongation and association to produce insoluble fibrils.



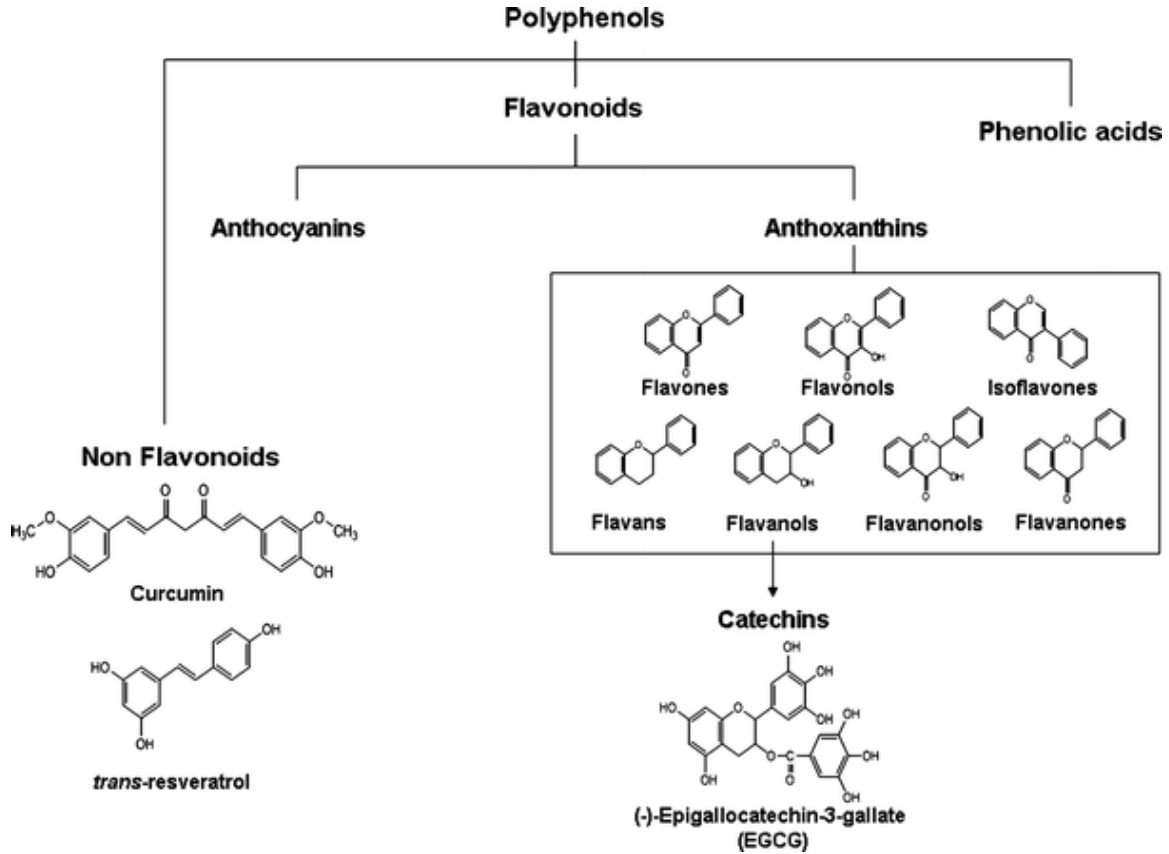


**Figure 1.3. Properties based categorization of polyphenols.**<sup>22</sup> The different categories are based upon their structure, intramolecular interactions, functional groups, and origin (natural or synthetic).

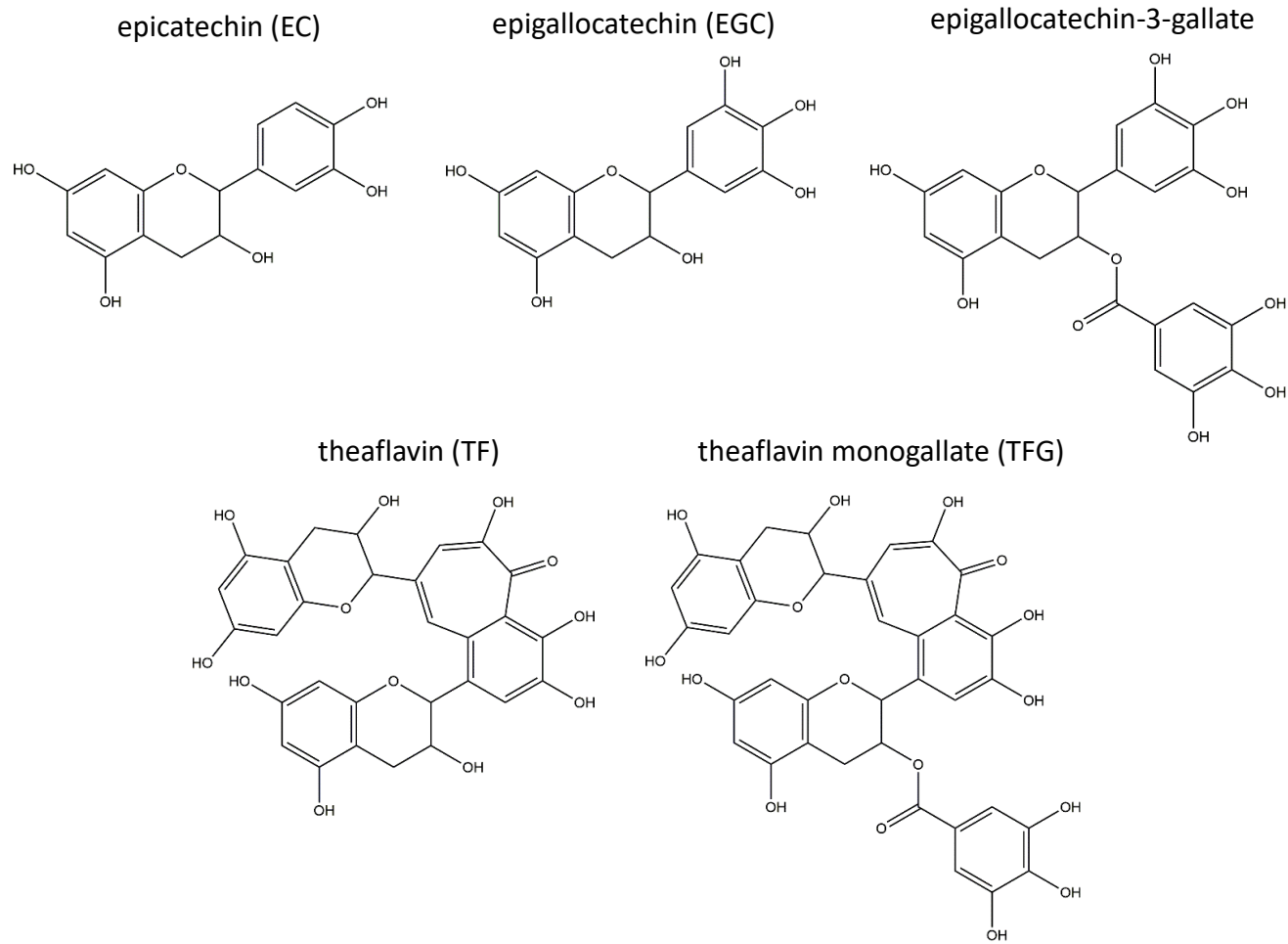


**Figure 1.4. Catechins and Theaflavins.** Catechin (EC, EGC, and EGCG) structures vary from hydroxylation to acetylation with a gallic acid. Theaflavin (TF and TFG) are the product of catechin oxidative coupling, during the tealeaf fermentation process. The theaflavin structures formed are dependent upon the catechins that were oxidatively coupled to produce the new derivative.

## CHAPTER 2: MATERIALS AND METHODS

### 2.1 Materials

(-)-Epicatechin, (-)-epigallocatechin, (-)-epigallocatechin gallate, theaflavin, and theaflavin monogallate were purchased from Sigma-Aldrich (St. Louis, MO) and stored at -4°C for catechins and at -20°C for theaflavins. A $\beta$ <sub>1-40</sub> and A $\beta$ <sub>1-42</sub> was purchased from AnaSpec, Inc. (San Jose, CA) and was stored at -20°C and -80°C respectively. Bovine serum albumin (BSA), Thioflavin T (ThT), sodium chloride (NaCl), sodium hydroxide (NaOH), phosphate buffered saline (PBS), and 1, 1, 1, 3, 3, 3-hexafluoro-2-propanol (HFIP) were purchased from Sigma Aldrich (St. Louis, MO). Dimethyl sulfoxide (DMSO) was purchased from VWR (Radnor, PA).

### 2.2 A $\beta$ <sub>1-40</sub> Monomer Purification

Lyophilized A $\beta$ <sub>1-40</sub> peptide was purified prior to experimentation. Fast protein liquid chromatography (FPLC) that utilizes size exclusion chromatography (SEC) on a Superdex 75 HR 10/300 column (GE Healthcare, Piscataway, NJ, USA) was used to remove any preformed aggregates and salts. Prior to injection A $\beta$ <sub>1-40</sub> was reconstituted in 50 mM NaOH at 2 mg/mL to minimize the formation of small aggregates. Remaining aggregates were excluded in 40 mM Tris-HCl (pH 8.0) via the purification process. To aid in the reduction of nonspecific A $\beta$  interaction with the dextran matrix of the column, the system was pretreated with bovine serum albumin (BSA, 2 mg/mL). Based on the UV (mAU) elution curve (Figure 2.1, red curve) the fractions of pure monomer were collected

for future experiments and additional large preformed aggregates were eluted in the void volume (9-11 mL). Concentrations of the collected fractions were determined using UV and the extinction coefficient of  $1450 \text{ M}^{-1}\text{cm}^{-1}$  at 280 nm.<sup>44,45</sup> SEC-purified  $\text{A}\beta_{1-40}$  monomer fractions were used fresh or stored at  $-4^{\circ}\text{C}$ , up to 4 days. This  $\text{A}\beta_{1-40}$  monomer was used for monomer aggregation,  $\text{fA}\beta$  preparation, production of soluble aggregates, and elongation assays.

### 2.3 Soluble $\text{A}\beta_{1-40}$ Aggregate Preparation and Purification

$\text{A}\beta_{1-40}$  soluble aggregates are intermediates between oligomers and fibrils. They were produced via the agitation (500 rpms) of 90-100  $\mu\text{M}$   $\text{A}\beta_{1-40}$  monomer combined with 50 mM NaCl in 40 mM Tris-HCl (pH 8.0). The sample was monitored for aggregation via thioflavin T (ThT) fluorescence. ThT is a benzathiole dye that binds to the  $\beta$ -sheet structure of  $\text{A}\beta$  aggregates, but not monomer or unordered species.<sup>46</sup> When bound, ThT undergoes a structural change and a shift in its Ex/Em to 450/485 nm. The fluorescence of the sample was monitored by combining 140  $\mu\text{L}$  of 10  $\mu\text{M}$  ThT and 10  $\mu\text{L}$  of sample. After the fluorescence surpasses a value of extensive aggregate formation, a 30  $\mu\text{L}$  aliquot of the agitated sample was centrifuged at 14,000 rpm for 5 min; the fluorescence of the supernatant was taken. A significant decrease in the fluorescent reading of the supernatant, relative to the unspun sample, is indicative of  $\text{A}\beta$  fibril formation.  $\text{A}\beta_{1-40}$  soluble aggregate aggregation was halted before extensive  $\text{fA}\beta$  formation. The hydrodynamic radius ( $R_H$ ) of the sample was also monitored using dynamic light scattering (DLS), to ensure the reaction was within soluble aggregates size range (60-100 nm). The sample was purified using FPLC on a SEC Superdex 75 HR 10/300 column in 40 mM Tris-

HCl (pH 8.0) elution buffer. To aid in the reduction of nonspecific A $\beta$  interaction with the dextran matrix of the column, the system was treated with BSA, 2 mg/mL, prior to A $\beta$ <sub>1-40</sub> injection. Figure 2.1 displays a typical soluble aggregate elution curve (black curve), where soluble aggregates were collected within the void volume and residual monomer was eluted with salt between 15-20 mL. A $\beta$ <sub>1-40</sub> soluble aggregate concentration within the collected fractions as determined by UV and a calculated extinction coefficient of 1450M<sup>-1</sup> cm<sup>-1</sup> corrected for light scattering. In addition, ThT fluorescence of isolated A $\beta$ <sub>1-40</sub> soluble aggregates was measured. Soluble A $\beta$ <sub>1-40</sub> aggregates were used in association and elongation assays. Soluble aggregates were stored up to 3 days and by using ThT concentration were re-evaluated before every experiment.

#### **2.4 Preparation of fA $\beta$**

A $\beta$ <sub>1-40</sub> monomer described from Section 2.2 was combined with NaCl for a final concentration of 60  $\mu$ M A $\beta$ <sub>1-40</sub>, 250 mM NaCl in 40mM Tris-HCl (pH 8.0). The mixture was vortexed at 800 rpm for 48 h (25°C) before centrifugation at 15,000 rpm for 15 min, the supernatant was removed and the fibril pellet was resuspended. ThT fluorescence readings, as described in Section 2.3 were taken before centrifugation and after resuspension and used to determine concentration of fA $\beta$ . The concentration was calculated by assuming the residual monomer was negligible, and multiplying the fraction of resuspended ThT fluorescence over pre-centrifugation ThT fluorescence by the initial monomer concentration.

## 2.5 Preparation of Catechins and Theaflavins

Catechins and theaflavins were respectively stored at  $-4^{\circ}\text{C}$  and  $-20^{\circ}\text{C}$ . Prior to each use catechins and theaflavins were prepared fresh by dissolving in filtered  $\text{dH}_2\text{O}$ .

## 2.6 Preparation of $\text{A}\beta_{1-42}$ Oligomers

$\text{A}\beta_{1-42}$  was reconstituted in cold HFIP to  $4\text{mg/mL}$  and incubated on ice (60 min), aliquoted and HFIP was allowed to evaporate overnight ( $25^{\circ}\text{C}$ ). The resulting  $\text{A}\beta_{1-42}$  films were stored at  $-80^{\circ}\text{C}$  until use.  $\text{A}\beta_{1-42}$  oligomers were formed by reconstituting the  $\text{A}\beta_{1-42}$  film to  $1.5\text{ mM}$  in DMSO with 10-fold molar excess polyphenol or equivalent volume of filtered  $\text{dH}_2\text{O}$  (control). Oligomerization was initiated by the addition of  $12\text{ mM}$  phosphate buffer (PBS, pH 7.4) containing  $1\text{ }\mu\text{M}$  NaCl to produce final concentrations of  $15\text{ }\mu\text{M}$   $\text{A}\beta_{1-42}$ ,  $150\text{ }\mu\text{M}$  polyphenol, 1% DMSO, and  $1\text{ mM}$  NaCl in PBS. The reaction was incubated for 30 min ( $25^{\circ}\text{C}$ ). Oligomers were then either immediately used for 8-anilino-1-naphthalenesulphonic acid (ANS) assay, diluted for cell treatment, or the oligomerization process was halted by the addition of Tween-20 (final concentration 0.1%).

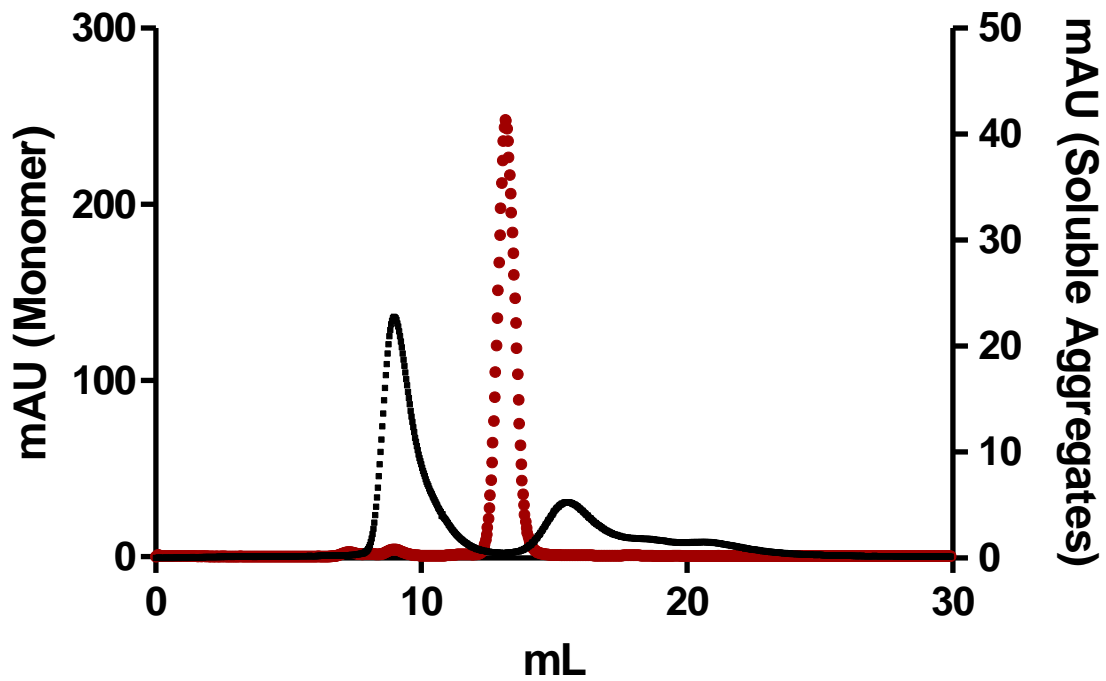


Figure 2.1. FPLC-SEC purification profile for A $\beta$ 1-40 monomer (red) and A $\beta$ 1-40 soluble aggregates (black). The FPLC utilizing SEC elutes large aggregates within the void volume followed by smaller monomer species of A $\beta$ 1-40 within the included volume.

CHAPTER 3: GREEN TEA CATECHINS AND BLACK TEA THEAFLAVINS MECHANISTICALLY  
INHIBIT AB AGGREGATION IN ALZHEIMER'S DISEASE

### 3.1 Introduction

Epidemiological studies support the abilities of green tea catechins and black tea theaflavins to attenuate AD. Further research is required to interpret the mechanism by which these polyphenols interfere in the disease process.<sup>21</sup> Previous studies have suggested that the inhibitory capabilities of some polyphenols are intrinsically altered dependent upon the mechanistic step at which they intervene, exhibiting conformation-dependent binding versus sequence specific binding.<sup>4,5,47,17</sup> To analyze the potential of catechins and theaflavins to interfere with the amyloidogenic pathway of A $\beta$ , it is crucial to first understand A $\beta$ 's secondary structure and intermolecular interactions to gain insight into potential mechanistic inhibition by polyphenols.

While fA $\beta$  are noncrystalline solid material and thus cannot be resolved via x-ray crystallography, several structures of A $\beta$  have been predicted by different techniques, including x-ray diffraction, nuclear magnetic resonance (NMR) spectroscopy, and computer simulation.<sup>18,48,49</sup> A widely used structural model of fA $\beta$ , proposed by Petkova et al. has given insight into the organization and intermolecular interactions of A $\beta$  (Figure 3.1a). Residues 1-8 are structurally disordered, while residues 12-24 and 30-40 adopt  $\beta$ -strand conformations and form parallel  $\beta$ -sheets by hydrogen bonding.<sup>48</sup> In the



amyloidogenic pathway, the initial random coil organization of A $\beta$  monomer converts to a  $\beta$ -sheet secondary structure, a cross- $\beta$ -sheet pattern, in which a single cross- $\beta$  unit is a double layered  $\beta$ -sheet structure with a hydrophobic core and a hydrophobic face. The only charged sidechains within the core of A $\beta$  are those of D23 and K28, these charged sidechains form a salt bridge to stabilize the  $\beta$ -sheet structure. The proposed binding of A $\beta$  is through hydrogen bonding, forming fibrils that contain two cross- $\beta$  units with their hydrophobic faces juxtaposed (Figure 3.1b). This model gives essential information towards the design of inhibitors of the amyloidogenic pathway of A $\beta$ .

Petkova et al.'s proposed model pinpoints several potential physicochemical features that would aid in the selection of a potential AD therapeutic. For example, compounds that interact with A $\beta$ 's hydrophobic core could potentially disrupt monomer-monomer interaction, destabilizing the nucleation of A $\beta$  oligomers. A sequence specific binding of A $\beta$  that recognizes residues 12-24, involved in the interaction between fA $\beta$  aggregates, would interfere with lateral association (Figure 3.1c). Alternatively, soluble aggregate elongation can potentially be inhibited by compound forming hydrogen bonds with amino or carboxyl groups of residues 12-24 or 30-40.

Catechins and theaflavins exhibit potential physicochemical features that are suggested to aid in the inhibition of the amyloidogenic aggregation of A $\beta$ . It was hypothesized that the aromatic rings of catechins and theaflavin would enable them to interact with the  $\pi$ - $\pi$  stacking of the phenylalanine residues at 19 and 20. Additionally, the abundance of hydroxyl groups in catechins and theaflavins (Figure 1.4) suggest a

higher potential to interact with hydrogen bonding of the amino and carboxyl groups of residues 12-24 and 30-40, potentially inhibiting elongation of soluble aggregates.

The approach of this aim differs from traditional investigation of potential therapeutics, by investigating the inhibitory capabilities of catechins, EC, EGC, and EGCG and theaflavins, TF and TFG, at the different mechanistic steps of A $\beta$  aggregation. A $\beta$  aggregation was investigated at three specific steps along the amyloidogenic pathway (Figure 1.2): oligomerization, the rate limiting step of A $\beta$  monomer oligomerization, elongation, A $\beta$  soluble aggregates are lengthened via the monomeric addition of A $\beta$  to N- or C-terminus, and association, A $\beta$  soluble aggregate growth via lateral interaction. Typical research focuses on overall A $\beta$  aggregation and early oligomerization. It was hypothesized that catechins and theaflavins will have unique inhibitory capabilities at the different mechanistic steps of A $\beta$  aggregation, effecting the overall A $\beta$  aggregation process. By analyzing the inhibitory capabilities of catechins and theaflavins at the different mechanistic steps, information was obtained on the importance of key structural elements. Knowing what structures are key to inhibit the varying mechanistic steps of A $\beta$  aggregation can aid in producing therapeutic drugs that are capable of targeting every mechanistic step of A $\beta$  aggregation, inhibiting the pathogenesis of AD.

## **3. 2 Materials and Methods**

### *3. 2. 1 Materials*

Laemmli buffer, 4-20% tris-glycine gels, Precision Plus Protein WesternC standard, Precision Protein Strep Tactin-HRP conjugate, and 0.2  $\mu$ m nitrocellulose membranes were purchased from Bio-Rad (Hercules, CA). Monoclonal antibody 6E10 was obtained from

Covance (Princeton, NJ). HRP-conjugated anti-mouse secondary antibody, Tween-20 and chemiluminescent reagents were purchased from VWR (Radnor, PA). 8-anilino-1-naphthalenesulphonic acid (ANS) was obtained from Research Organics (Cleveland, OH). 300-mesh formvar-supported copper grids and uranyl acetate were purchased from Electron Microscopy Science (Hatfield, PA).

### 3. 2. 2 Assessment of $A\beta_{1-42}$ Oligomer Size via SDS-PAGE and Western Blot Analysis

To determine if the presence of catechins or theaflavins alters the oligomer size distribution, Tween-20 (final concentration 0.1%) stabilized  $A\beta_{1-42}$  oligomer products made in the absence (control) or presence of the polyphenols described in Section 2.6 were mixed 1:1 with Laemmli buffer for size characterization using SDS-PAGE and Western blot.  $A\beta_{1-42}$  oligomer samples and Precision Plus Protein WesternC standard were loaded onto a 4-20% Tris-glycine gel and electrophoresed (120V) using a Mini-PROTEAN Tetra Cell (Bio-Rad). Protein was electrotransferred (14 V, 12 min) onto a 0.2  $\mu\text{m}$  nitrocellulose membrane via semi-dry transfer cell (Bio-Rad) and blocked (overnight, 4°C) using 5% dry nonfat milk in phosphate buffered saline containing 0.002% Tween (PBS-T). The membrane was probed (1h) with 6E10 monoclonal antibody (1:2000), a sequence-specific antibody that binds to the N-terminal region of  $A\beta$ . The membrane was then washed (5 min) three times with PBS-T before incubating (45 min) with HRP-conjugated anti-mouse secondary antibody (1:200) and Precision Protein Strep Tactin-HRP conjugate (1:200). After incubation with the secondary, the membrane was washed (5 min) three times before being placed in enhanced chemiluminescence reagents for 2 min. Images were obtained using the Gel Doc<sup>TM</sup> XRS+ imaging system (Bio-Rad), and

Image Lab software (Bio-Rad) was used for volumetric analysis of oligomer species within the 25-100 kDa and 100-250 kDa size ranges. Results are presented as fraction of control.

### 3. 2. 3 Evaluation of A $\beta$ <sub>1-42</sub> Oligomer Conformation via ANS Spectroscopy

ANS spectroscopy was used to evaluate the influence of catechins and theaflavins on oligomer conformation. ANS is a small molecular dye that undergoes a blue shift and an increase in fluorescence when bound to exposed hydrophobic residues of a protein or peptide. This dye has been extensively used in protein folding analysis to identify the presence of exposed hydrophobic residues and is commonly used as an indicator of A $\beta$  aggregate conformation, specifically oligomer conformation.<sup>49,50,51</sup> ANS was solubilized in DMSO at 50 mM and stored at 4°C. ANS was further diluted in 12 mM phosphate buffer (7.4) and added to oligomers made in the absence (control) or presence of catechins or theaflavins as described in Section 2.6, to a final concentration of 1  $\mu$ M A $\beta$ <sub>1-42</sub>, 10  $\mu$ M polyphenol, and 100  $\mu$ M ANS. Fluorescence emission from 400 to 600 nm with excitation at 350 nm was measured using an LS-45 luminescence spectrophotometer (Perkin Elmer, Waltham, MA). ANS fluorescence values were determined as the integrated area under the curve (IAUC) from 450-550 nm with blank (polyphenol with ANS) subtraction. Results are presented as fraction of control.

### 3. 2. 4 Determination of the Rate of A $\beta$ <sub>1-40</sub> Elongation

An elongation assay was utilized to evaluate the capabilities of catechins and theaflavins to alter the rate of A $\beta$ <sub>1-40</sub> soluble aggregate lengthening via monomer addition, or elongation.<sup>45,52,53</sup> SEC-purified soluble aggregates described in Section 2.4 were diluted in 40 mM Tris-HCl (pH 8.0) and incubated (15 min) alone (positive control)

or in the presence of 25-fold molar excess of catechins or theaflavins. Elongation was initiated by the addition of  $A\beta_{1-40}$  monomer (Section 2.2) for final concentrations of 2  $\mu\text{M}$   $A\beta_{1-40}$  soluble aggregates, 50  $\mu\text{M}$  polyphenol, and 30  $\mu\text{M}$   $A\beta_{1-40}$  monomer.  $A\beta_{1-40}$  soluble aggregates incubated in the absence of  $A\beta_{1-40}$  monomer, NaCl, and polyphenols served as a negative control and reflected the stability of the soluble aggregates.  $A\beta_{1-40}$  monomer incubated in the absence of  $A\beta_{1-40}$  soluble aggregates, NaCl, and polyphenols served as a negative control and reflected the stability of the monomer. Once initiated, the elongation reaction was placed in a quartz cuvette (path length 1 cm) for continual monitoring of  $R_H$  via DLS by a Dyna Pro Temperature-Controlled Microsampler and DynaPro Titan power source (Wyatt Technology Corporation, Santa Barbara, CA). Elongation rates were determined by linear regression of temporal increase in  $R_H$ . Results were normalized to the positive control.

### 3. 2. 5 Determination of the Rate of $A\beta_{1-40}$ Association

An association assay was used to evaluate the capabilities of catechins and theaflavins to attenuate the rate of lateral binding of  $A\beta_{1-40}$  soluble aggregates, or association.<sup>45,52,53</sup> SEC-purified soluble aggregates described in Section 2.4 were diluted in 40 mM Tris-HCl (pH 8.0) and incubated (15 min) alone (positive control) or in the presence of 25-fold molar excess of catechins or theaflavins. Association was initiated by the addition of physiological NaCl concentration for final concentrations of 2  $\mu\text{M}$   $A\beta_{1-40}$  soluble aggregates, 50  $\mu\text{M}$  polyphenol, and 150 mM NaCl. Once initiated, the association reaction was placed into a quartz cuvette (path length 1 cm) for continual monitoring of  $R_H$  via DLS of Dyna Pro Temperature-Controlled Microsampler and DynaPro Titan power

source (Wyatt Technology Corporation, Santa Barbra, CA).  $A\beta_{1-40}$  soluble aggregates incubated in the absence of NaCl and polyphenols served as a negative control and reflected the stability of the soluble aggregates. Association rates were determined by linear regression of temporal increase in  $R_H$ . Results were normalized to the positive control.

### 3. 2. 6 Evaluation of $A\beta_{1-40}$ Monomer Aggregation

SEC-purified  $A\beta_{1-40}$  monomer (Section 2.2) was diluted to a final concentration of 20  $\mu$ M  $A\beta_{1-40}$  monomer, 100  $\mu$ M polyphenol or equivalent solvent volume (control), and 150 mM NaCl in 40 mM Tris-HCl (pH 8.0). Samples were continuously vortexed at 500 rpm until  $A\beta_{1-40}$  aggregates plateaued. At pre-determined time intervals, a 30  $\mu$ L aliquot of the samples was removed and the extent of aggregation was evaluated using one of three  $A\beta$  aggregate detection methods: ThT fluorescence, dot blot analysis utilizing structure specific (larger  $A\beta$  aggregates) antibody LOC detection, and DLS intensity.

$A\beta_{1-40}$  monomer aggregation exhibited the characteristic lag period, growth phase, and plateau. From these graphs, the plateau portion of the experiment was determined and the average of the plateau was used to normalize all data points (each to their corresponding graphs). Inhibition was evaluated by determining the lag extent and plateau reduction. Lag extent was determined as the time required for a significant change in the detected  $A\beta$  aggregates to occur normalized to the control. Plateau reduction was determined as fraction of control plateau.

### 3. 2. 7 Evaluation of $A\beta_{1-40}$ Monomer Aggregation by ThT Fluorescence

$A\beta_{1-40}$  monomer aggregation was monitored via ThT fluorescence by combining 140  $\mu\text{L}$  of 10  $\mu\text{M}$  ThT dye and 10  $\mu\text{L}$  of the sample. Fluorescence emission from 400 to 600 nm with excitation at 450 nm was measured using an LS-45 luminescence spectrophotometer. Measurements were evaluated by calculating the area under the curve from 470-500 nm. Results are presented as the change in fluorescence over time.

### 3. 2. 8 Evaluation of $A\beta_{1-40}$ Monomer Aggregation by LOC Antibody Detection

$A\beta_{1-40}$  monomer aggregation was monitored via dot blot analysis using LOC antibody detection performed by adding 4 $\mu\text{L}$  of sample drop-wise onto a 0.1  $\mu\text{m}$  nitrocellulose membrane. The membrane was dried (9 min) at 25°C before placed into 5% nonfat milk in PBS-T (overnight, at 4°C). The membrane was probed (1h) with LOC (1:5000) and then washed (5 min) three time with PBS-T before incubation (45 min) with HRP-conjugated anti-rabbit secondary antibody (1:200) and Precision Protein Strep Tactin-HRP conjugate (1:200). After incubation with the secondary the membrane was washed (5 min) three times before being placed in enhanced chemiluminescence reagents for 2 min. Images were obtained using the Gel Doc<sup>TM</sup> XRS+ imaging system (Bio-Rad), and Image Lab software (Bio-Rad) was used for volumetric analysis to determine the intensity of each dot. Results are presented as the change in adjusted volume (intensity) over time.

### 3. 2. 9 Evaluation of $A\beta_{1-40}$ Monomer Aggregation by DLS Intensity

$A\beta_{1-40}$  monomer aggregation was monitored via DLS intensity. The sample's DLS intensity was determined by loading the sample into a quartz cuvette (path length 1 cm)

for continual monitoring using a Dyna Pro Temperature-Controlled Microsampler and DynaPro Titan power source (Wyatt Technology Corporation, Santa Barbra, CA). Because A $\beta$  monomer aggregation results in the production of a wide range of aggregate species, monitoring its  $R_H$  is not practical. Instead, the more global parameter of intensity was monitored. Results are presented as increase in intensity over time.

### 3. 2. 10 Evaluation of LOC and ThT Binding of A $\beta$ Aggregates

Assessment of catechins' and theaflavins' ability to alter ThT and LOC binding signals was performed to facilitate selection of the most effective technique for monitoring A $\beta_{1-40}$  monomer aggregation. For ThT analysis, fA $\beta_{1-40}$  (Section 2.4) were diluted to the equivalent of loading 15  $\mu$ L A $\beta$  monomer aggregation assay (1:5 molar ratio of A $\beta$ : polyphenol) into 140  $\mu$ L 10  $\mu$ M ThT, for a final concentration of 1.93  $\mu$ M fA $\beta$  in 40 mM Tris-HCl (pH 8.0), 9.67  $\mu$ M polyphenol or solvent (control), and 9.03  $\mu$ M ThT. Sample fluorescence was analyzed as in Section 3.2.7. For LOC analysis, fA $\beta_{1-40}$  diluted to 10  $\mu$ M in 40mM Tris-HCl (pH 8.0) with 100  $\mu$ M polyphenol or solvent (control) was added drop-wise (4 $\mu$ L) onto a 0.1  $\mu$ m nitrocellulose membrane. The membrane was dried (9 min) at 25°C before being placed into 5% nonfat milk in PBS-T (overnight, at 4°C). The membrane was probed (1h) with LOC (1:5000) and then washed (5 min) three time with PBS-T before incubation (45 min) with HRP-conjugated anti-rabbit secondary antibody (1:200) and Precision Protein Strep Tactin-HRP conjugate (1:200). After incubation with the secondary, the membrane was washed (5 min) three times before being placed in enhanced chemiluminescence reagents for 2 min. LOC binding was analyzed as in Section 3.2.8 all samples were quantified and reported as a fraction of the control.



### 3. 2. 11 Transmission Electron Microscopy

Transmission electron microscopy (TEM) negative staining technique was implemented to view the fA $\beta$  end product of A $\beta$ <sub>1-40</sub> monomer aggregation, described in Section 3.2.6—Section 3.2.9. Negative staining employs a dye that stains the background, but not the protein itself. TEM transmits a beam of electrons through a sample; the electrons are scattered by the stain and only permitted to pass through the sample. This imaging technique allows for qualitative evaluation of the effect of catechins and theaflavins on the morphology of the fA $\beta$ <sub>1-40</sub>.

Samples were gridded by placing 20  $\mu$ L of the end product of A $\beta$ <sub>1-40</sub> monomer aggregation reaction onto a 300-mesh formvar-supported copper grid and incubating (3 min). The remaining solution was wicked off, and this process was repeated a total of three times. Grids were negatively stained by incubation (8 min) sample side down on a 20  $\mu$ L droplet of 2% uranyl acetate before solution was wicked off, and the grids dried overnight (4°C). Grids were imaged using a TEM-1400 Plus Electron Microscope (JEOL) at 120kV.

### 3. 2. 12 Statistical Analysis

Prism 5 software (Graphpad Software, La Jolla, CA) was used for all statistical analysis. A one-way analysis of variance (ANOVA) with Dunnett test was used to compare all samples to the respective control, and an unpaired t-test was used for comparison between samples.  $p < 0.05$  was considered significant. All values are expressed as the mean  $\pm$  SEM.

### 3.3 Results

#### 3.3.1 Theaflavins Modulate A $\beta$ Oligomer Size and Structure

To evaluate the ability of catechins and theaflavins to alter oligomerization, A $\beta_{1-42}$  oligomers were formed in the absence (control) or presence of each polyphenol. The size distribution of resulting oligomers was assessed using SDS-PAGE and Western blot. Separation of the oligomer products by 4-20% Tris-glycine gel (Figure 3.3a) revealed that only theaflavins are able to reduce the formation of oligomers in both the 25-100 kDa and 100-250 kDa (Figure 3.3b) size ranges. The A $\beta_{1-42}$  oligomer result indicates a clear distinction in the inhibitory capability of catechins and their phenolic derivatives, theaflavins. In their monomeric form, the catechins have no effect, but when they are oxidatively coupled to form phenolic derivatives, theaflavins, they are able to significantly reduce the amount of larger oligomers formed (100-250 kDa). TFG is the only compound that is also able to significantly reduce the formation of small (25-100 kDa) oligomers.

Studies have shown a direct correlation between A $\beta$  aggregate structure and toxicity as well as the potential to undergo further aggregation.<sup>17,18</sup> The ability of catechins and theaflavins to alter the conformation of A $\beta_{1-42}$  oligomers was determined via ANS (Figure 3.4). ANS binds to exposed hydrophobic residues of proteins and has been commonly used to determine A $\beta$  aggregate conformation.<sup>51</sup> Oligomers formed in the presence of catechins do not exhibit significantly altered ANS fluorescence when compared to native oligomers. A $\beta_{1-42}$  oligomers made in the presence of TFG, however, exhibit increased ANS fluorescence, suggesting an altered oligomer conformation.

### 3. 3. 2 Catechins and Theaflavins Inhibit Growth of $A\beta_{1-40}$ Soluble Aggregate Intermediates

Elongation and association are the two late-stage mechanistic steps of  $A\beta$  aggregation, which occur simultaneously to produce insoluble  $fA\beta$  that deposit as neuritic plaques. Assays that isolate the growth mechanisms were utilized to evaluate the ability of catechins and theaflavins to alter the late-stages of  $A\beta_{1-40}$  soluble aggregate growth by monomeric lengthening, or elongation, and lateral binding, or association.

Elongation growth was initiated by addition of  $A\beta_{1-42}$  monomer resulting in monomeric growth. Accuracy of elongation was determined by no individual change in the native monomer and soluble aggregate size. When soluble  $A\beta_{1-40}$  aggregates were pre-incubated in the presence of catechins and theaflavins prior to initiation of elongation via addition of monomer, all compounds were significantly able to reduce the rate of elongation by greater than 60% (Figure 3.5). EGCG was the superior inhibitor, completely abrogating elongation.

Association growth was initiated by addition of physiological salt resulting in lateral growth. Accuracy of association was determined by no change of native soluble aggregates size. When incubation of  $A\beta_{1-40}$  soluble aggregates with catechins and theaflavins was followed by addition of physiological salt to initiate association, varying inhibitory capabilities were observed for catechins and theaflavins (Figure 3.5). As compounds are derived from the parent compound EC, hydroxylation to EGC, and acetylation of EGC with gallic acid to form EGCG, capacity to attenuate association increased ( $p < 0.05$  EC to EGC,  $p < 0.01$  EGC to EGCG and  $p < 0.001$  EC to EGCG). Catechins,

EGC and EGCG, and theaflavins, TF and TFG, are all able to significantly reduce the rate of association.

For both growth mechanisms, elongation and association, EGCG displays superior inhibition. EGCG is able to completely abrogate both late-stage mechanistic-aggregation steps of A $\beta$ .

### 3. 3. 3 Congruence between A $\beta$ <sub>1-40</sub> Monitoring Techniques and Polyphenol Interaction

A $\beta$  aggregation was monitored simultaneously using three different methods of aggregate detection, ThT, LOC antibody detection, and DLS intensity, to verify the validity of using these techniques interchangeably. The results of each technique were reported as a fraction of their control's plateau for comparison purposes (Figure 3.6a).

When normalized to their control's plateau, the extent of total aggregation was analogous between the three A $\beta$  aggregate monitoring techniques. All techniques exhibited equivalent fractions of plateau at the same three phases of A $\beta$ <sub>1-40</sub> monomer aggregation, lag period, growth phase, and plateau. These results demonstrate that these three methods of monitoring A $\beta$  aggregation can be used interchangeably.

Polyphenols have exhibited the capability to compete with ThT and LOC for interaction with A $\beta$ <sub>1-40</sub> binding sites. To ensure that the compounds within this study do not interfere with A $\beta$  aggregate detection, detection of fA $\beta$ <sub>1-40</sub> by ThT and LOC was performed in the absence and presence of catechins and theaflavins (Figure 3.6b). ThT and LOC competition is indicated by lowered detection in the presence of the compound than in its absence. The presence of EGCG, TF, and TFG resulted in reduced detection of ThT and LOC. Thus, for these compounds, DLS intensity was utilized to monitor the extent

of A $\beta$ <sub>1-40</sub> monomer aggregation. EC and EGC exhibited no significant reduction of ThT or LOC, and the monitoring technique of LOC antibody detection was used for further A $\beta$ <sub>1-40</sub> monomer aggregation analysis.

### *3.3.4 Theaflavins Reduce the Extent of A $\beta$ <sub>1-40</sub> Monomer Aggregation, while both Catechins and Theaflavins Alter fA $\beta$ <sub>1-40</sub> Morphology*

The capabilities of catechins and theaflavins to reduce the extent of A $\beta$ <sub>1-40</sub> monomer aggregation was monitored by LOC antibody detection for EC and EGC (Figure 3.7a) and DLS intensity for EGCG (Figure 3.7b), TF, and TFG (Figure 3.7c). Inhibitory capabilities of polyphenols were evaluated via two parameters, lag time, the time required for nucleation to occur and the plateau, the overall amount of A $\beta$  aggregates formed (Figure 3.6d).

Catechins and theaflavins exhibit a trend for altered time required for nucleation, but it does not reach significance. EC and EGC shorten the time required for nucleation to occur. EGCG and TF extend the time required for nucleation to occur by approximately 40%, TFG extends the time required for nucleation by approximately 120%. There is a statistical increase in lag extension from EC and EGC to EGCG ( $p < 0.05$  EC to EGCG and EGC to EGCG). The plateau value of monomer aggregations performed in the presence of catechins has no significant difference from the control plateau, thus catechins do not reduce the amount of aggregates formed. Monomer aggregations performed in the presence of TF and TFG had significantly reduced plateau values compared to the control, significantly reducing the overall amount of A $\beta$  aggregates formed in their presence by 58% and 79%, respectively. As shown in Figure 3.6d, an inverse relationship is observed

between the plateau and lag time for both catechins and theaflavins. The superior inhibitor of  $A\beta_{1-40}$  monomer aggregation is TFG, capable of extending time required for nucleation and significantly reducing total amount of  $A\beta$  aggregate formation.

To observe the effects of catechins and theaflavins on the morphology of aggregates formed in their presence, the end products of the  $A\beta_{1-40}$  monomer aggregation were gridded and negatively stained for TEM analysis (Figure 3.8). Typical morphology of  $fA\beta_{1-40}$ , exhibited by the control displays a network of thick long spindle-like structures that spread across the image, having no defined beginning or end. A defined morphology change is observed for  $fA\beta_{1-40}$  made in the presence of each studied compound.  $fA\beta_{1-40}$  formed in the presence of EC and EGC have shortened  $fA\beta$ , indicating reduced elongation, and reduced thickness with hydroxylation of the compound, indicating reduced association.  $fA\beta_{1-40}$  formed in the presence of EGCG have been reduced to very short, singular, fibril strands.  $fA\beta_{1-40}$  formed in the presence of TF have unchanged or slightly increased thickness and the length of  $fA\beta_{1-40}$  clusters are short in comparison to the control. TFG has the most pronounced effect on  $fA\beta_{1-40}$  morphology.  $fA\beta_{1-40}$  formed in its presence are very short, thin fibrils that are dispersed across the TEM grids.

### 3.4 Discussion

This aim investigated the capability of green tea catechins and their phenolic derivatives, theaflavins, to inhibit  $A\beta$  aggregation via mechanistic inhibition.  $A\beta$  undergoes aggregation to form insoluble  $fA\beta$  that deposit as extracellular neuritic plaques, hallmarks of AD.<sup>4,5</sup>  $A\beta$  first nucleates to form oligomers that then coalesce into

soluble aggregates. Soluble aggregates are simultaneously thickened through lateral association and lengthened through elongation via monomer addition to form insoluble fibrils. Catechins and theaflavins ability to alter individual mechanistic steps of oligomerization, soluble aggregate elongation, and soluble aggregate association, as well as the cumulative A $\beta$  aggregation process and morphology of resulting aggregates were determined.

Evidence suggests that before A $\beta$  monomer can oligomerize it undergoes misfolding; the exact mechanism of misfolding and its accompanied conformation change to oligomers is still not known.<sup>40,54</sup> Current research has shown that A $\beta$  oligomers are the most toxic A $\beta$  species,<sup>13-15</sup> placing emphasis on preventing the misfolding and subsequent oligomerization of A $\beta$  or pushing it to less toxic larger species. Another proposed method of altering oligomer toxicity<sup>18</sup> and propensity to aggregate is structural modification, or altering oligomer conformation.<sup>17</sup> Theaflavins, but not catechins, are able to modulate A $\beta$  oligomer formation. TF significantly reduces large (100-250 kDa) oligomers, while TFG significantly reduces both the larger and smaller (25-100 kDa) oligomer species. Moreover, TFG is the only compound able to significantly alter oligomer conformation, evidenced by heightened ANS fluorescence indicative of increased exposed hydrophobic regions within oligomers formed in its presence. TF also increases ANS fluorescence, although this increase does not reach significance.

Inhibition of A $\beta$  aggregation as an AD therapeutic approach arose from the correlation between aggregate accumulation as extracellular neuritic plaques and neurodegeneration association with AD.<sup>6,7</sup> The primary hallmark of AD, extracellular

neuritic plaques, are composed of insoluble fA $\beta$  that deposit as long spindle like structures that exhibit clusters of lateral association. The morphology of fA $\beta$  is a result of the simultaneous soluble aggregate growth via elongation and association. Inhibition of the mechanistic steps of soluble aggregate growth has the potential to attenuate the production of insoluble fA $\beta$ . Analysis of catechins' and theaflavins' inhibitory effect on soluble aggregate growth reveals that all compounds significantly attenuate the rate of A $\beta$ <sub>1-40</sub> soluble aggregate elongation. Petkova et al.'s model of A $\beta$  fibril formation indicates a compound that forms hydrogen bonds with the amino or carboxyl groups of residues 12-24 or 30-40 can potentially inhibit the A $\beta$  soluble aggregate growth via elongation. The substantial number of hydroxyl groups within catechins and theaflavins possess a high propensity to form hydrogen bonds, providing a potential explanation for the capability of all compounds examined to significantly decrease the rate of soluble aggregate elongation. In contrast, catechins and theaflavins capability to attenuate A $\beta$ <sub>1-40</sub> soluble aggregate growth via association follows a structural trend. Hydroxylation of EC to EGC statistically increases the compound's capability to attenuate the rate of soluble aggregate growth via lateral binding. This statistical trend continues with gallic acid acetylation of EGC to EGCG. TF, the phenolic derivative of EC and EGC, displays association inhibition congruent with its precursor EGC. However, TFG, the phenolic derivative of EGC and EGCG, shows a decreased attenuation of association, over TF. Overall, association results indicate that EGCG is the superior inhibitor of soluble aggregate growth, displaying the capability to attenuate both elongation and association.



Previous research has suggested that polyphenols can bind to A $\beta$  by two methods, sequence specific binding or conformation dependent binding.<sup>17</sup> Results from this aim illustrate catechins' capabilities to only effect A $\beta$  soluble aggregate growth, suggesting conformation dependent binding of A $\beta$ . Conversely, theaflavins exhibit the ability to affect every mechanistic step of A $\beta$  aggregation, suggesting the compounds' capabilities to recognize several A $\beta$  structures.

The resulting fibrillar product of A $\beta$  aggregation is a summation of the different mechanistic steps. Therefore, the inhibitory capabilities of the compounds at oligomerization, elongation, and association steps can influence both the overall aggregation propensity and aggregate morphology. Ability of catechins and theaflavins to alter propensity of A $\beta$  to aggregate is directly comparable to their ability to inhibit A $\beta$  oligomerization, with only the theaflavins able to significantly reduce the overall amount of A $\beta$  aggregates formed in their presences. Catechins have little effect on extent of aggregation. However, they and their phenolic derivatives, theaflavins, have pronounced effect on aggregate morphology. A robust analysis is formed by comparing the morphological TEM images of fA $\beta$  produced.

fA $\beta$  made in the presence of EC is characterized by short well-defined lengths compared to that of native fA $\beta$ . This observed morphology parallels with EC's ability to significantly reduce the rate of soluble aggregate elongation. The addition of a hydroxyl group at the 3' position from EC to EGC increases the capability of the compound to alter fA $\beta$  morphology. fA $\beta$  made in the presence of EGC exhibits short well-defined lengths as well limited lateral association compared to native fA $\beta$ . This morphological change is

congruent with EGC's increased ability to reduce association over EC. The acetylation of EGC with gallic acid at position 3 to form EGCG results in further altered fA $\beta$  morphology. EGCG produces fA $\beta$  with extremely short spindle-like structures with no lateral association. The pronounced lack of length and thickness of the resulting fibrils can be attributed to the mechanistic inhibitory capabilities of EGCG to attenuate soluble aggregate growth. Fibrils are still produced in the presence of EGCG due to its inability to inhibit A $\beta$  oligomer formation. Though catechins are unable to reduce the amount of A $\beta$  aggregates formed in the overall A $\beta_{1-40}$  monomer aggregation process, the TEM images aligned with their mechanistic inhibitory capabilities reveals their ability to alter the morphology of fA $\beta$  produce. Structure-toxicity relationship research has indicated a direct correlation between fA $\beta$  morphology and toxicity<sup>18</sup>, this relationship could potential explain the correlation of treatment with EGCG and reduced A $\beta$  toxicity besides its antioxidant capabilities.<sup>47,55,56</sup>

Catechins phenolic derivatives, theaflavins, in addition to reducing the propensity of A $\beta$  to aggregate alter fA $\beta$  morphology. TF has a reduced effect on fA $\beta$  morphology compared to that of its catechin predecessors, as shown by the formation of fA $\beta$  with short well-defined spindle-like lengths with equivalent native fA $\beta$  lateral association. Due to the additive nature of the mechanistic steps of A $\beta$  aggregation, the superior capability of TF to reduce the elongation rate appears to negate its mechanistic inhibition of association. Of the catechins and theaflavins, TFG has the most pronounced effect on the morphology of fA $\beta$  made in its presence. When closely examined, the morphology of the A $\beta$  produced in the presence of TFG exhibits both reduced length and thickness, as well as altered

morphology of the typically  $fA\beta$  spindle like conformation. The  $A\beta$  conformation produced by the presence of TFG more closely resembles an intermediate conformation between oligomers and soluble aggregates based on the TEM classification by Fändrich 2006.<sup>49</sup> While TFG's capability to inhibit the late stages of  $A\beta$  aggregation is not as pronounced as EGCG,  $A\beta$  morphological comparison shows TFG has a more pronounced effect on  $fA\beta$  formation. The difference in the mechanistic inhibitory capabilities of TFG compared to EGCG is its ability to alter conformation and formation of  $A\beta$  oligomers. These results place emphasis on alteration of  $A\beta$  at the earlier oligomeric formation.

Epidemiological<sup>28-30</sup> and therapeutic research<sup>20,27,35,55,57-60</sup> on catechins and more recently theaflavins supports the growing recognition of their protective role against neurodegeneration. Therapeutic research into the inhibitory capabilities of catechins has focused on their ability to inhibit the earlier oligomerization process and the overall aggregation of  $A\beta$ . Previous *in vitro* studies have shown the most promising therapeutic catechin polyphenol to be EGCG,<sup>60,61</sup> due to its ability to attenuate  $A\beta$  monomer aggregation.<sup>55,62,63</sup> From this aim and other papers<sup>64</sup> it has been determined that the  $A\beta$  aggregate detection method of ThT is not a viable monitoring technique for EGCG. Results have shown that EGCG competes with ThT for binding of  $A\beta$ ,<sup>64</sup> resulting in discrepancies between studies on the extent of EGCG capability to inhibit  $A\beta$  aggregation.<sup>60,63</sup> What is agreed upon is that EGCG does have an effect on  $A\beta$  aggregates produced in its presence<sup>11,55,62-66</sup> which has been correlated with reduce  $A\beta$  cytotoxicity.<sup>47,63,65,67</sup> By analyzing the mechanistic inhibitory capability of catechins and their phenolic derivatives, theaflavins, it was revealed that the addition of the gallate group aids theaflavin inhibitory

capability at oligomerization and overall aggregation, and the addition of a hydroxyl at the 3' position and a gallate group at the 3 position aids in catechins inhibitory capability at association. Of the catechins, EGCG is the superior inhibitor, capable of attenuating A $\beta$  soluble aggregate growth. It was determined that while catechins are only able to recognize A $\beta$  soluble aggregate conformation they are still able to alter the resulting fA $\beta$  morphology, potentially aiding in their ability to attenuate A $\beta$  cytotoxicity. Theaflavins are the only compounds able to significantly reduce the extent of A $\beta$  aggregation, drawing a direct correlation between compounds capability to reduce A $\beta$  aggregate formation and early modification of A $\beta$  oligomerization.

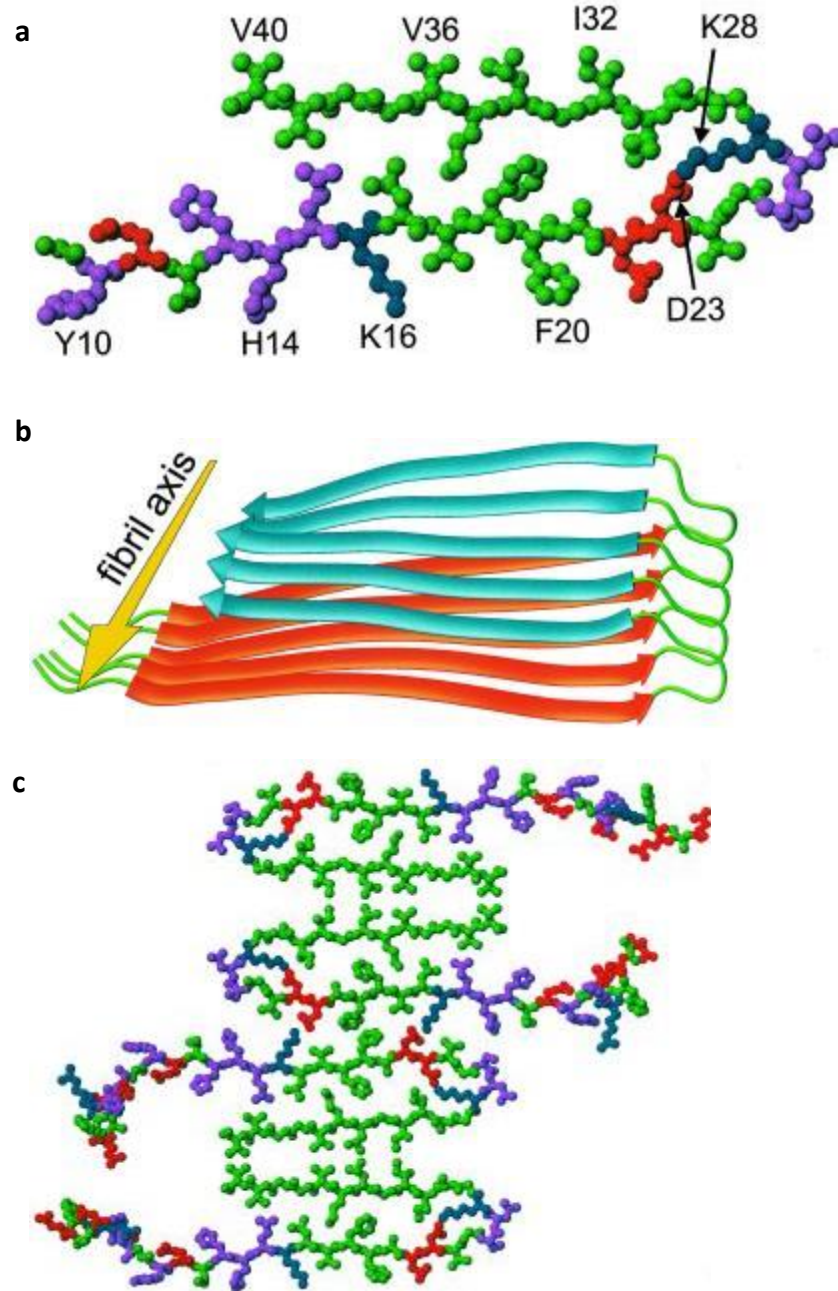


**Figure 3.1. Petkova et al. model of A $\beta$  secondary structure and potential fibrillar interaction.**<sup>48</sup> (a) Depicts the secondary structure of a single cross  $\beta$ -sheet unit of A $\beta$ , residues 1-8 are structurally disordered and not shown, while residues 12-24 and 30-40 adopt  $\beta$ -strand conformations and form parallel  $\beta$ -sheets by hydrogen bonding. (b) Depicts the proposed binding of A $\beta$  through hydrogen bonding, forming fibrils that contain two cross- $\beta$  units with their hydrophobic faces juxtaposed. (c) Depicts the proposed model of fA $\beta$  association, formed by juxtaposing the hydrophobic faces of two cross- $\beta$  units.

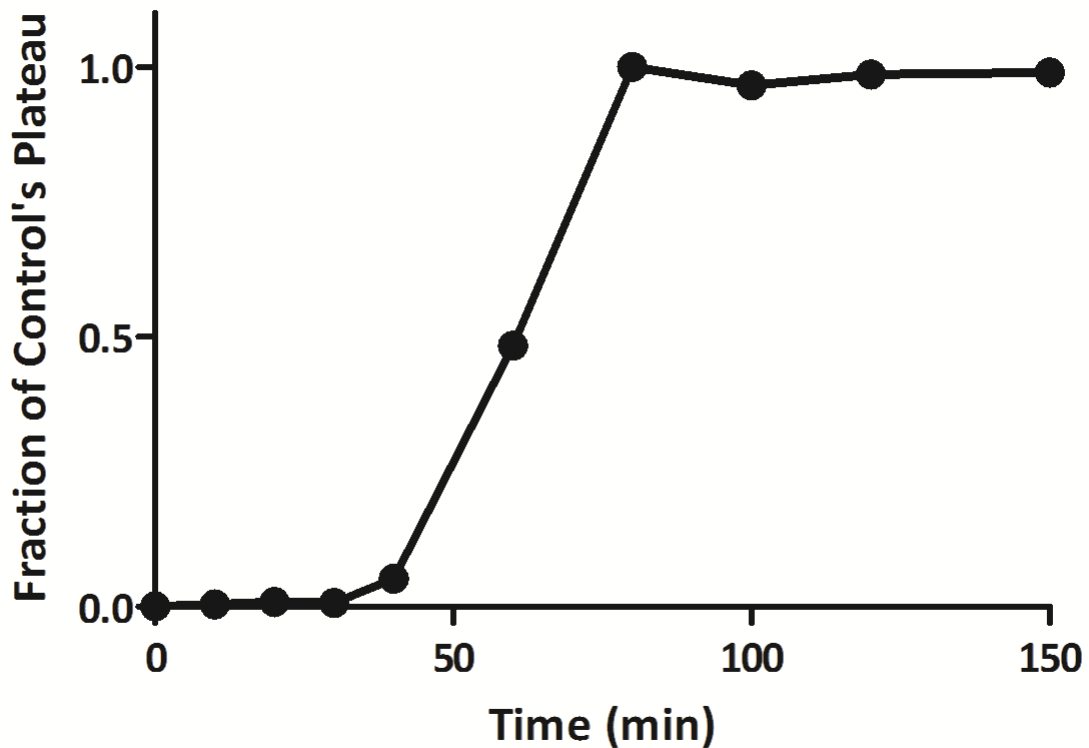


**Figure 3.1. A $\beta$ 1-40 monomer aggregation.** A $\beta$ 1-40 monomer aggregation exhibits three stages: the lag period, a rate limiting step where oligomerization occurs; the growth phase, a period of soluble aggregate growth through elongation and association into fA $\beta$ ; and a plateau phase, where insoluble fA $\beta$ , soluble aggregates, and oligomers are in equilibrium.

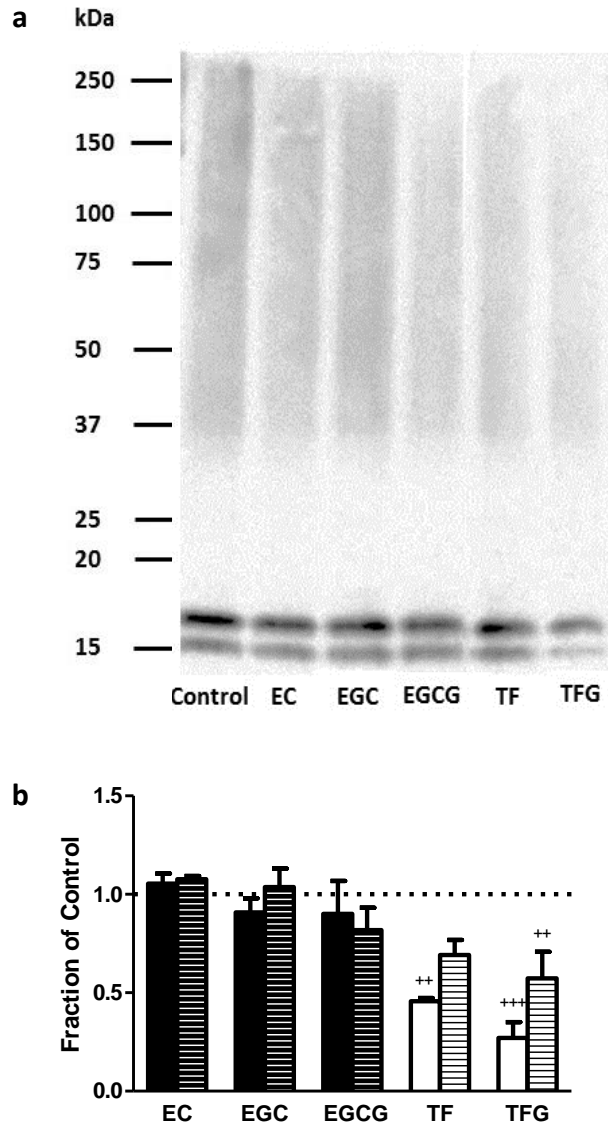


**Figure 3.3. Ability of catechins and theaflavins to inhibit A $\beta$ <sub>1-42</sub> oligomer formation.** A $\beta$ <sub>1-42</sub> is incubated alone (control, indicated by dashed line at one) or in the presence of catechins, or theaflavins prior to dilution. Oligomerization is initiated via the dilution of DMSO-solubilized A $\beta$ <sub>1-42</sub> in 12 mM phosphate containing 1 $\mu$ M NaCl to final concentrations of 15  $\mu$ M A $\beta$ <sub>1-42</sub>, 1% DMSO, 150  $\mu$ M polyphenol. **(a)** A $\beta$ <sub>1-42</sub> oligomer products resolved by SDS-PAGE using a 4-20% Tris-glycine gel were transferred to nitrocellulose membrane and probed with 6E10 antibody. **(b)** Volumetric analysis was performed for oligomer sizes of 100-250 kDa (solid bars) and 25-100 kDa (striped bars). Error bars represent SEM n=3-4. \*p<0.05, \*\*p<0.01, \*\*\*p<0.001 for sample versus control.

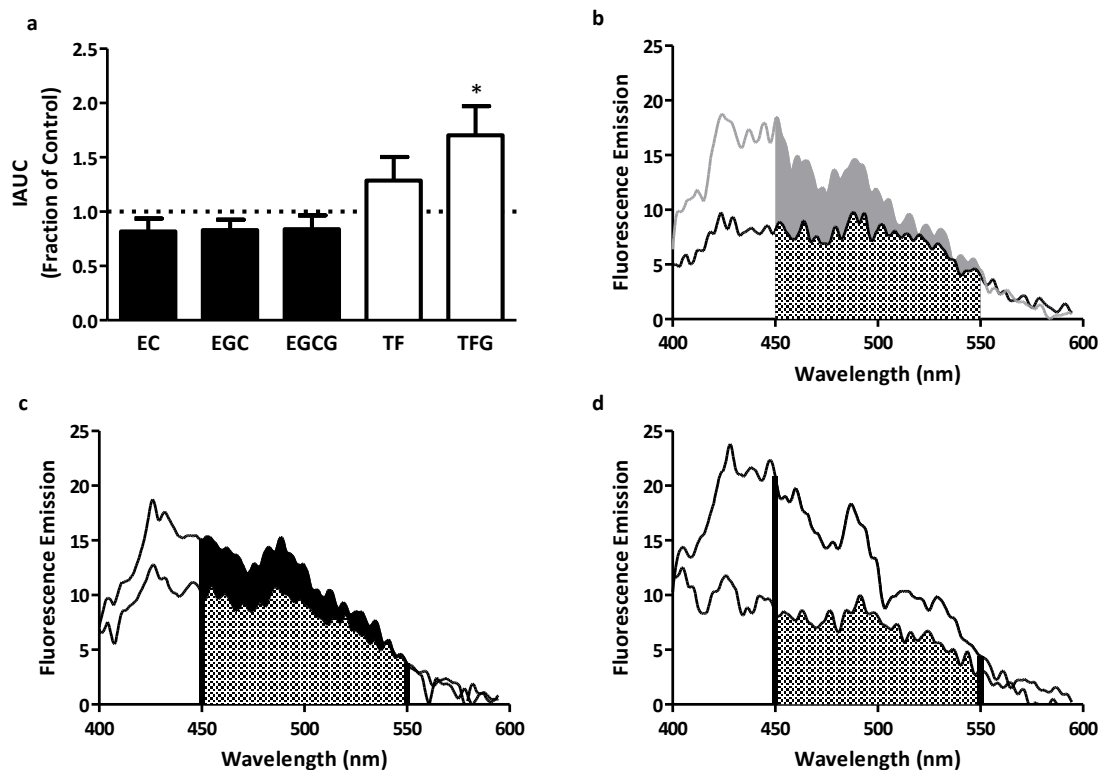


**Figure 3.4. Altered conformation of A $\beta$ 1-42 oligomers confirmed by ANS.** A $\beta$ <sub>1-42</sub> oligomers were prepared as in Figure 3.3 and were incubated alone (control, indicated by dashed line at one) or in the presence of catechins (closed bars), or theaflavins (open bars). Oligomers were diluted with ANS for a final concentration of 1  $\mu$ M A $\beta$ , 10  $\mu$ M polyphenol, and 100  $\mu$ M ANS. ANS emission data is shown for the control (**panel b**), EGC (**panel c**), and TFG (**panel d**). (a) Fluorescence was determined as the IAUC (450-550 nm) (solid area) following blank subtraction (pattern area) and normalized to the control. Parameters are expressed as mean  $\pm$  SEM, n=3. \*p < 0.05 for sample versus control.



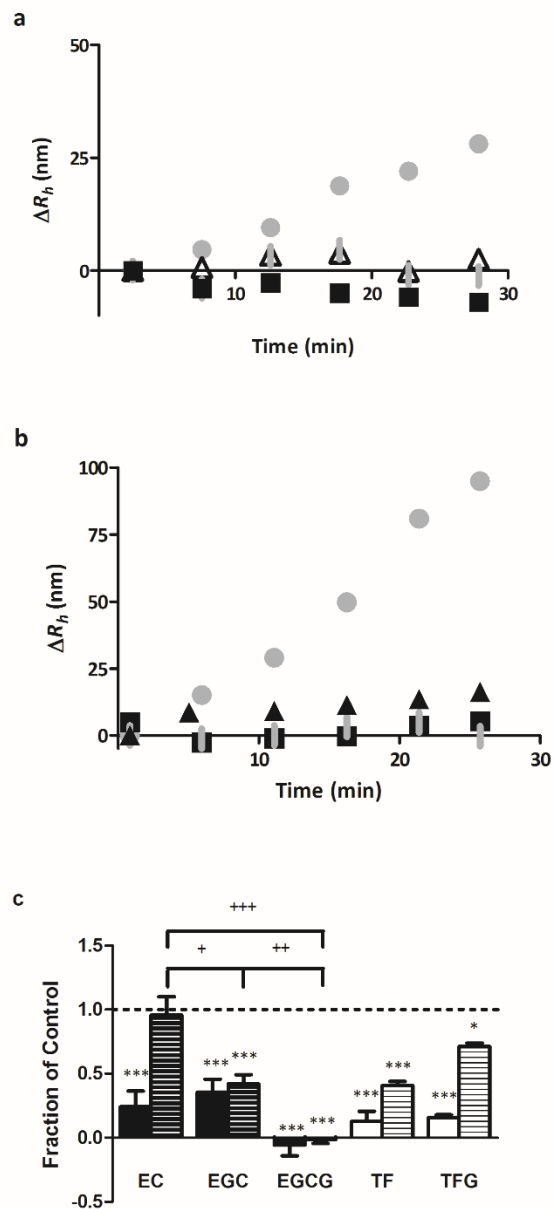


**Figure 3.5. Effect of catechins and theaflavins on soluble A $\beta$ <sub>1-40</sub> aggregate growth.** 2  $\mu$ M A $\beta$ <sub>1-40</sub> soluble aggregates in 40 mM Tris-HCl (pH 8.0), was incubated alone (control, ●), or in the presence of 50  $\mu$ M EC, EGC (▲), EGCG (■), TF or TFG (△). Elongation (**panel a**) and association (**panel b**) were initiated by the addition of 30  $\mu$ M A $\beta$ <sub>1-40</sub> monomer and 150 mM NaCl, respectively. Native soluble A $\beta$ <sub>1-40</sub> aggregate incubated alone and in the absence of monomer or NaCl served as a negative control (■). Samples were monitored by the DLS for  $R_h$ . The rate of soluble aggregate growth was determined by linear regression. Results are expressed as fraction of control (control indicated by the dashed line at 1); elongation (solid bars) and association (pattern bars) (**panel c**). Error bars represent SEM, n=3-4. \*p<0.05, \*\*\*p<0.001 sample versus control. +p<0.05, ++p<0.01, and +++p<0.001 between samples.

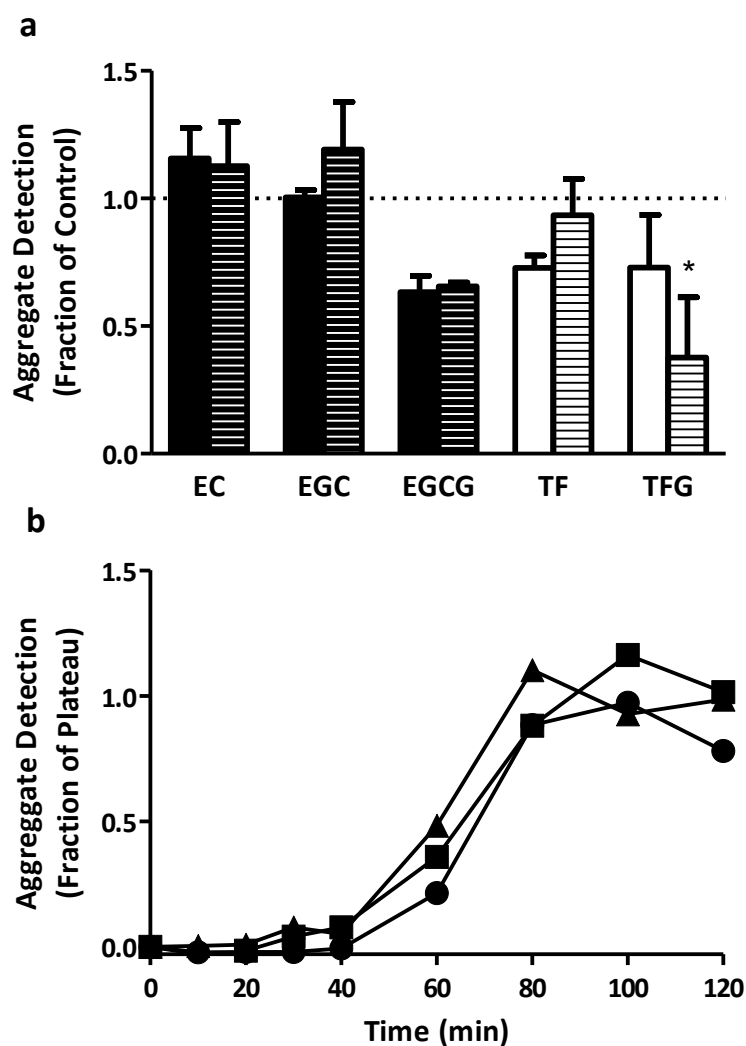


**Figure 3.6. Comparison of different A $\beta$ <sub>1-40</sub> monomer aggregation monitoring techniques.** (a) For ThT analysis, fA $\beta$ <sub>1-40</sub> was diluted to the equivalent of loading 15  $\mu$ L A $\beta$  monomer aggregation assay (1:5 molar ratio of A $\beta$ : polyphenol) into 140  $\mu$ L 10  $\mu$ M ThT, for a final concentration of 1.93  $\mu$ M fA $\beta$  in 40 mM Tris-HCl (pH 8.0), 9.67  $\mu$ M polyphenol or solvent (control), and 9.03  $\mu$ M ThT (solid bars). For LOC analysis fA $\beta$ <sub>1-40</sub> were diluted to 10  $\mu$ M in 40mM Tris-HCl (pH 8.0) in the absence (control) or presence of 100  $\mu$ M catechins or theaflavins. Each sample was dotted on 0.1  $\mu$ M nitrocellulose paper right before and after the catechin or theaflavin was added. Each dot was evaluated by densitometric analysis using LOC antibody detection (pattern bars). All samples were quantified and reported as a fraction of the control (control indicated by the dashed line at one). SEC-purified A $\beta$ <sub>1-40</sub> monomer was diluted to 20  $\mu$ M in 40 mM Tris-HCl (pH 8.0) containing 150 mM NaCl, the sample was then vortexed at 500 rpm. The amount of aggregation was monitored by three techniques simultaneously. 1) ThT fluorescence using the area under the curve from 470-500 nm (■, panel b), this was accomplished by combining 140  $\mu$ L of 10  $\mu$ M ThT dye with 10  $\mu$ L of the sample. 2) LOC, large A $\beta$  aggregate antibody, each dot was quantified by densitometric analysis (●, panel b). 3) DLS intensity (▲, panel b). All monitoring techniques are displayed as fraction of control's plateau (panel b). Error bars represent SEM, n=3. \*p<0.05.

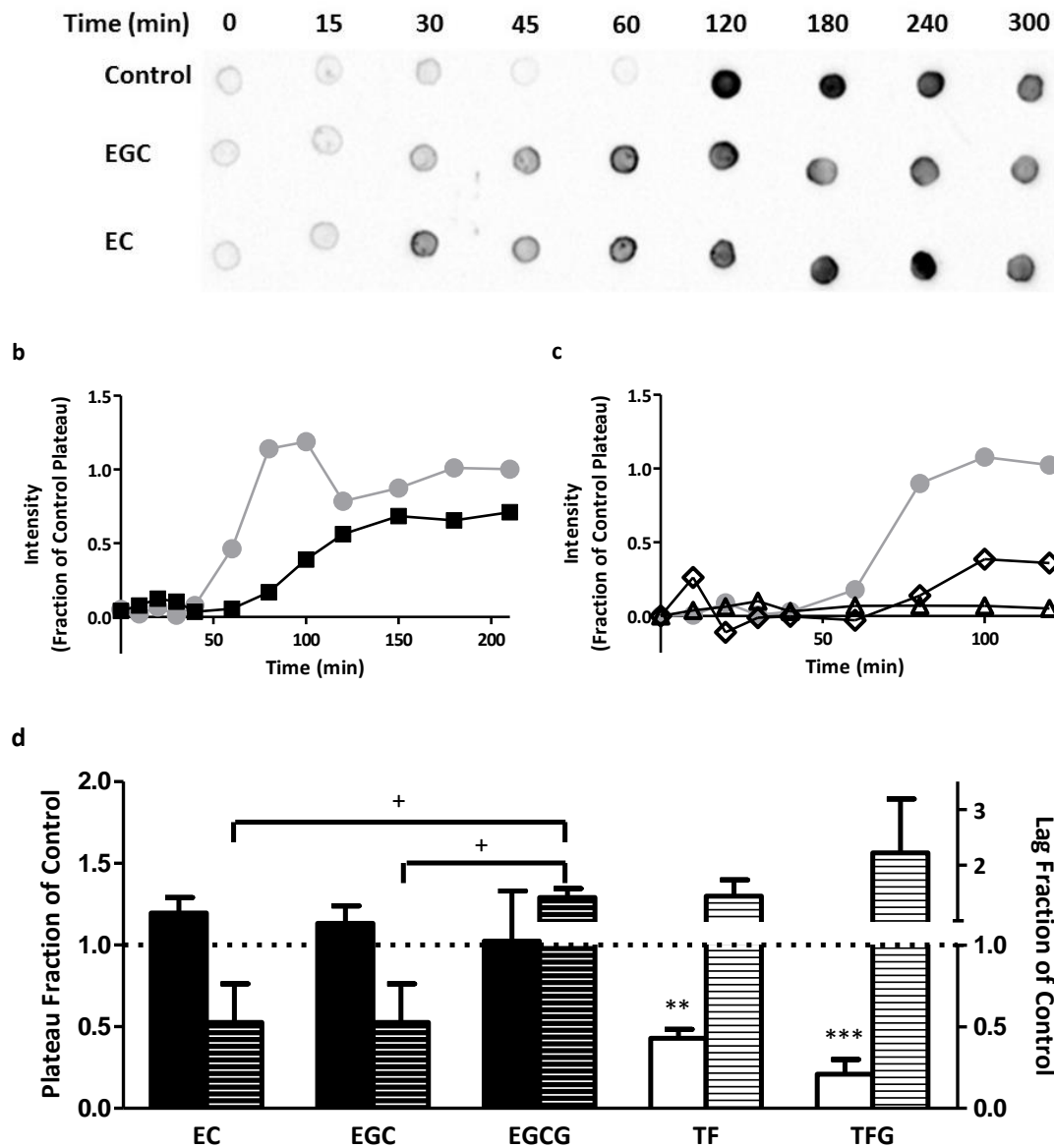


**Figure 3.7. Effect of catechins and theaflavins on A $\beta$ <sub>1-40</sub> monomer aggregation.** SEC-purified A $\beta$ <sub>1-40</sub> monomer was diluted to 20  $\mu$ M in 40mM Tris-HCl (pH 8.0) containing 150 mM NaCl, samples were vortexed at 500 rpm alone (control, ●) or in the presence of 100  $\mu$ M EC, EGC, EGCG (■) (**panel a and b**), TF (◇), or TFG (△) (**panel c**). Extent of aggregation, for the EC and EGC, was evaluated via dot blot by LOC antibody detection. Each dot was quantified (**panel a**) and reported as the fraction of control plateau (**panel d**). The extent of aggregation, for EGCG (**panel b**) and theaflavins (**panel c**) were monitored via the intensity of DLS readings and graphed as fraction of control plateau. Values were determined by averaging the plateau values of the control and sequentially dividing all samples values by this average. All compounds' inhibitory capabilities were expressed as fraction of control (control indicated by dashed line at one) and evaluated for plateau reduction (solid bars) and lag extension (pattern bars) (**panel d**). Error bars represent SEM, n=3-4. \*\*p<0.01, \*\*\*p<0.001 sample versus control; †p<0.05, THP grouped comparison; †p<0.05, between samples.

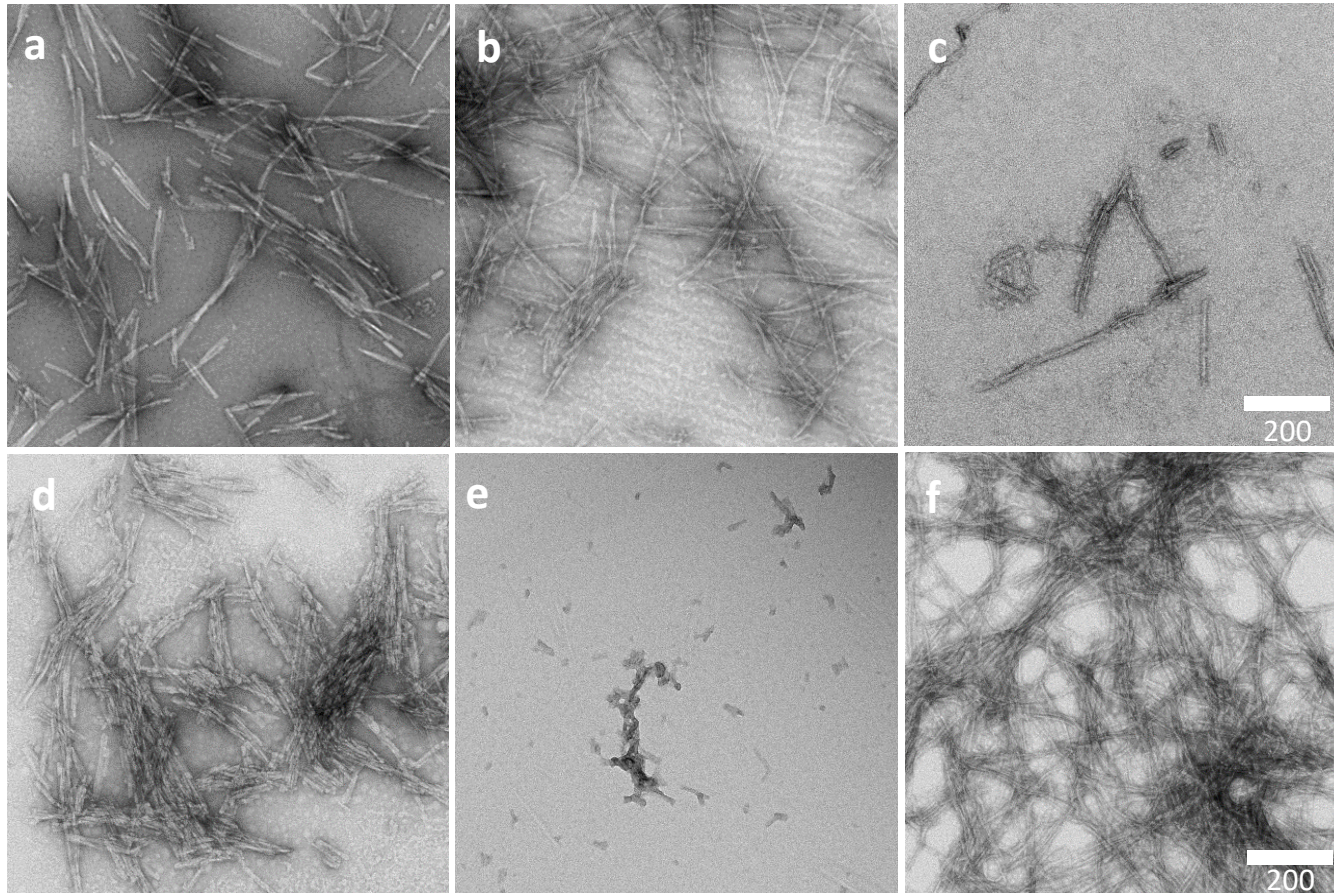


**Figure 3.8. Morphology of A $\beta$ <sub>1-40</sub> aggregates formed in presence of catechins and theaflavins.** Samples are composed of SEC-purified A $\beta$ <sub>1-40</sub> monomer diluted to 20  $\mu$ M in 40 mM Tris-HCl (pH 8.0) containing 150 mM NaCl, incubated under agitation alone (control, **f**) or in the presence of 100  $\mu$ M catechin or theaflavin, EC (**a**), EGC (**b**), EGCG (**c**), TF (**d**), and TFG (**e**). Extent of monomer aggregation was evaluated by negative staining at a point in the equilibrium plateau. All samples were analyzed by TEM at 25 K magnification and are shown relative to a scale bar of 200 nm.

CHAPTER 4: GREEN TEA CATECHINS AND BLACK TEA THEAFLAVINS ALTER KEY RNA  
EXPRESSION IN ALZHEIMER'S DISEASE

**4.1 Introduction**

The amyloid cascade hypothesis pinpoints the amyloidogenic cleavage of APP as the initial step in the pathogenesis of AD. Because of the limited expression of APP within the cell membrane, the amyloidogenic and non-amyloidogenic pathways compete for substrate in the process of APP proteolysis.<sup>66,68</sup> In the amyloidogenic pathway, APP is cleaved sequentially by BACE1 and  $\gamma$ -secretase to produce sAPP $\beta$  and A $\beta$ . Alternatively, in the non-amyloidogenic pathway, APP is sequentially cleaved by  $\alpha$ -secretase and  $\gamma$ -secretase to produce sAPP $\alpha$  and  $\alpha$ -CTF, or C83 (Figure 4.1). Intense focus has been given to the investigation of APP proteolysis and A $\beta$  amyloidogenic aggregation as possible targets for AD therapy. This aim will investigate the capabilities of catechins and theaflavins to alter the A $\beta$ <sub>1-42</sub> oligomer-induced expression of key RNAs in AD.

A $\beta$ <sub>1-42</sub> oligomers can act as cell stressors altering key RNA expression and upsetting the precarious balance of APP proteolytic cleavage.<sup>42</sup> A $\beta$ <sub>1-42</sub> oligomers cause the upregulation of lncRNA antisense transcript for BACE1 (BACE1-AS), resulting in a rapid feed forward mechanism of BACE1 upregulation.<sup>42,41,69,70</sup> BACE1-AS levels have been shown to be elevated in individuals with AD. As an antisense transcript, BACE1-AS has a complementary nucleotide sequence to BACE1 mRNA. When these complimentary sequences bind, BACE1 mRNA is stabilized and its transcription promoted. BACE1, as the

rate limiting enzyme of APP cleavage,<sup>69</sup> when increased shifts the balance of APP cleavage towards the amyloidogenic pathway.<sup>71</sup>

A disintegrin and metalloproteinase (ADAM) family encompasses approximately 40 known ADAMs. Of those 40, 12 are catalytically active ADAMS that have the potential to mediate the proteolytic cleavage of cell surface integral membrane proteins within their juxtamembrane regions, releasing a soluble protein ectodomain into the extracellular spaces.<sup>72</sup> This process is commonly known as ectodomain shedding, making the ADAMs involved often referred to as sheddases.<sup>72</sup> ADAM9, ADAM10, and ADMAM17 are type 1 transmembrane glycoproteins responsible for ectodomain shedding and possess  $\alpha$ -secretase activity capable of proteolytic cleavage of APP.<sup>72-74</sup> While ADAM9, ADAM10, and ADAM 17 are putative  $\alpha$ -secretases, the most prominent ADAM to exhibit  $\alpha$ -secretase activity is ADAM10.<sup>75,76</sup> An alternative to the main strategy of therapeutic research in AD, development of A $\beta$  aggregation inhibitors, is the production of non-amyloidogenic pathway promoters, including upregulation of ADAM9, ADAM17, and ADAM10.

As an alternative to reducing the amyloidogenic pathway or promoting the non-amyloidogenic pathway, A $\beta$  production can be attenuated through reduction of APP or  $\gamma$ -secretase. By reducing either or both of these proteins, resources for the production of the amyloidogenic peptide A $\beta$  are limited.  $\gamma$ -secretase is a multi-subunit membrane-embedded protease complex, comprised of 4 integral membrane proteins: presenilin1 (PS1) or PS2, nicastrin, Aph-1 (anterior pharynx-defective 1), and Pen-2 (presenilin enhancer 2).<sup>77</sup> PS1 or PS2 acts as the catalytic subunit, while the other members allow for



stabilization and maturation of the  $\gamma$ -secretase complex. Since the 1995 identification of the involvement of PSEN1 and PSEN2 (PS1 and PS2 genes, respectively) mutations with familial AD, the inhibition of  $\gamma$ -secretase has been investigated as a potential therapeutic strategy.<sup>78-80</sup>  $\gamma$ -secretase inhibitors also block the proteolytic cleavage of the Notch receptor resulting in *in vivo* toxicity, thus undermining the inhibition of  $\gamma$ -secretase as a reliable therapeutic.<sup>79</sup> Alternatively, compounds that modulate versus inhibit  $\gamma$ -secretase possess greater therapeutic potential for AD. As a key catalytic subunit, this aim focuses on PS1 mRNA expression in relation to potential  $\gamma$ -secretase alterations.

The consumption of green tea and black tea is becoming widely regarded for its diverse health benefits. Epidemiological<sup>28-30</sup> and therapeutic research<sup>20,27,35,55,57-60</sup> of green tea and black tea components attribute the primary health benefits of the beverages to their respective composition of monomeric catechin polyphenols and their phenolic oligomers, theaflavins. Research from Chapter 3 divulged the ability of catechins and theaflavins to inhibit A $\beta$  aggregation, but that approach focuses upon only one of the avenues in which they can interfere with the amyloidogenic pathway of AD. This aim expands the knowledge of catechins and theaflavins as potential therapeutics by investigating their ability to alter the processing of APP to release A $\beta$ . In this aim, the capability of catechins and theaflavins to alter A $\beta$ <sub>1-42</sub> oligomer-induced expression of key AD-associated mRNAs was determined.

## 4. 2 Materials and Methods

### 4. 2. 1 Materials

XTT was purchased from Sigma-Aldrich (St. Louis, MO). OxiSelect™ Oxygen Radical Antioxidant Capacity (ORAC) activity assay was purchased from Cell BioLabs (San Diego, CA). N-methyl dibenzopyrazine methyl sulfate (PMS) and E.Z.N.A. Total RNA isolation kit I were purchased from VWR (Radnor, PA). Random Primers, MgCl<sub>2</sub>, dNTP, and GoScript Reverse Transcriptase were purchased from Promega (Madison, WI). RNase Inhibitor (human placenta) was purchased from New England BioLabs Inc. (Ipswich, MA). PowerUp SYBR Green Mater Mix was obtained from ThermoFisher Scientific (Waltham, MA). Ki67, APP, PS1, BACE1, ADAM9, ADAM10, and β-actin RNA primers were purchased from Integrated DNA Technologies (Coralville, IA); sequences can be found in Table 4.1.

### 4. 2. 2 Evaluation of the Effect of Catechins and Theaflavins on Cell Viability

To ensure that catechins and theaflavins do not induce cytotoxicity, an XTT assay was used to evaluate the effect of catechins and theaflavins on the viability of SH-SY5Y human neuroblastoma cells. The XTT cell viability assay is a colorimetric assay that detects cellular metabolic activity. In the assay, the yellow tetrazolium salt, XTT, is reduced to a highly colored formazan dye by dehydrogenase enzymes in cells that are metabolically active. This conversion only occurs in viable cells, creating an inverse correlation between the amount of formazan produced and cellular toxicity. In a 96-well plate, cells were seeded at 50,000 cells/well and allowed to settle and adhere (24 h) in a 1:1 mixture of Ham's F12K medium and DMEM. Medium was supplemented with 10% FBS, 100 units/mL penicillin, and 100 µg/mL streptomycin. All cultures were maintained at 37°C in a humid



atmosphere of 5% CO<sub>2</sub> and 95% air. Seeded wells were then incubated in the absence (negative control) or presence of 20 µM polyphenol or 0.2% Triton-X (positive control) for 30 min. Wells were then treated with XTT in conjunction with PMS, an electron coupling reagent that significantly improves the efficiency of XTT transport into cells, for 24 h. Metabolically active cells, viable cells, produce dehydrogenase enzyme reducing XTT to highly colored formazan shifting the absorbance. The absorbance was analyzed at 450 nm. Results are expressed as fraction of control, and catechins and theaflavins were classified as nontoxic if their levels of XTT reduction were not statistically lower than the negative control.

#### *4. 2. 3 Evaluation of Catechins' Antioxidant Capacity*

An oxygen radical antioxidant capacity (ORAC) activity assay was utilized to evaluate the antioxidant capacity of catechins. The ORAC activity assay utilizes a fluorescein probe that is oxidized by peroxy radicals produced by free radical initiators. As the probe is oxidized over time, the fluorescence is quenched. The presence of an antioxidant compound prolongs the quenching of the fluorescence by blocking the peroxy radical oxidation until the antioxidant activity in the sample is depleted. 1 µM catechin was combined with the 1 X fluorescein solution (30 min) followed by the addition of the free radical initiator. The samples were then immediately evaluated for fluorescence at an excitation and emission of 480 and 520 nm, respectively, for 90 min at 1 min intervals. This allowed the assay to be monitored to completion, or until depletion of the fluorescence. The data was graphed as absorbance versus time, and the area under the curve was determined and compared to the standard curve of Trolox, vitamin E analog

(a known good antioxidant), to assess the ORAC value. Results are expressed as ORAC value in comparison to Trolox ORAC value of one.

#### 4. 2. 4 *SH-SY5Y Cell Culturing for PCR experiments*

Human neuroblastoma SH-SY5Y cells were seeded in a 6-well plate at 1,000,000 cells/well in 10% FBS and allowed to settle and adhere (24 h) in a 1:1 mixture of Ham's F12K medium and DMEM. Medium was supplemented with 10% FBS, 100 units/mL penicillin, and 100 µg/mL streptomycin. All cultures were maintained at 37°C in a humid atmosphere of 5% CO<sub>2</sub> and 95% air. Cell treatments were diluted in 1 mL of 1% FBS, 10 units/mL penicillin, and 10 µg/mL streptomycin before being added to cells. Cell treatments included untreated cells and cells treated with vehicle (containing DMSO and H<sub>2</sub>O solvent substituted for Aβ and polyphenols, respectively) which served as negative controls. SH-SY5Y cells were treated for 72 h; to prevent cell apoptosis via starvation, 1 mL of 1% FBS was added every 24 h after the initial PCR treatment.

#### 4. 2. 5 *PCR Treatment*

Before the capabilities of catechins and theaflavins to alter the Aβ<sub>1-42</sub> oligomer-induced expression of mRNAs were determined, the effect of excess catechins and theaflavins alone was evaluated. Catechins and theaflavins were dissolved in filtered dH<sub>2</sub>O to 3 mM before dilution to a final concentration of 10 µM polyphenol in 1% FBS media for cell treatment.

The ability of catechins and theaflavins to alter the Aβ<sub>1-42</sub> oligomer induced expression of AD-associated mRNAs through antiaggregation, antioxidant, and synergistic capabilities was analyzed via three treatments, respectively: oligomers were made in the

presence of polyphenols, native oligomers were combined with excess polyphenol, and oligomers were made in the presence of polyphenols combined with an excess of polyphenols. All results were normalized to the vehicle treatment.

Catechins and theaflavins were evaluated for their capability to alter  $A\beta_{1-42}$  oligomer-induced expression of key AD-associated mRNAs through their ability to alter oligomerization, including alterations of oligomer size distribution and conformation.  $A\beta_{1-42}$  oligomers, described in Section 2.6, were made in the absence (control) or presence of a 1:10 molar ratio of catechins or theaflavins. Following oligomerization, oligomers were immediately diluted to a final concentration of 0.1  $\mu\text{M}$   $A\beta_{1-42}$  and 0  $\mu\text{M}$  (control) or 1  $\mu\text{M}$  polyphenol in media containing 1% FBS.

The antioxidant capabilities of catechins and theaflavins to alter  $A\beta_{1-42}$  oligomer-induced expression of key AD-associated mRNAs were also evaluated.  $A\beta_{1-42}$  oligomers, described in Section 2.6, were made in the absence of catechins or theaflavins. Following oligomerization,  $A\beta_{1-42}$  oligomers were immediately diluted to a final concentration of 0.1  $\mu\text{M}$   $A\beta_{1-42}$  oligomers in 1% FBS media, containing 0  $\mu\text{M}$  (control) or 10  $\mu\text{M}$  polyphenol.

Finally, catechins and theaflavins were evaluated for their ability to modify  $A\beta_{1-42}$  oligomer-induced expression of key AD-associated mRNAs through synergistic capabilities, including both inhibition of oligomerization and antioxidant capabilities, simultaneously. For this treatment,  $A\beta_{1-42}$  oligomers, described in Section 2.6, were made in the presence of a 1:10 molar ratio of catechins or theaflavins. Following oligomerization,  $A\beta_{1-42}$  oligomers were immediately diluted to a final concentration of 0.1

$\mu\text{M}$   $\text{A}\beta_{1-42}$  oligomers and 0  $\mu\text{M}$  (control) or 1 $\mu\text{M}$  polyphenol in 1% FBS media, containing 0  $\mu\text{M}$  (control) or 10  $\mu\text{M}$  polyphenol.

#### 4. 2. 6 Isolation and Quantification of RNA

E.Z.N.A. RNA isolation kit I was utilized for total RNA isolation following 72 h treatment. Treatment media was aspirated, and cells were immediately lysed with TRK Lysis Buffer and scraped from their culture. Cell isolates were homogenized before being precipitated with 70% EtOH via agitation (1200 rpm, 1.5 min). Total lysate was spun through a HiBind RNA Mini column, trapping only the RNA within the filter. The RNA was washed with 500  $\mu\text{L}$  of RNA Wash Buffer I once, followed by two 500  $\mu\text{L}$  washes with RNA Wash Buffer II (twice) via column centrifugation. RNA was isolated from the column via incubation (5 min) in DNase free  $\text{H}_2\text{O}$  (70°C). Isolated RNA was diluted 1:50 in 10 mM Tris-HCl (pH 8.0) containing 1 mM EDTA (TE buffer). Isolated RNA concentrations were determined using absorbance at 260 nm, measured on a Life Science UV/Vis Spectrophotometer DU 730 (Beckman Coulter, Brea, CA), and an extinction coefficient of 0.025 [(mg/ml)<sup>-1</sup>cm<sup>-1</sup>]. Purity of the sample was determined by the ratio of the nucleic acid absorbance to the protein absorbance (A260/A280). Only samples having a ratio between 1.8 and 2.1 were used for PCR. Isolated RNA was stored at -80°C for up to 1 year.

#### 4. 2. 7 Determination of Relative RNA Expression via qRT-PCR

Reverse transcription was first initiated by the dilution of RNA to 1  $\mu\text{g}$  and addition of 1  $\mu\text{g}$  of random primers in DNase free  $\text{H}_2\text{O}$  for a total volume of 12  $\mu\text{L}$ . RNA-random primer mixture was heated for 5 min at 90°C before incubation (30 min) on ice. 4  $\mu\text{L}$  of Reverse Transcriptase buffer, 2  $\mu\text{L}$  of  $\text{MgCl}_2$ , 1  $\mu\text{L}$  dNTP, 1  $\mu\text{L}$  RNase Inhibitor, and 1  $\mu\text{L}$

Reverse Transcriptase were added to the RNA-random primer mixture for final concentrations of 47.62  $\mu\text{M}$  RNA, 47.62  $\mu\text{M}$  random primers, 2.38 mM  $\text{MgCl}_2$ , 0.476 mM dNTP, 40 U RNase inhibitor, and 1 U reverse transcriptase in reverse transcriptase buffer. The reverse transcriptase mixture was then incubated (1 h) at 42°C before temperature was increased to 92°C (10 min). cDNA produced was diluted 1:2 with DNase free  $\text{H}_2\text{O}$  and stored at -20°C until further use, up to 2 months.

Upon arrival, forward and reverse primers of Ki67, APP, PS1, ADAM9, ADAM10, BACE1, and  $\beta$ -actin were diluted to 100  $\mu\text{M}$  with TE buffer and stored at 4°C (Table 4.1). qRT-PCR was performed in triplicate for each sample and primer, with a  $\beta$ -actin reference sequence on each plate. The qRT-PCR contained a final concentration of 2  $\mu\text{M}$  forward primer, 2  $\mu\text{M}$  reverse primer, and 25 ng cDNA in DNase free  $\text{H}_2\text{O}$  and 5  $\mu\text{L}$  PowerUp SYBR Green Master Mix for a final volume of 10  $\mu\text{L}$ . Samples were loaded into a DNase free 96 well plate and placed into the CFX96 Real-Time System and C1000 Thermal Cycler (Bio-Rad, Hercules, CA). Using Bio-Ras CFX Manager 3.1 the instrument was programed to the following parameters for all mRNAs: 95°C (4 min); 40 cycles of the sequence 95°C (30 sec), 56°C (30 sec), and 72°C (30 sec); 72°C (5 min); and a melting curve. A comparative threshold cycle ( $C_t$ ) was determined for each reference sequence. For each sample, the reference sequence  $C_t$  values were normalized using Equation 4.1. Samples were then normalized to the control using Equation 4.2. Relative mRNA expression levels are reported as an n-fold difference of the sample to vehicle.

$$\Delta C_t = C_{t_{\text{sample}}} - C_{t_{\beta\text{-actin}}} \quad \text{Equation 4.1}$$

$$\Delta\Delta C_t = \Delta C_{t_{\text{sample}}} - \Delta C_{t_{\text{vehicle}}} \quad \text{Equation 4.2}$$

### 4.3 Results

#### 4.3.1. Catechins and Theaflavins do not Significantly Alter Cell Viability

The ability of catechins and theaflavins to alter cell viability was determined by their ability to reduce XTT to a highly colored formazan dye by dehydrogenase enzymes, found only in metabolically active cells. Treatment with catechins and theaflavins alone resulted in formazan dye absorbance similar to the vehicle (Figure 4.2), indicated that the presence of catechins and theaflavins do not alter the viability of cells.

#### 4.3.2. Catechins Exhibit Antioxidant Capacity

Catechins antioxidant capacities were determined via an ORAC activity assay. Antioxidant capabilities were evaluated as the polyphenol's ability to delay decay of the fluorescent probe by free radicals in relation to Trolox, a vitamin E analog. EGC and EGCG exhibited capabilities similar to Trolox, and EC expressed significantly increased antioxidant capacity compared to Trolox (Figure 4.3).

#### 4.3.3. Catechins and Theaflavins have Negligible Effect on Key AD-associated mRNA Expressions

To ensure accurate interpretation of catechins and theaflavins capability to alter A $\beta$ <sub>1-42</sub> oligomer-induced expression of key AD-associated mRNAs, their effect on the mRNAs in the absence of A $\beta$  oligomers was determined. Utilizing the highest polyphenol treatment concentration employed, the effect of 10  $\mu$ M polyphenol treatment (72h) on the RNA expression of Ki67, APP, PS1, ADAM9, ADAM10, and BACE1 was determined (Figure 4.4). Results display no significant change in mRNA expression relative to the

vehicle treatment, displaying that catechins and theaflavins alone have negligible effect on the expression of key AD-associated mRNAs investigated.

#### 4. 3. 4. *A $\beta$ <sub>1-42</sub> Oligomers have Negligible Effect on Ki67 mRNA*

Ki67 protein is a marker for cell proliferation,<sup>69</sup> Ki67 mRNA was utilized to determine if cellular treatments resulted in altered cell proliferation.<sup>41</sup> Results represent Ki67 mRNA expression for antiaggregation treatment (Figure 4.5a) and antioxidant treatment (Figure 4.5b), as explained in Section 4.2.5. Ki67 mRNA expression was unchanged by the presence of native or catechin and theaflavin modified A $\beta$ <sub>1-42</sub> oligomers, confirming that these treatments do not alter proliferation of SH-SY5y cells.

#### 4. 3. 5. *Catechins Alter A $\beta$ <sub>1-42</sub> Oligomer-induced Expression of APP mRNA*

APP, a type 1 transmembrane protein, has the potential to undergo proteolytic cleavage by BACE1 and  $\gamma$ -secretase to produce the amyloidogenic peptide A $\beta$ . A $\beta$  a known cell stressor, at concentrations of 0.1  $\mu$ M native A $\beta$ <sub>1-42</sub> oligomers resulted in the upregulation of APP mRNA expression (Figure 4.6). Catechins and theaflavins were investigated for their ability to attenuate this oligomer-induced upregulation of APP mRNA. This upregulation was attenuated via EGCG antiaggregation (Figure 4.6a) capability and EGC antioxidant (Figure 4.6b) capability. In fact, mRNA levels for these treatments were maintained slightly below that of the vehicle.

#### 4. 3. 6. *Catechins and Theaflavins Fail to Downregulate PS1 mRNA Expression*

mRNA of PS1, the catalytic activity subunit of the  $\gamma$ -secretase complex, was used in reference to potential reduce  $\gamma$ -secretase activity, limiting the amyloidogenic cleavage of APP. Native A $\beta$ <sub>1-42</sub> oligomers and modified oligomers formed in the presence of

catechins and theaflavins did not significantly downregulate PS1 mRNA expression (Figure 4.7a). Alternatively, oligomers modified via TFG antioxidant capabilities resulted in the upregulated of PS1 mRNA (Figure 4.7b).

#### *4. 3. 7. Catechins Modified A $\beta$ Oligomers to Upregulate ADAM10 mRNA, but not ADAM9 mRNA Expression*

ADAM9 and ADAM10, sheddases with  $\alpha$ -secretase activity, can cleave APP to promote the non-amyloidogenic pathway. Thus, shift the balance away from the amyloidogenic pathway. The presence of native A $\beta$ <sub>1-42</sub> oligomers did not result in altered ADAM9 (Figure 4.8) or ADAM10 (Figure 4.9) mRNA expression. Additionally, modification of oligomers by catechin and theaflavin antiaggregation (Figure 4.8a) and antioxidant (Figure 4.8b) capabilities failed to alter expression of ADAM9 mRNA. Similarly, catechin and theaflavin antioxidant (Figure 4.9b) capabilities failed to alter ADAM10 mRNA, but through modulation of oligomerization (Figure 4.9a), EGC and EGCG upregulated ADAM10 mRNA.

#### *4. 3. 8. Catechins Attenuate A $\beta$ <sub>1-42</sub> Oligomer-induced Expression of BACE1 mRNA*

Sequential cleavage of APP by BACE1 and  $\gamma$ -secretase results in the production of the amyloidogenic peptide A $\beta$ . Data has previously identified A $\beta$  as cell stressor, capable of upregulating BACE1 mRNA expression.<sup>41,69</sup> Results in this aim show congruent capabilities with the presence of native A $\beta$ <sub>1-42</sub> oligomers resulting in the significant upregulation of BACE1 mRNA (Figure 4.10). All catechins investigated were able to attenuate the oligomer-induced upregulation of BACE1 mRNA through antiaggregation



capabilities (Figure 4.10a), maintaining vehicle-like expression levels. In contrast, theaflavin modified oligomers still expressed significant upregulation of BACE1 mRNA.

The antioxidant capacity of catechins and theaflavins to attenuate the oligomer-induced upregulation of BACE1 mRNA show, that only EC possesses the ability to attenuate the BACE1 mRNA upregulation (Figure 4.10b), resulting in expression levels similar to the vehicle. EGCG and TF displayed no antioxidant effect towards the reduction of oligomer-induced upregulation of BACE1 mRNA, exhibiting significantly upregulated BACE1 mRNA congruent to native oligomers.

Due to the individual antiaggregation and antioxidant capabilities of catechins and theaflavins, a synergistic treatment was performed to assess their combined antiaggregation and antioxidant potential. Synergistic results of EC express continued attenuation of oligomer-induced upregulation of BACE1 mRNA (Figure 4.10c). Additionally, the combined synergetic treatment of TF reduced the upregulation of oligomer-induced BACE1 mRNA expression ( $p < 0.05$ ).

#### **4. 4 Discussion**

Epidemiological and research studies have associated catechins, abundantly found in green tea, and theaflavins, abundantly found in black tea, with reduced incidence of cognitive decline. This research sought to identify the manner in which catechins and theaflavins act as potential therapeutics of AD. Focusing on the amyloid cascade hypothesis, Chapter 3 identified the ability of catechins and theaflavins to mechanistically attenuate A $\beta$  aggregation, resulting in altered fA $\beta$  morphology. Current research has, and continues to, identify the most toxic species of the A $\beta$  aggregation pathway way as

oligomers formed at the early stages of aggregation,<sup>15,81,82</sup> placing emphasis on early inhibition. Results from Chapter 3 identified theaflavins as the only compounds capable of inhibiting oligomer formation and altering oligomer conformation. The inability of catechins to alter A $\beta$  oligomers does not appear to diminish their potential at AD therapeutics. *In vitro* cell assays and *in vivo* models have shown a correlation between catechins and attenuation of A $\beta$ -induced cytotoxicity and cognitive impairment.<sup>3,17,38,40,65</sup> Research has attributed catechins AD therapeutic potential to their ability antioxidant capacity to scavenge ROS and act as metal-chelators.<sup>24,26,58,83,84</sup> ORAC results concurred with previous research that all catechins are good antioxidants. Additionally, research has shown theaflavins as effective antioxidants, capabilities analogous to catechins.<sup>31,85-88</sup> A $\beta$  is a source of ROS, the peptide in the presence of metal ions such as iron and copper generates free radicals via Fenton reaction.<sup>24</sup> The resulting oxidative stress is able to induce the upregulation of amyloidogenic cleavage of APP<sup>26,89,90</sup> and potentiate its toxic effect. An additional AD therapeutic strategy, to inhibition of A $\beta$  aggregation, is the alteration of the APP cleavage from the amyloidogenic pathway.

This research took a novel approach by analyzing the capability of catechins and theaflavins to alter A $\beta$ <sub>1-42</sub> oligomer-induced expression of key AD-associated mRNAs involved in APP processing to release A $\beta$ . Catechins and theaflavins antiaggregation and antioxidant capacity were assessed to alter oligomer-induced expression of key mRNAs in three parts: 1) ability to reduce APP and PS1 mRNA, thus reducing the initial substrate available for amyloidogenic cleavage, 2) ability to promote the non-amyloidogenic

pathway by upregulating ADAM9 or ADAM10 mRNA, and 3) ability to attenuate the amyloidogenic pathway by inhibiting BACE1 mRNA.

A $\beta$ <sub>1-42</sub> oligomers upregulated APP mRNA expression, congruent with previously seen research.<sup>41</sup> This shifted the initial focus of reducing APP mRNA expression to finding a potential therapeutic to prevent this upregulation. Oligomer-induced upregulation of APP mRNA is attenuated for oligomers made in the presence of EGCG and modified via antioxidant capacity of EGC. These results align with the data that indicates the neuroprotective action of EGCG may occur through more mechanisms than just promotion of non-amyloidogenic APP cleavage.<sup>11</sup>

In response to the second component of this aim, catechins and theaflavins ability to upregulate the expression of key non-amyloidogenic mRNAs were analyzed. It was revealed that native and modified oligomers by catechins and theaflavins had no effect on ADAM9. Additionally, ADAM10 mRNA expression was not altered by native oligomers. However, oligomers made in the presence of EGC and EGCG resulted in significantly upregulated ADAM10 mRNA. These results align with previous studies that show incubation with EGCG promotes the non-amyloidogenic cleavage of APP to produce sAPP $\alpha$  via  $\alpha$ -secretase,<sup>47,56,57,83</sup> specifically the putative  $\alpha$ -secretase ADAM10.<sup>68,91</sup> It is important to note that the most prominent ADAM to exhibit  $\alpha$ -secretase activity is ADAM10.<sup>76</sup> This indicates the potential to upregulate the non-amyloidogenic cleavage of APP by  $\alpha$ -secretase.

The third component of this aim was to investigate the capabilities of catechins and theaflavins to inhibit the amyloidogenic cleavage of APP by attenuating BACE1 mRNA

expression. Congruent with previously research, BACE1 mRNA expression is upregulated by A $\beta$ .<sup>42</sup> Oligomers made in the presence of all catechins attenuated oligomer-induced upregulation of BACE1 mRNA, while through antioxidant and synergistic capabilities EC was able to attenuate of oligomer-induced upregulation of BACE1 mRNA. Through the studied capabilities of catechin and theaflavins to alter oligomer-induced expression of key AD-associated mRNAs, it was determined that theaflavins do not alter or interact with oligomers in a manner that aids in the reduction of initial APP and  $\gamma$ -secretase substrates, promote the non-amyloidogenic pathway, or attenuate the amyloidogenic pathway.

A $\beta$ <sub>1-42</sub> oligomer-induced upregulation of APP and BACE1 mRNA are congruent with other research,<sup>41</sup> indicate the ability of A $\beta$  to increase the APP substrate that can undergo proteolytic cleavage as well as a shift towards its amyloidogenic cleavage, supporting the feed-forward mechanism of A $\beta$  production.<sup>41,42,70,92</sup> It is thought that A $\beta$  may act as a transcription factor within the regulatory regions of AD-associated genes.<sup>93</sup> This oligomer-induced expression of key AD-associated mRNAs identifies several points of actions, as potential therapeutic must attenuate. EC displays antiaggregation, antioxidant, and synergistic capabilities to attenuate oligomer-induced upregulation of BACE1 mRNA. These results are congruent with mice models exhibiting EC capability to only alter  $\beta$ -secretase cleavage of APP, though effective at 100 nM concentrations.<sup>38</sup> EGC and EGCG exhibit capabilities as antiaggregants and antioxidants to not only attenuate the oligomer-induced upregulation of APP and BACE1 mRNA but also to modify oligomers that result in the upregulation of ADAM10. These results illustrate the capability of

catechins to maintain initial APP substrate levels while shifting the upregulation of the amyloidogenic cleavage to the non-amyloidogenic cleavage.

**Table 4.1. Primer Sequences.**

Primer Sequence	Forward		Reverse		
APP	5'	ACGAAGAAGCCACAGAGA	3'	5' TTCATTCTCATCCCCAGGTG	3'
PS1	5'	GGTAAAGCCTCAGCAACAG	3'	5' AAACAAGCCCAAAGGTGAT	3'
BACE1	5'	GCAGGGCTACTACGTGGAGA	3'	5' CAGCACCCACTGCAAAGTTA	3'
ADAM10	5'	ATGGGAGGTCAGTATGGGAATC	3'	5' ACTGCTCTTTTGGCA CGCT	3'
ADAM9	5'	AAGAATTGTCACTGTGAAAATGGCT	3'	5' CATTGTATGTAGGTCCACTGTCCAC	3'
Ki67	5'	TGGGTCTGTTATTGATGAGCC	3'	5' TGA CTTCCTTCCATTCTGAAGAC	3'
$\beta$ -actin	5'	AAAGACCTGTACGCCAACAC	3'	5' GTCATACTCCTGCTTGCTGAT	3'

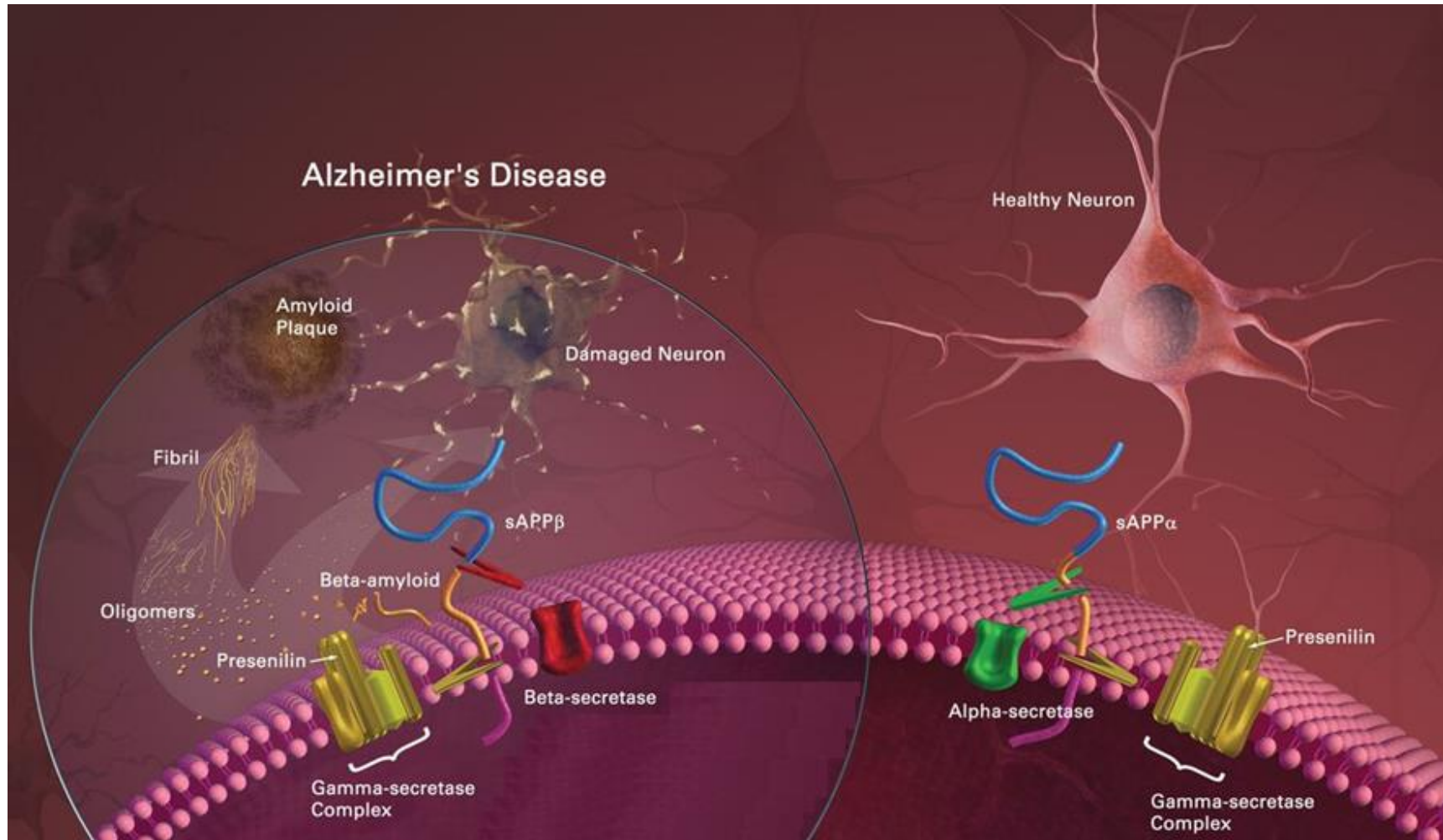


**Figure 4.1. Amyloidogenic and non-amyloidogenic cleavage of APP.**<sup>43</sup> In the amyloidogenic pathway BACE1 and  $\gamma$ -secretase sequentially cleave APP to produce A $\beta$  peptide that can then aggregate. Alternatively, in the non-amyloidogenic pathway  $\alpha$ -secretase and  $\gamma$ -secretase sequentially cleave APP.

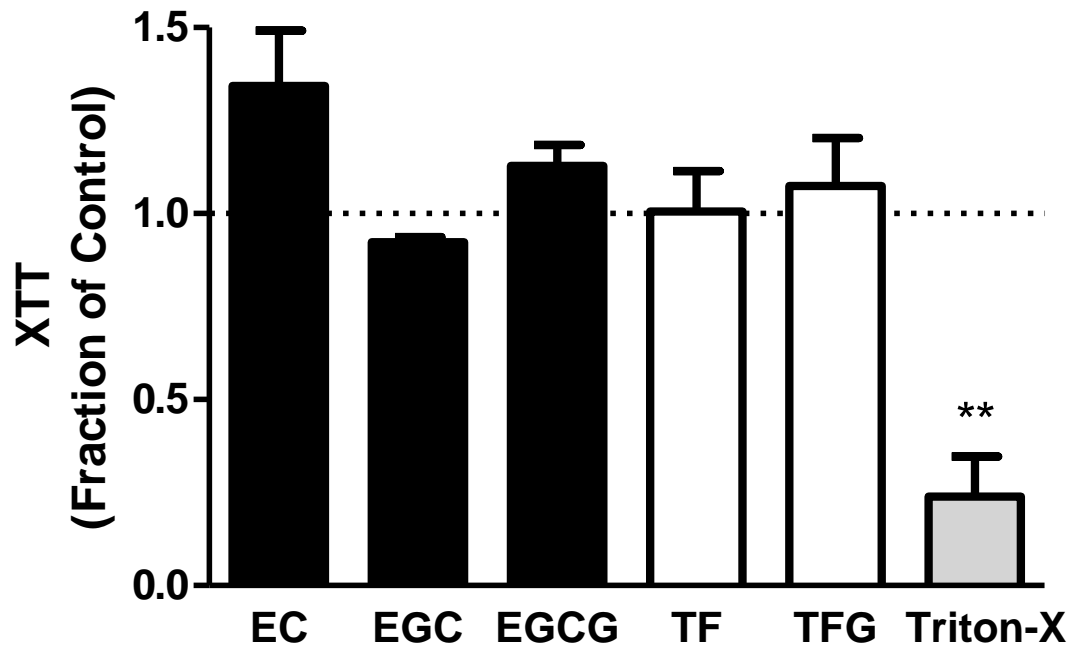


**Figure 4.2. Cell viability after treatment with catechins and theaflavins.** Human neuroblastoma SH-SY5Y cells were incubated in the absence (control, indicated by dash line at 1) or presence of 20  $\mu$ M polyphenol or 0.2% Triton-X (negative control) for 30 min. Cells were assessed for metabolic activity using XTT as described in Section 4.2.2. Error bars indicate SEM n=3-4, \*\*p<0.01, compared to control.



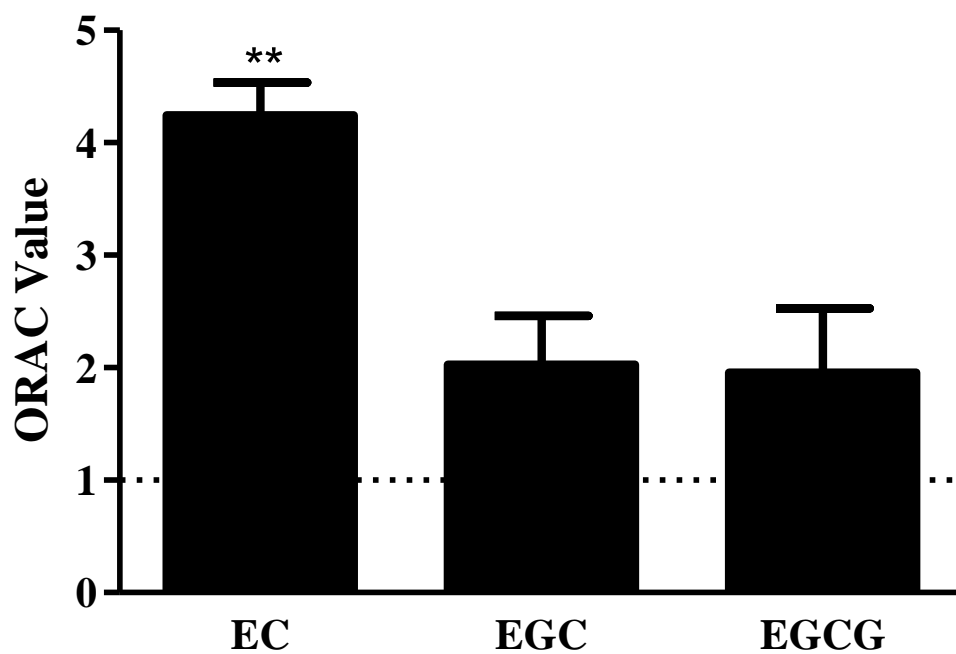


**Figure 4.3. Antioxidant capacity of catechins.** 1  $\mu$ M EC, EGC or EGCG was incubated with 1X fluorescein solution, for assessment of antioxidant capacity using an ORAC assay, described in Section 4.2.3. Data is shown as ORAC value relative to Trolox (indicated by dashed line at 1). Error bars represent SEM n=3-4, \*\*p<0.01, compared to control.

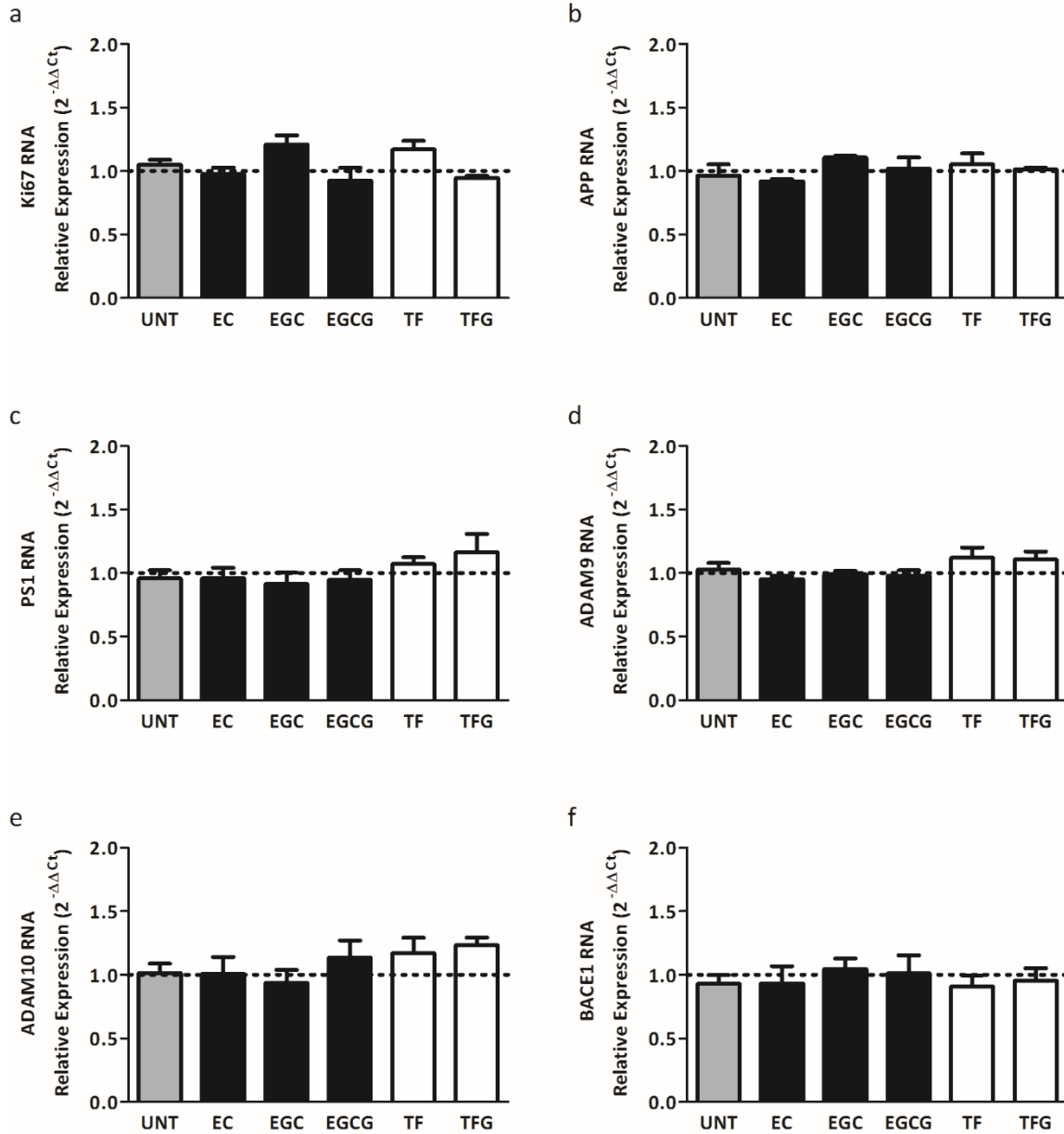


**Figure 4.4. Catechins and theaflavins alone have negligible effect on AD-associated mRNAs.** Human neuroblastoma SH-SY5Y cells were incubated in the absence (vehicle, indicated by dashed line at 1) or presence of 10  $\mu$ M polyphenol. RNA was isolated with E.Z.N.A RNA Kit 1 followed by reverse transcription and qRT-PCR as detailed in Section 4.2.5. Expression relative to the vehicle (dashed line at one) was determined for Ki67 (panel a), APP (panel b), PS1 (panel c), ADAM9 (panel d), ADAM10 (panel e), and BACE1 (panel f). Error bars represent SEM, n=3-4.

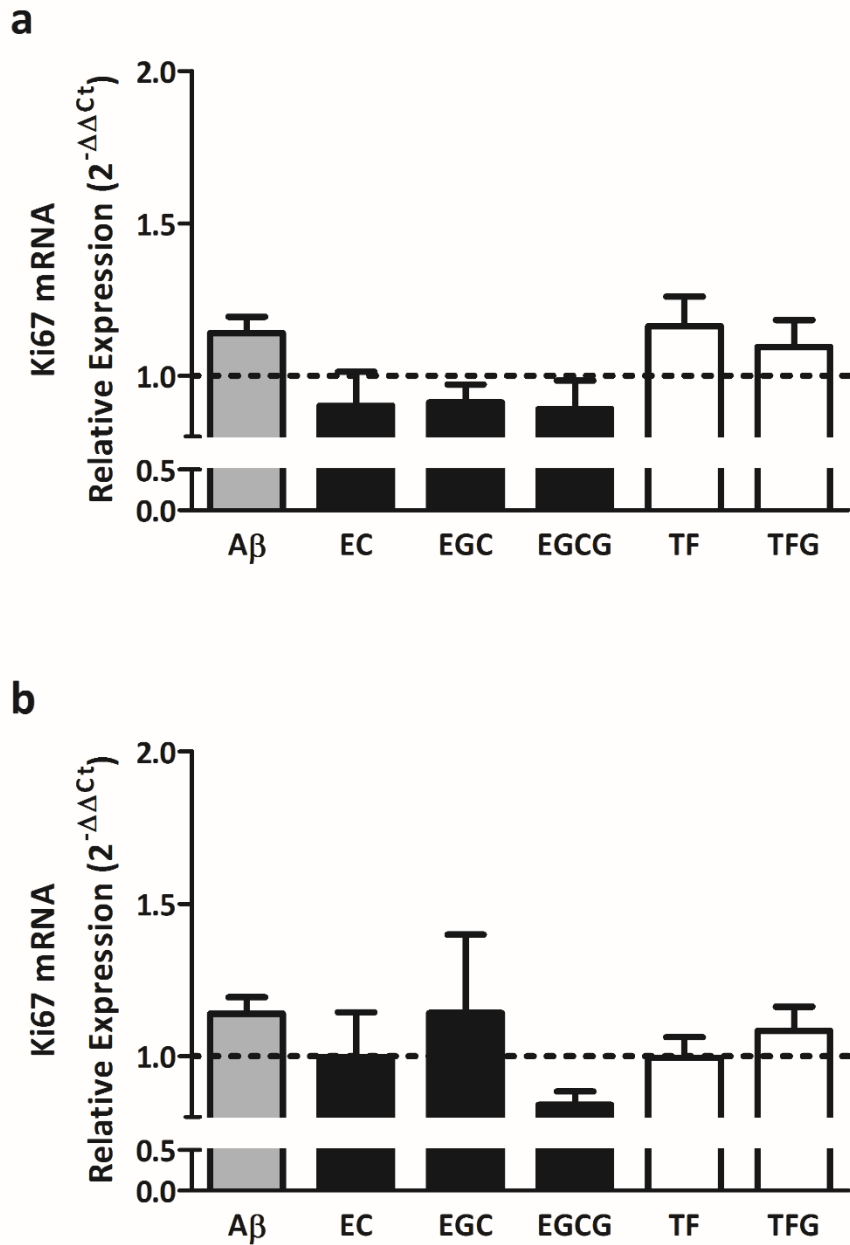


**Figure 4.5. Cell treatments display negligible effect on Ki67 mRNA.** SH-SY5Y cells were treated for 72 h with a final concentration of 0.1  $\mu\text{M}$   $\text{A}\beta_{1-42}$  oligomers made in the absence or presence of 10-fold molar excess polyphenol (**panel a**), or final concentrations of 0.1  $\mu\text{M}$  native  $\text{A}\beta$  oligomers and 10  $\mu\text{M}$  polyphenol (**panel b**). RNA was isolated with E.Z.N.A RNA Kit 1 followed by reverse transcription and qRT-PCR as detailed in Section 4.2.5. Expression relative to the vehicle (dashed line at one) was determined for Ki67 mRNA. **Error bars represent SEM; n=8 for treatment with  $\text{A}\beta$  alone and n=3-4 for treatment with polyphenols.**

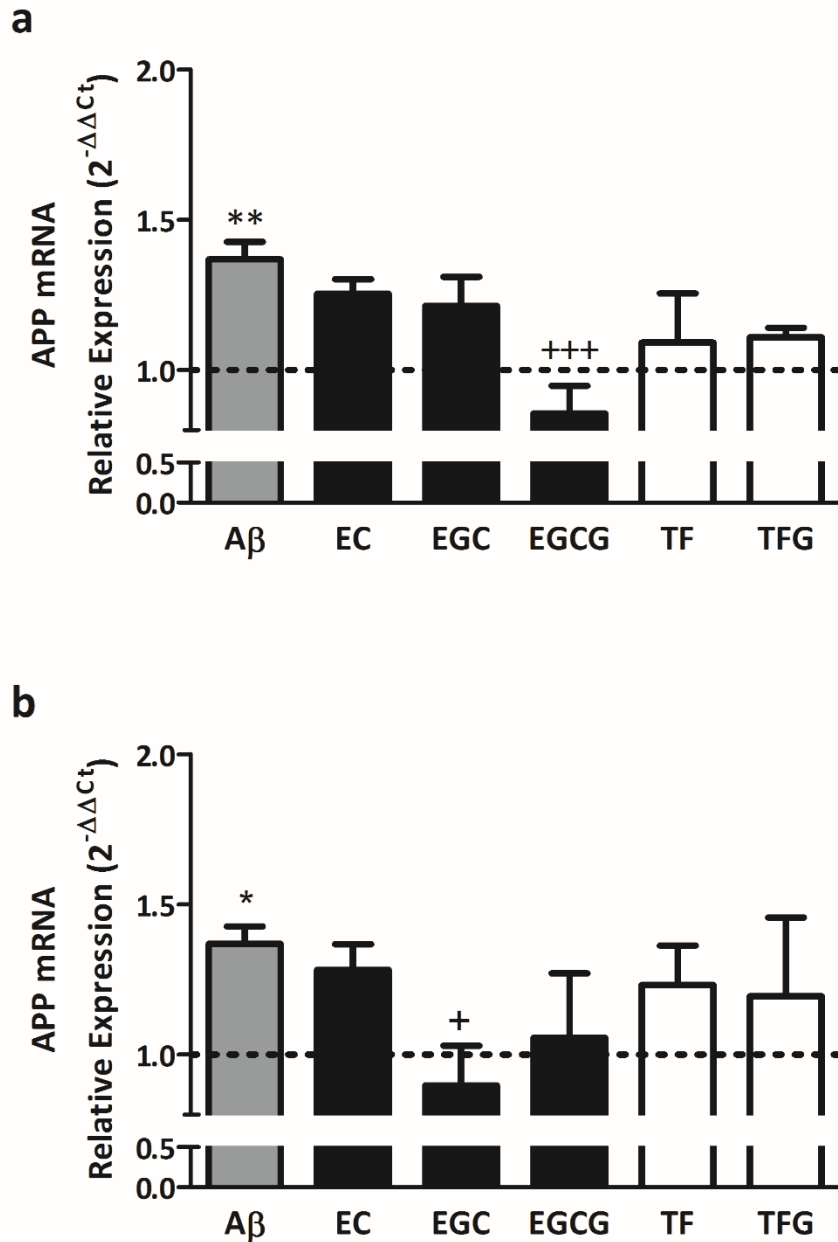


**Figure 4.6. Effect of catechins and theaflavins on Aβ<sub>1-42</sub> oligomers-induced upregulation of APP mRNA.** SH-SY5Y cells were treated for 72 h with a final concentration of 0.1 μM Aβ<sub>1-42</sub> oligomers made in the absence or presence of 10-fold molar excess polyphenol (**panel a**), or final concentrations of 0.1 μM native Aβ oligomers and 10 μM polyphenol (**panel b**). RNA was isolated with E.Z.N.A RNA Kit 1 followed by reverse transcription and qRT-PCR as detailed in Section 4.2.5. Expression relative to the vehicle (dashed line at one) was determined for Ki67 mRNA. Error bars represent SEM; n=8 for treatment with Aβ alone and n=3-4 for treatment with polyphenols and \*p<0.05, \*\*p<0.01 for sample versus vehicle, and +++p<0.01 for samples versus native Aβ oligomers.

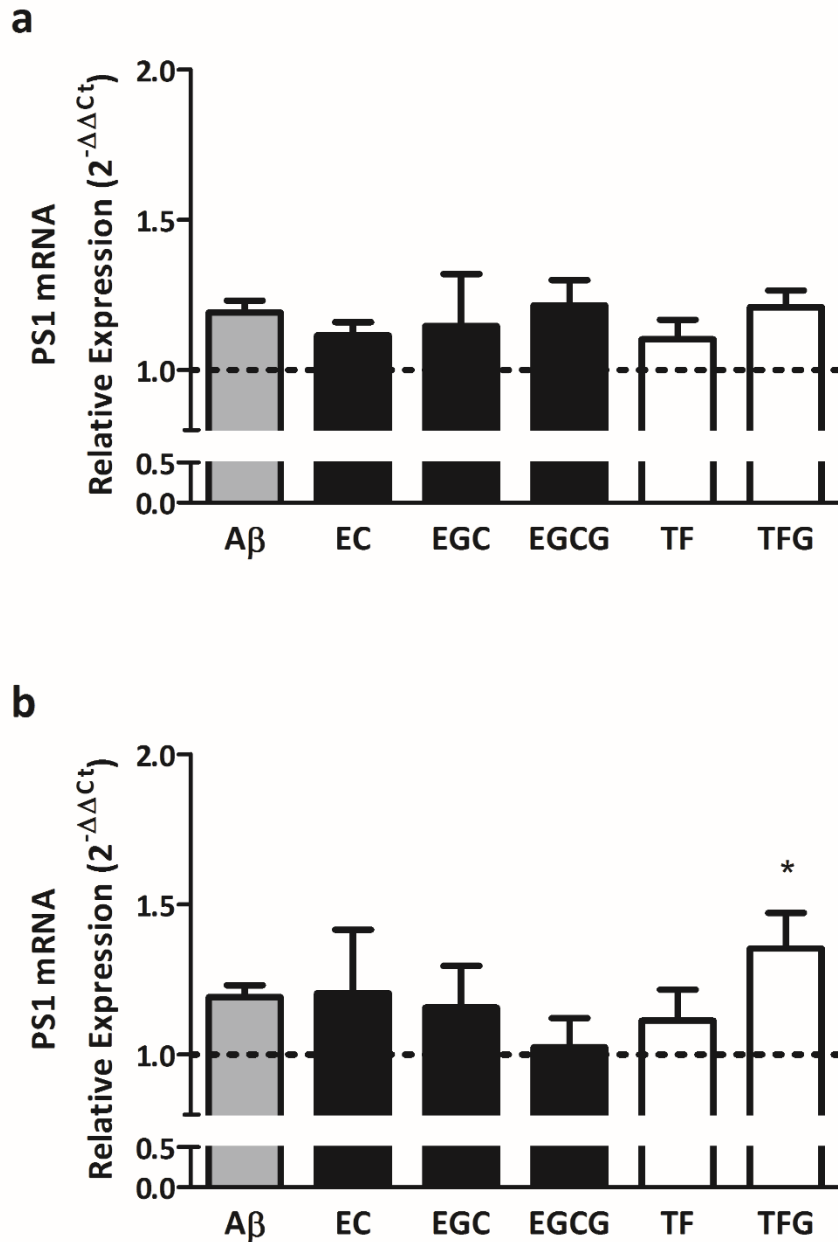


**Figure 4.7. Effect of catechins and theaflavins on PS1 mRNA expression.** SH-SY5Y cells were treated for 72 h with a final concentration of 0.1  $\mu$ M A $\beta$ 1-42 oligomers made in the absence or presence of 10-fold molar excess polyphenol (**panel a**), or final concentrations of 0.1  $\mu$ M native A $\beta$  oligomers and 10  $\mu$ M polyphenol (**panel b**). RNA was isolated with E.Z.N.A RNA Kit 1 followed by reverse transcription and qRT-PCR as detailed in Section 4.2.5. Expression relative to the vehicle (dashed line at one) was determined for Ki67 mRNA. Error bars represent SEM; n=8 for treatment with A $\beta$  alone and n=3-4 for treatment with polyphenols.

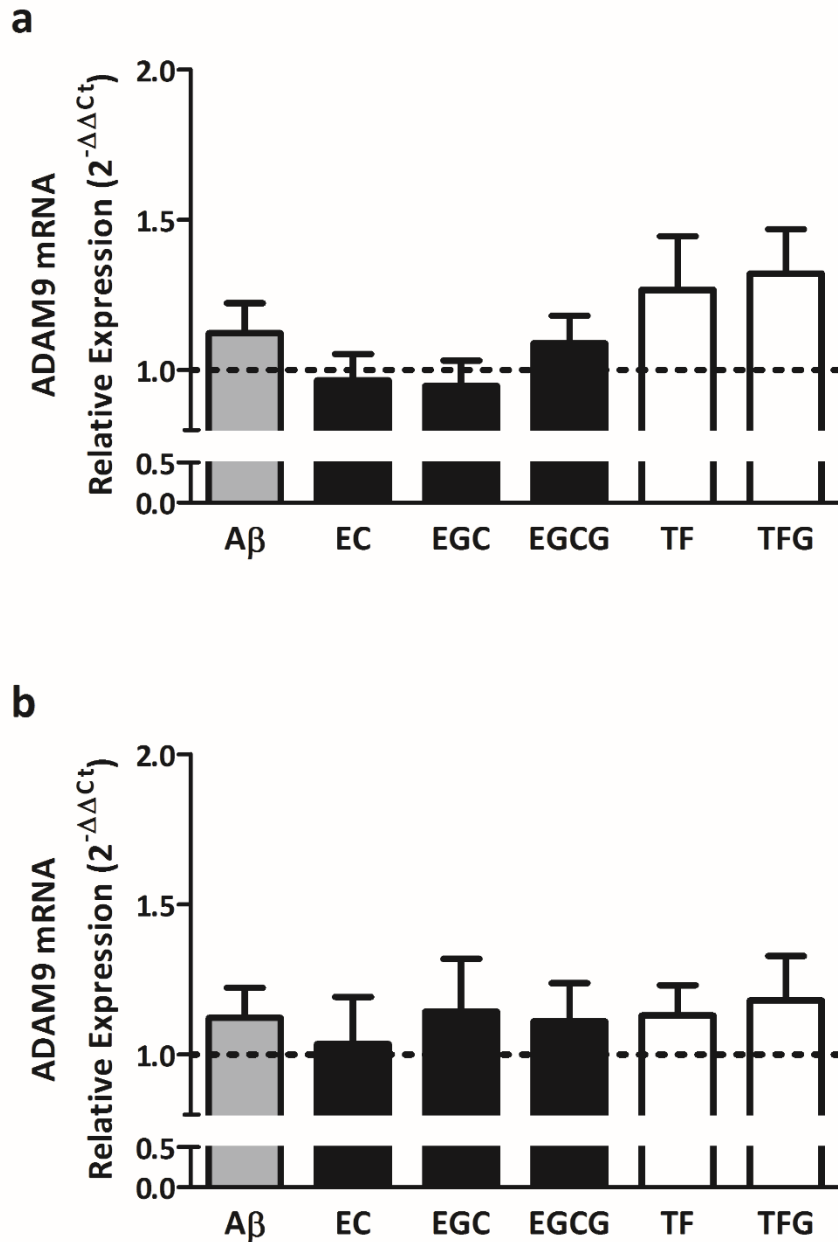


**Figure 4.8. Effect of catechins and theaflavins on ADAM9 mRNA expression.** SH-SY5Y cells were treated for 72 h with a final concentration of 0.1  $\mu$ M A $\beta$ 1-42 oligomers made in the absence or presence of 10-fold molar excess polyphenol (**panel a**), or final concentrations of 0.1  $\mu$ M native A $\beta$  oligomers and 10  $\mu$ M polyphenol (**panel b**). RNA was isolated with E.Z.N.A RNA Kit 1 followed by reverse transcription and qRT-PCR as detailed in Section 4.2.5. Expression relative to the vehicle (dashed line at one) was determined for Ki67 mRNA. Error bars represent SEM; n=8 for treatment with A $\beta$  alone and n=3-4 for treatment with polyphenols

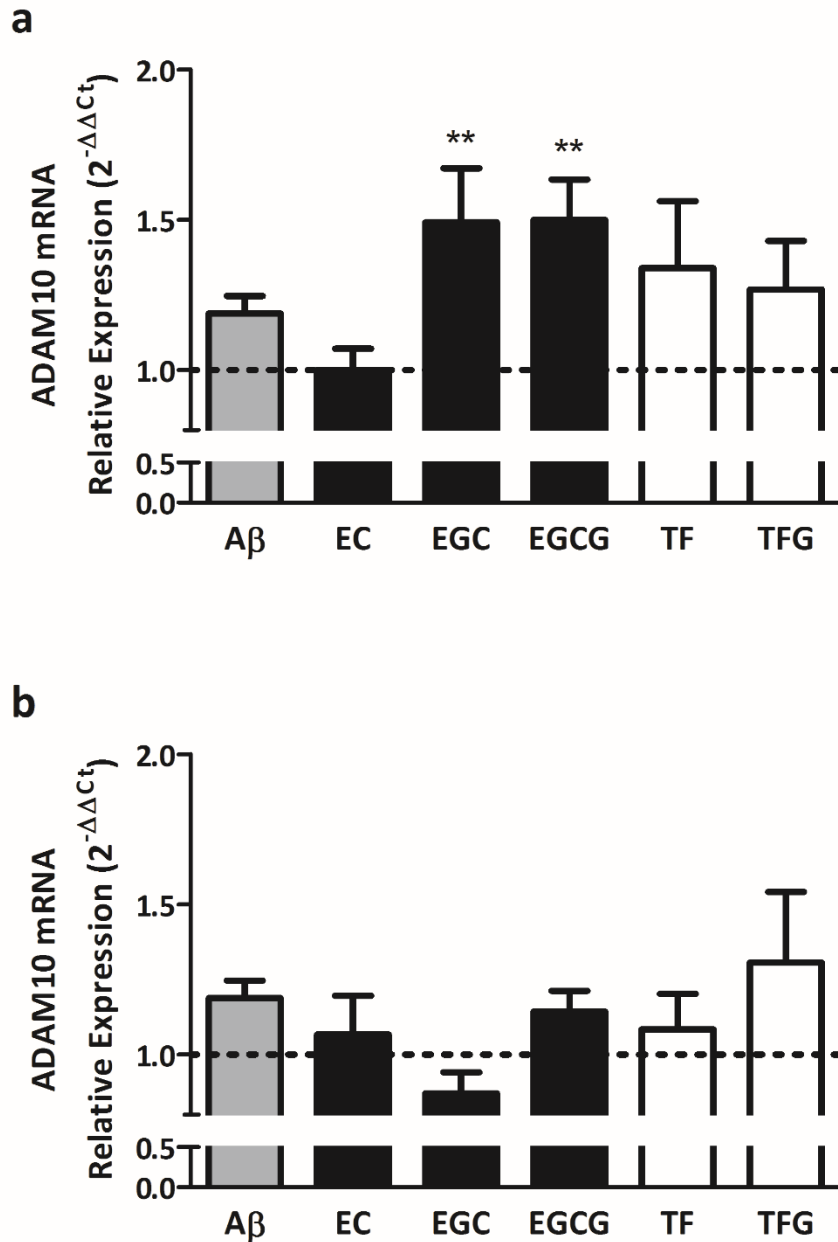


**Figure 4.9. Effect of catechins and theaflavins on ADAM10 mRNA expression.** SH-SY5Y cells were treated for 72 h with a final concentration of 0.1  $\mu\text{M}$  A $\beta$ 1-42 oligomers made in the absence or presence of 10-fold molar excess polyphenol (**panel a**), or final concentrations of 0.1  $\mu\text{M}$  native A $\beta$  oligomers and 10  $\mu\text{M}$  polyphenol (**panel b**). RNA was isolated with E.Z.N.A RNA Kit 1 followed by reverse transcription and qRT-PCR as detailed in Section 4.2.5. Expression relative to the vehicle (dashed line at one) was determined for Ki67 mRNA. Error bars represent SEM; n=8 for treatment with A $\beta$  alone and n=3-4 for treatment with polyphenols and \*p<0.05 modified oligomers versus native oligomers.

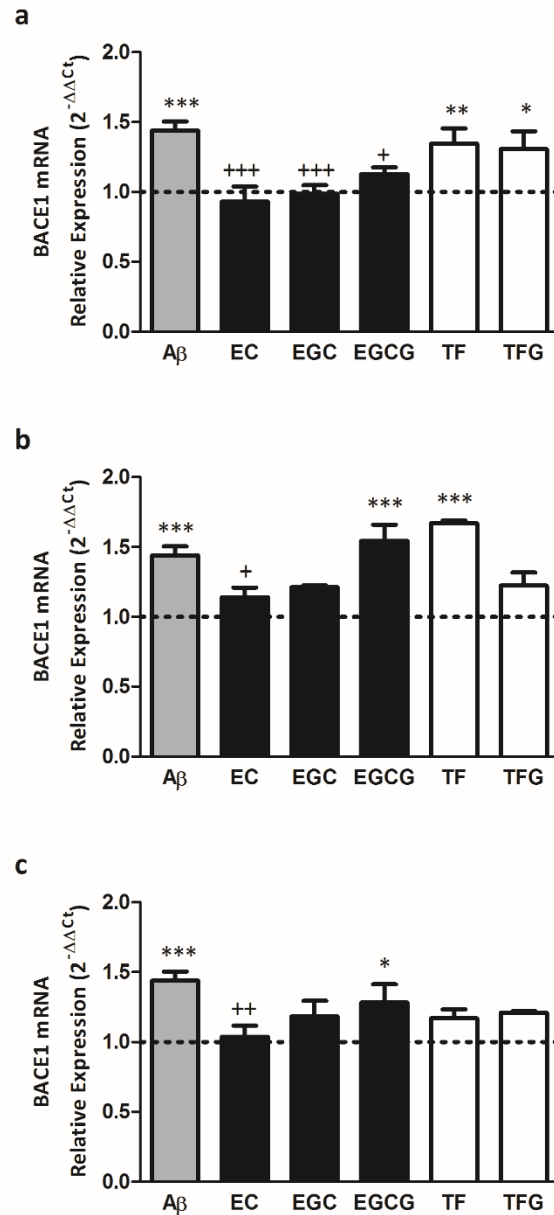


**Figure 4.10. Effect of catechins and theaflavins on Aβ<sub>1-42</sub> oligomers-induced upregulation of BACE1 mRNA.** SH-SY5Y cells were treated for 72 h with a final concentration of 0.1 μM Aβ<sub>1-42</sub> oligomers made in the absence or presence of 10-fold molar excess polyphenol (**panel a**), or final concentrations of 0.1 μM native Aβ oligomers and 10 μM polyphenol (**panel b**), or final concentrations of 0.1 μM Aβ oligomers made in the absence (Aβ control) or presence of 10-fold molar excess polyphenol and 10 μM polyphenol (**panel c**). RNA was isolated with E.Z.N.A RNA Kit 1 followed by reverse transcription and qRT-PCR as detailed in Section 4.2.5. Expression relative to the vehicle (dashed line at one) was determined for Ki67 mRNA. Error bars represent SEM; n=8 for treatment with Aβ alone and n=3-4 for treatment with polyphenols +p<0.05 and ++p<0.01 modified oligomers versus native oligomers.



## CHAPTER 5: CONCLUSIONS

AD currently affects an estimated 5.4 million Americans. This number is anticipated to reach 13.8 million in 2050, placing prominence for a therapeutic. Current AD therapeutic research investigates many facets of the disease, including but not limited to amyloidogenic pre- and post-processing of A $\beta$ , a key protein in AD pathogenesis. Epidemiological studies have shown a direct correlation between green tea, rich in catechin polyphenols, and black tea, rich in theaflavin polyphenols, consumption with reduced incidence of cognitive decline.<sup>29,30</sup> Based on these and other studies supporting the natural cognitive health benefits of catechins and theaflavins, this study sought to identify their potential as AD therapeutics targeting the amyloidogenic pre- and post-processing of A $\beta$ . In this study, catechins' and theaflavins' potential to act as multi-target therapeutic drugs for AD was analyzed for their ability to 1) alter the mechanistic aggregation of A $\beta$  and 2) alter basal and A $\beta$ <sub>1-42</sub> oligomer-induced expression of key AD-associated mRNAs.

In Chapter 3, catechins and theaflavins' capability to attenuate the mechanistic aggregation of A $\beta$  was determined. The polyphenols examined varied in their derivation from the original parent compound EC. EC hydroxylates to EGC; EGC undergoes gallic acid acetylation to form EGCG. Theaflavins are produced during fermentation by the oxidative coupling of catechins. EC and EGC oxidatively couple to form TF, and EGC and EGCG

oxidatively couple to form TFG. Mechanistic aggregation results show that catechins displayed inhibitory capabilities only at the late stages, suggesting structural recognition of only large aggregates, while theaflavins exhibit inhibitory capabilities at every mechanistic step of the pathway, suggesting the capability to recognize multiple aggregate conformations.

The ability of catechins and theaflavins to alter the overall  $A\beta_{1-40}$  monomer aggregation proved to be congruent with the summation of the inhibitory capabilities at the individual mechanistic steps of  $A\beta$  aggregation, as shown by altered morphology of  $fA\beta$  made in their presence. Catechins were unable to inhibit the earlier oligomerization process of  $A\beta$  aggregation, but were able to significantly reduce the rate of elongation and association. Due to their inability to inhibit the early oligomerization, catechins were unable to reduce the total  $A\beta$  aggregates formed, but because of the late stage inhibitory capabilities, catechins were able to alter the morphology  $fA\beta$  made in their presence. Fibrils made in the presence of catechins displayed decreasing lateral association and length from EC to EGC to EGCG, trending with structural derivation. Theaflavins exhibit similar inhibitory capabilities as catechins towards soluble aggregate growth, but are additionally able to reduce  $A\beta_{1-42}$  oligomer formation and the total amount of  $A\beta$  aggregates formed in their presence. This result suggests that the amount of total  $A\beta$  aggregates formed is more dependent upon the earlier nucleation phase of aggregate growth. TFG, the phenolic derivative of EGC and EGCG, showed prominent attenuation of both large (100-250 kDa) and small (25-100 kDa) oligomer species as well as moderate to significant attenuation of the rate of elongation and association. The sum of its

capabilities at every mechanistic step resulted in the most altered form of A $\beta$  morphology, which closely resembled an intermediate conformation between oligomers and soluble aggregates.<sup>49</sup>

Chapter 3 analyzed catechins and theaflavins capabilities to attenuate the post-processing aggregation of A $\beta$ . To expand on their innate abilities to reduce cognitive impairment, Chapter 4 examined their capabilities to alter the pre-processing of A $\beta$  from APP. Chapter 4 research took a novel approach by analyzing the capability of catechins and theaflavins to alter A $\beta$ <sub>1-42</sub> oligomer-induced expression of key AD-associated mRNAs. Catechins' and theaflavins' ability to alter the production of A $\beta$  was analyzed in three parts: 1) the ability to reduce APP and PS1 mRNA, 2) the ability to promote the non-amyloidogenic pathway by upregulating ADAM9 or ADAM10 mRNA, and 3) the ability to attenuate the amyloidogenic pathway by inhibiting BACE1 mRNA. Results showed that catechins, over theaflavins, displayed capabilities to alter A $\beta$ -oligomer induced expression of key AD-associated mRNAs. Congruent with previous observations, A $\beta$ <sub>1-42</sub> acts as cell stressor resulting in the upregulation of APP and BACE1 mRNA.<sup>41</sup> These results are not only indicative of A $\beta$ 's potential to increase the amyloidogenic cleavage of APP but its potential to increase APP, producing more initial substrate to undergo proteolytic cleavage. Results demonstrate that catechins possess the potential to prevent the amyloidogenic cleavage of APP and promote non-amyloidogenic cleavage. All catechins exhibits the capability to attenuate oligomer-induced upregulation of BACE1 through antiaggregation capabilities and thus the potential to reduce the amyloidogenic cleavage of APP. A $\beta$ <sub>1-42</sub> oligomers made in the presence of EGC and EGCG exhibit the capability to

upregulate ADAM10 mRNA. Upregulation of ADAM10, the most prominent ADAM with  $\alpha$ -secretase activity, has the potential to promote the non-amyloidogenic cleavage of APP.<sup>75,76</sup> Additionally, EGC and EGCG are able to attenuate the  $A\beta_{1-42}$  oligomer-induced upregulation of APP mRNA for oligomers made in its presence. This effect has the potential to prevent upregulation of APP that can lead to more amyloidogenic cleavage.

In summary, this study demonstrated that catechins and theaflavins are able to mechanistically inhibit aggregation of  $A\beta$ . It was found that the overall amount of  $A\beta$  aggregates formed and the resulting  $fA\beta$  morphology is dependent upon the mechanistic step in which the compounds intervene. Only catechins were able to alter  $A\beta_{1-42}$  oligomer-induced expression of multiple AD-associated mRNAs, showing potential to attenuate the amyloidogenic and promote non-amyloidogenic cleavage of APP. Combined, these studies identify the capabilities of catechins to alter the pre-processing and post-processing of  $A\beta$ , supporting their potential to act as multi-target therapeutics.

## CHAPTER 6: FUTURE PERSPECTIVES

Catechins and theaflavins exhibited the capability to alter fA $\beta$  morphology made in their presence, presenting potential therapeutic benefits to attenuate A $\beta$ -induced toxicity, based on direct correlation between fA $\beta$  morphology and toxicity.<sup>18</sup> Future studies to analyze the ability of catechins and theaflavins to alter the toxicity of A $\beta$  aggregates formed in their presence will substantiate the potential of these compounds as therapeutics.

Additionally, catechins were identified in Chapter 4 to alter expression of key AD-associated mRNAs. This action translates to the potential to alter expression of key proteins involved in the amyloidogenic and non-amyloidogenic cleavage of APP. Future studies will analyze protein expression of cell isolates from treatments congruent to Section 4.2.4 PCR treatments, probing for BACE1, APP, and ADAM10 proteins. Results congruent with PCR will provide stronger evidence that catechins, through antiaggregation and antioxidant capabilities, are able to attenuate the feed-forward mechanism of A $\beta$  production by down regulating APP and BACE1 expression, while upregulating ADAM10 expression. Resulting in attenuation of the amyloidogenic and promotion of the non-amyloidogenic pathway.

## REFERENCES

1. 2016 ALZHEIMER ' S DISEASE FACTS AND FIGURES. *Alzheimer's & Dementia* **12**, (2016).
2. *Alzheimer ' s Disease Medications*. (2008).
3. Lee, Y.-J. *et al.* Epigallocatechin-3-gallate prevents systemic inflammation-induced memory deficiency and amyloidogenesis via its anti-neuroinflammatory properties. *J. Nutr. Biochem.* **24**, 298–310 (2013).
4. Ono, K. *et al.* Potent anti-amyloidogenic and fibril-destabilizing effects of polyphenols in vitro: implications for the prevention and therapeutics of Alzheimer's disease. *J. Neurochem.* **87**, 172–181 (2003).
5. Taniguchi, S. *et al.* Inhibition of heparin-induced tau filament formation by phenothiazines, polyphenols, and porphyrins. *J. Biol. Chem.* **280**, 7614–23 (2005).
6. Oddo, S. Amyloid deposition precedes tangle formation in a triple transgenic model of Alzheimer's disease. *Neurobiol. Aging* **24**, 1063–1070 (2003).
7. Hardy, J. & Selkoe, D. J. The amyloid hypothesis of Alzheimer's disease: progress and problems on the road to therapeutics. *Science* **297**, 353–6 (2002).
8. Hardy, J. & Higgins, G. Alzheimer's Disease: The Amyloid Cascade Hypothesis. *Science (80-. )*. **256**, (1992).
9. Pimplikar, S. W. Reassessing the amyloid cascade hypothesis of Alzheimer's disease. *Int J Biochem Cell Biol* **41**, 1261–1268 (2009).
10. Roychaudhuri, R., Yang, M., Hoshi, M. M. & Teplow, D. B. Amyloid beta-protein assembly and Alzheimer disease. *J. Biol. Chem.* **284**, 4749–53 (2009).
11. Lin, C.-L., Chen, T.-F., Chiu, M.-J., Way, T.-D. & Lin, J.-K. Epigallocatechin gallate (EGCG) suppresses beta-amyloid-induced neurotoxicity through inhibiting c-Abl/FE65 nuclear translocation and GSK3 beta activation. *Neurobiol. Aging* **30**, 81–92 (2009).
12. Suo, C. & Moss, M. A. Study of Polyphenols and Naphthalimide Analogs As Inhibitors of Amyloid-beta Protein Aggregation in Alzheimer's Disease. (2011).
13. Hsai, A. Y. *et al.* Plaque-independent disruption of neural circuits in Alzheimer's disease mouse models. *Proc. Natl. Acad. Sci. U. S. A.* **96**, 3228–33 (1999).
14. Mc Donald, J. M. *et al.* The presence of sodium dodecyl sulphate-stable A $\beta$  dimers is strongly associated with Alzheimer-type dementia. *Brain* **133**, 1328–1341 (2010).
15. Benilova, I., Karran, E. & De Strooper, B. The toxic A $\beta$  oligomer and Alzheimer's disease: an emperor in need of clothes. *Nat. Neurosci.* **15**, 349–57 (2012).
16. Yankner, B. a & Lu, T. Amyloid beta-protein toxicity and the pathogenesis of Alzheimer disease. *J. Biol. Chem.* **284**, 4755–9 (2009).
17. Porat, Y., Abramowitz, A. & Gazit, E. Inhibition of amyloid fibril formation by polyphenols: structural similarity and aromatic interactions as a common inhibition

- mechanism. *Chem. Biol. Drug Des.* **67**, 27–37 (2006).
18. Ritter, C. *et al.* 3D structure of Alzheimer ' s amyloid- $\beta$  ( 1 – 42 ) fibrils. *Proc. Natl. Acad. Sci. U. S. A.* **102**, 17342–17347 (2005).
  19. Ono, K., Naiki, H. & Yamada, M. The development of preventives and therapeutics for Alzheimer's disease that inhibit the formation of  $\beta$  -amyloid Fibrils ( fA  $\beta$  ), as well as destabilize preformed fA  $\beta$ . *Curr. Pharm. Des.* **12**, 4357–4375 (2006).
  20. Ono, K. *et al.* Effects of grape seed-derived polyphenols on amyloid beta-protein self-assembly and cytotoxicity. *J. Biol. Chem.* **283**, 32176–87 (2008).
  21. Bastianetto, S., Krantic, S. & Quirion, R. Polyphenols as Potential Inhibitors of Amyloid Aggregation and Toxicity : Possible Significance to Alzheimer ' s Disease. *Mini-Reviews Med. Chem.* **8**, 429–435 (2008).
  22. Rossi, L., Mazzitelli, S., Arciello, M., Capo, C. R. & Rotilio, G. Benefits from dietary polyphenols for brain aging and Alzheimer's disease. *Neurochem. Res.* **33**, 2390–400 (2008).
  23. Zhang, H.-Y., Liu, Y.-H., Wang, H.-Q., Xu, J.-H. & Hu, H.-T. Puerarin protects PC12 cells against beta-amyloid-induced cell injury. *Cell Biol. Int.* **32**, 1230–7 (2008).
  24. Choi, D.-Y., Lee, Y.-J., Hong, J. T. & Lee, H.-J. Antioxidant properties of natural polyphenols and their therapeutic potentials for Alzheimer's disease. *Brain Res. Bull.* **87**, 144–53 (2012).
  25. Smith, W. W., Gorospe, M. & Kusiak, J. W. Signaling Mechanisms Underlying A Toxicity : Potential Therapeutic Targets for Alzheimer ' s Disease. *CNS Neurol. Disord. Targets* **5**, 355–361 (2006).
  26. Tabaton, M., Zhu, X., Perry, G., Smith, M. a & Giliberto, L. Signaling effect of amyloid- $\beta$ (42) on the processing of A $\beta$ PP. *Exp. Neurol.* **221**, 18–25 (2010).
  27. Ramdani, D., Chaudhry, A. S. & Seal, C. J. Chemical composition, plant secondary metabolites, and minerals of green and black teas and the effect of different tea-to-water ratios during their extraction on the composition of their spent leaves as potential additives for ruminants. *J. Agric. Food Chem.* **61**, 4961–7 (2013).
  28. Nurk, E. *et al.* Intake of flavonoid-rich wine, tea, and chocolate by elderly men and women is associated with better cognitive test performance. *J. Nutr.* 120–127 (2009). doi:10.3945/jn.108.095182.oxidant
  29. Ng, T.-P., Feng, L., Niti, M., Kua, E.-H. & Yap, K.-B. Tea consumption and cognitive impairment and decline in older Chinese adults. *Am. J. Clin. Nutr.* **88**, 224–31 (2008).
  30. Kuriyama, S. *et al.* Green tea consumption and cognitive function : a cross-sectional study from the Tsurugaya Project. *Am J Clin Nutr.* **83**, 355–361 (2006).
  31. Leung, L. K. *et al.* Theaflavins in black tea and catechins in green tea are equally effective antioxidants. *J. Nutr.* **131**, 2248–2251 (2001).
  32. Sang, S. *et al.* Chemical studies of the antioxidant mechanism of theaflavins : radical reaction products of theaflavin 3 , 3 % -digallate with hydrogen peroxide. **44**, 5583–5587 (2003).
  33. Menet, M.-C., Sang, S., Yang, C. S., Ho, C.-T. & Rosen, R. T. Analysis of theaflavins and thearubigins from black tea extract by MALDI-TOF mass spectrometry. *J. Agric. Food Chem.* **52**, 2455–61 (2004).

34. Manach, C. Polyphenols : food sources and bioavailability . *Am J Clin Nutr. Am. J. Clin. Nutr.* **79**, 727–747 (2004).
35. Natsume, M. *et al.* Structures of (-)-epicatechin glucuronide identified from plasma and urine after oral ingestion of (-)-epicatechin: Differences between human and rat. *Free Radic. Biol. Med.* **34**, 840–849 (2003).
36. Abd El Mohsen, M. M. *et al.* Uptake and metabolism of epicatechin and its access to the brain after oral ingestion. *Free Radic. Biol. Med.* **33**, 1693–1702 (2002).
37. Wang, J. *et al.* Brain-Targeted Proanthocyanidin Metabolites for Alzheimer’s Disease Treatment. *J. Neurosci.* **32**, 5144–5150 (2012).
38. Cox, C. J. *et al.* Dietary (-)-epicatechin as a potent inhibitor of  $\beta\gamma$ -secretase amyloid precursor protein processing. *Neurobiol. Aging* **36**, 178–187 (2015).
39. Ferruzzi, M. G. *et al.* Bioavailability of gallic acid and catechins from grape seed polyphenol extract is improved by repeated dosing in rats: Implications for treatment in Alzheimer’s Disease. *J. Alzheimers Dis.* **18**, 113–124 (2010).
40. Cheng, B. *et al.* Inhibiting toxic aggregation of amyloidogenic proteins: A therapeutic strategy for protein misfolding diseases. *Biochim. Biophys. Acta - Gen. Subj.* **1830**, 4860–4871 (2013).
41. Liu, T. *et al.* Attenuated ability of BACE1 to cleave the amyloid precursor protein via silencing long noncoding RNA BACE1-AS expression. *Mol. Med. Rep.* **10**, 1275–81 (2014).
42. Faghihi, M. A. *et al.* Expression of a noncoding RNA is elevated in Alzheimer’s disease and drives rapid feed-forward regulation of  $\beta$ -secretase expression. *Nat. Med.* **14**, 723–730 (2008).
43. National Institute of Aging. *Alzheimer’s Disease:Unraveling the Mystery. National Institute on Aging* (2008).
44. Gill, S. C. & von Hippel, P. H. Calculation of protein extinction coefficients from amino acid sequence data. *Analytical biochemistry* **182**, 319–26 (1989).
45. Nichols, M. R. *et al.* Growth of beta-amyloid(1-40) protofibrils by monomer elongation and lateral association. Characterization of distinct products by light scattering and atomic force microscopy. *Biochemistry* **41**, 6115–27 (2002).
46. LeVine, H. Thioflavine T interaction with synthetic Alzheimer’s disease beta-amyloid peptides: detection of amyloid aggregation in solution. *Protein Sci.* **2**, 404–10 (1993).
47. Haque, A. M., Hashimoto, M., Katakura, M., Hara, Y. & Shido, O. Green tea catechins prevent cognitive deficits caused by Abeta1-40 in rats. *J. Nutr. Biochem.* **19**, 619–26 (2008).
48. Petkova, A. T. *et al.* A Structural Model for Alzheimer’ s  $\beta$ -Amyloid Fibrils Based on Experimental Constraints from Solid State NMR. *Proc Natl Acad Sci U S A* **99**, 16742–16747 (2002).
49. Fändrich, M. Oligomeric intermediates in amyloid formation: Structure determination and mechanisms of toxicity. *J. Mol. Biol.* **421**, 427–440 (2012).
50. Bolognesi, B. & Wilson, M. R. ANS Binding Reveals Common Features of Cytotoxic Amyloid Species. **5**, 735–740 (2010).



51. Lindgren, M. & Hammarström, P. Amyloid oligomers: Spectroscopic characterization of amyloidogenic protein states. *FEBS J.* **277**, 1380–1388 (2010).
52. Davis, T. J. *et al.* Comparative Study of Inhibition at Multiple Stages of Amyloid- $\beta$  Self-Assembly Provides Mechanistic Insight. **76**, 405–413 (2009).
53. Pryor, N. E., Moss, M. a & Hestekin, C. N. Unraveling the Early Events of Amyloid- $\beta$  Protein (A $\beta$ ) Aggregation: Techniques for the Determination of A $\beta$  Aggregate Size. *Int. J. Mol. Sci.* **13**, 3038–72 (2012).
54. Chiti, F. & Dobson, C. M. Protein misfolding, functional amyloid, and human disease. *Annu. Rev. Biochem.* **75**, 333–366 (2006).
55. Mandel, S. a, Amit, T., Weinreb, O., Reznichenko, L. & Youdim, M. B. H. Simultaneous manipulation of multiple brain targets by green tea catechins: a potential neuroprotective strategy for Alzheimer and Parkinson diseases. *CNS Neurosci. Ther.* **14**, 352–65 (2008).
56. Levites, Y., Amit, T., Mandel, S. & Youdim, M. B. H. Neuroprotection and neurorescue against A $\beta$  toxicity and PKC-dependent release of nonamyloidogenic soluble precursor protein by green tea polyphenol (-)-epigallocatechin-3-gallate. *FASEB J.* **17**, 952–954 (2003).
57. Mandel, S. a, Amit, T., Kalfon, L., Reznichenko, L. & Youdim, M. B. H. Targeting multiple neurodegenerative diseases etiologies with multimodal-acting green tea catechins. *J. Nutr.* **138**, 1578S–1583S (2008).
58. Mandel, S. & Youdim, M. B. H. Catechin polyphenols: Neurodegeneration and neuroprotection in neurodegenerative diseases. *Free Radic. Biol. Med.* **37**, 304–317 (2004).
59. Ramassamy, C. Emerging role of polyphenolic compounds in the treatment of neurodegenerative diseases: a review of their intracellular targets. *Eur. J. Pharmacol.* **545**, 51–64 (2006).
60. Grelle, G. *et al.* Black tea theaflavins inhibit formation of toxic amyloid- $\beta$  and  $\alpha$ -synuclein fibrils. *Biochemistry* **50**, 10624–10636 (2011).
61. Ebrahimi, A. & Schluesener, H. Natural polyphenols against neurodegenerative disorders: potentials and pitfalls. *Ageing Res. Rev.* **11**, 329–45 (2012).
62. Wang, S.-H., Liu, F.-F., Dong, X.-Y. & Sun, Y. Thermodynamic analysis of the molecular interactions between amyloid beta-peptide 42 and (-)-epigallocatechin-3-gallate. *J. Phys. Chem. B* **114**, 11576–11583 (2010).
63. Ehrnhoefer, D. E. *et al.* EGCG redirects amyloidogenic polypeptides into unstructured, off-pathway oligomers. *Nat. Struct. Mol. Biol.* **15**, 558–66 (2008).
64. Palhano, F. L., Lee, J., Grimster, N. P. & Kelly, J. W. Toward the molecular mechanism(s) by which EGCG treatment remodels mature amyloid fibrils. *J. Am. Chem. Soc.* **135**, 7503–10 (2013).
65. Bieschke, J. *et al.* EGCG remodels mature alpha-synuclein and amyloid-beta fibrils and reduces cellular toxicity. *Proc. Natl. Acad. Sci. U. S. A.* **107**, 7710–5 (2010).
66. Rezai-Zadeh, K. *et al.* Green tea epigallocatechin-3-gallate (EGCG) modulates amyloid precursor protein cleavage and reduces cerebral amyloidosis in Alzheimer transgenic mice. *J. Neurosci.* **25**, 8807–14 (2005).

67. Baptista, F. I., Henriques, A. G., Silva, A. M. S., Wiltfang, J. & Da Cruz E Silva, O. a B. Flavonoids as therapeutic compounds targeting key proteins involved in Alzheimer's disease. *ACS Chem. Neurosci.* **5**, 83–92 (2014).
68. Fernandez, J. W., Rezai-Zadeh, K., Obregon, D. & Tan, J. EGCG functions through estrogen receptor-mediated activation of ADAM10 in the promotion of non-amyloidogenic processing of APP. *FEBS Lett.* **584**, 4259–67 (2010).
69. Modarresi, F. *et al.* Knockdown of BACE1-AS Nonprotein-Coding Transcript Modulates Beta-Amyloid-Related Hippocampal Neurogenesis. *Int. J. Alzheimers. Dis.* **2011**, 929042 (2011).
70. Wilusz, J. E., Sunwoo, H. & Spector, D. L. Long noncoding RNAs: functional surprises from the RNA world. *Genes Dev.* **23**, 1494–504 (2009).
71. Randall, a D., Witton, J., Booth, C., Hynes-Allen, a & Brown, J. T. The functional neurophysiology of the amyloid precursor protein (APP) processing pathway. *Neuropharmacology* **59**, 243–67 (2010).
72. Parkin, Edward, and Harris, B. A disintegrin and metalloproteinase (ADAM)-mediated ectodomain sheddin of ADAM10. *J. Neurochem.* **108**, 1464–1479 (2009).
73. Chasseigneaux, Stephani and Allinquant, B. Functions of A $\beta$ , sAPP $\alpha$  and sAPP $\beta$ : similarities and differences. *J. Neurochem.* **120**, 99–108 (2012).
74. Thathiah, A. & Strooper, B. De. The role of G protein-coupled receptors in the pathology of Alzheimer's disease. **12**, 9–11 (2011).
75. Moss, M. L. *et al.* ADAM9 Inhibition Increases Membrane Activity of ADAM10 and Controls  $\alpha$ -Secretase Processing of Amyloid Precursor. *J. Biol. Chem.* **286**, 40443–40451 (2011).
76. Marshall, A. J., Rattray, M. & Vaughan, P. F. T. Chronic hypoxia in the human neuroblastoma SH-SY5Y causes reduced expression of the putative  $\alpha$ -secretases, ADAM10 and TACE, without altering their mRNA levels. **99**, (2006).
77. Morishima-Kawashima, M. Molecular mechanism of the intramembrane cleavage of the  $\beta$ -carboxyl terminal fragment of amyloid precursor protein by Inhibition and Modulation of  $\gamma$ -Secretase. *Front. Physiol.* **5**, 1–7 (2014).
78. Cacquevel, M., Aeschbach, L., Houacine, J. & Fraering, P. C. Alzheimer's disease-linked mutations in presenilin-1 result in a drastic loss of activity in purified  $\gamma$ -secretase complexes. *PLoS One* **7**, 1–13 (2012).
79. Wolfe, M. S. Inhibition and Modulation of  $\gamma$ -Secretase for Alzheimer's Disease. *Neurotherapeutics* **5**, 158–164 (2009).
80. Nik, S. H. M. *et al.* Alzheimer's disease-related peptide PS2V plays ancient, conserved roles in suppression of the unfolded protein response under hypoxia and stimulation of ??-secretase activity. *Hum. Mol. Genet.* **24**, 3662–3678 (2015).
81. Bieler, N. S., Knowles, T. P. J., Frenkel, D. & Vácha, R. Connecting macroscopic observables and microscopic assembly events in amyloid formation using coarse grained simulations. *PLoS Comput. Biol.* **8**, e1002692 (2012).
82. Turner, J. P. *et al.* Rationally designed peptoids modulate aggregation of amyloid-beta 40. *ACS Chem. Neurosci.* **5**, 552–558 (2014).
83. Reznichenko, L. *et al.* Reduction of iron-regulated amyloid precursor protein and  $\beta$ -amyloid peptide by (-)-epigallocatechin-3-gallate in cell cultures: Implications for

- iron chelation in Alzheimer's disease. *J. Neurochem.* **97**, 527–536 (2006).
84. Williams, R. J. & Spencer, J. P. E. Flavonoids, cognition, and dementia: actions, mechanisms, and potential therapeutic utility for Alzheimer disease. *Free Radic. Biol. Med.* **52**, 35–45 (2012).
  85. Yang, Z. *et al.* Radical-scavenging abilities and antioxidant properties of theaflavins and their gallate esters in H<sub>2</sub>O<sub>2</sub>-mediated oxidative damage system in the HPF-1 cells. *Toxicol. Vitr.* **22**, 1250–1256 (2008).
  86. Kimutai, S. *et al.* Determination of residual catechins, polyphenolic contents and antioxidant activities of developed Theaflavin-3,3'-Digallate rich black teas. *Food Nutr. Sci.* **7**, 180–191 (2016).
  87. Lorenz, M. *et al.* Green and black tea are equally potent stimuli of NO production and vasodilation: new insights into tea ingredients involved. *Basic Res. Cardiol.* **104**, 100–110 (2009).
  88. Zhang, J. *et al.* Neuroprotective Effects of Theaflavins Against Oxidative Stress-Induced Apoptosis in PC12 Cells. *Neurochem. Res.* 1–9 (2016). doi:10.1007/s11064-016-2069-8
  89. Tong, Y. *et al.* Oxidative stress potentiates BACE1 gene expression and A $\beta$  generation. *J. Neural Transm.* **112**, 455–469 (2005).
  90. Tamagno, E. *et al.*  $\beta$ -site APP cleaving enzyme up-regulation induced by 4-hydroxynonenal is mediated by stress-activated protein kinases pathways. *J. Neurochem.* **92**, 628–636 (2005).
  91. Obregon, D. F. *et al.* ADAM10 Activation Is Required for Green Tea (–)-Epigallocatechin-3-gallate-induced  $\alpha$ -Secretase Cleavage of Amyloid Precursor Protein. *J. Biol. Chem.* **281**, 16419–16427 (2006).
  92. Maloney, M. T., Minamide, L. S., Kinley, A. W., Boyle, J. a & Bamberg, J. R. Beta-secretase-cleaved amyloid precursor protein accumulates at actin inclusions induced in neurons by stress or amyloid beta: a feedforward mechanism for Alzheimer's disease. *J. Neurosci.* **25**, 11313–11321 (2005).
  93. Bailey, J. a, Maloney, B., Ge, Y.-W. & Lahiri, D. K. Functional activity of the novel Alzheimer's amyloid  $\beta$ -peptide interacting domain (A $\beta$ ID) in the APP and BACE1 promoter sequences and implications in activating apoptotic genes and in amyloidogenesis. *Gene* **488**, 13–22 (2011).